The Hong Kong Polytechnic University

Department of Rehabilitation Sciences

EFFECT OF LOW INTENSITY PULSED ULTRASOUND ON RHBMP-4 INDUCED OSTEOGENESIS IN A SPINAL FUSION MODEL

WANG XIAOYUN

A thesis submitted in partial fulfillment of the requirements for the Degree of Doctor of Philosophy

September 2008

CERTIFICATE OF ORIGINALITY

I hereby declare that this thesis is my own work and that, to the best of my knowledge and belief, it reproduces no material previously published or written, nor material that has been accepted for the award of any other degree or diploma, except where due acknowledgement has been made in the text.

_____(Signature of Candidate)

WANG XIAOYUN (Name of Candidate)

May. 4 2009 (Date)

Abstract of thesis entitled "effect of low intensity pulsed ultrasound on rhBMP-4 induced osteogenesis in a spinal fusion model" submitted by Wang xiaoyun for the degree of Doctor of Philosophy at the Hong Kong Polytechnic University in September 2008

ABSTRACT

Low intensity pulsed ultrasound (LIPU) has been proven effective in enhancing bone repair. It is well known that LIPU can effectively enhance bone healing in fresh fracture, delayed-union or non-union, bone defect and bone distraction. However, few studies have reported the effect of LIPU on ectopic ossification, which is the formation of bone in extraskeletal tissues. Moreover, the precise biological mechanisms underlying the effect of LIPU enhanced bone repair remain unclear. LIPU is a form of acoustic wave that can be transmitted through and into biological tissue to deliver mechanical energy. It is important therefore, to relate the mechanical basis of ultrasound to the sensitivity of the target biological tissues to the mechanical stimuli through its mechano-sensory nerve fibers which secrete calcitonin gene related peptide (CGRP). To date, little evidence is available on this relationship.

The aim of the present study is to investigate the effect of LIPU on the recombinant human bone morphogenetic protein-4 (rhBMP-4) induced ectopic ossification and the role of CGRP-positive nerve in ectopic ossification and its response to ultrasound stimulation.

Sixty 30-week old (around 4.5kg) New Zealand white rabbits were used as the experimental animals for this study. All animals underwent a single level non-decorticated bilateral posterolateral intertransverse process fusion at L5–L6 by implantation of poly (d,l-lactic acid) (PDLLA) incorporated with rhBMP-4. LIPU treatment was applied unilaterally on the body surface over the implantation site daily, starting at day 2 after operation. Rabbits were randomly allocated into 10 groups according to the application of different doses of rhBMP-4 (low dose or high dose) and different treatment durations of LIPU (3 days, 1 week, 3 weeks, 7 weeks and 12 weeks). Animals were sacrificed after the LIPU treatment was completed. The new bone formation at the fusion site was assessed using radiography, peripheral quantitative computed tomography (pQCT) and microscopy after animals to be sacrificed at the end of the experiment. The innervation of CGRP expressing sensory nerve in the fusion area was detected through immunofluorescent microscopy.

The x-ray, pQCT and light microscopy results showed that LIPU treatment could significantly enhance rhBMP-4 induced ectopic ossification in the present study. New bone formation was observed via intramembranous ossification and endochondral ossification on the sham LIPU side of all groups, indicating that the application of rhBMP-4 could effectively induce ectopic ossification. Moreover, more new bone tissues were found in the high dose rhBMP-4 groups

than in low dose rhBMP-4 groups at week 7 and week 12 postoperation, suggesting the apparent dose-dependent effect of rhBMP-4 on inducing and promoting ectopic ossification. On the other hand, LIPU treatment effectively enhanced rhBMP-4 induced ectopic ossification. The pQCT results showed that bone mineral content (BMC) and bone volume were significantly higher on the LIPU treated side than those on the sham LIPU side at week 7 and week 12 postoperation in both the low and high dose rhBMP-4 groups. Histological results also showed that the percentage of new cartilage tissue was significantly higher on the LIPU treated side than that on the sham LIPU side at week 3 and 7 postoperation, suggesting that LIPU could enhance rhBMP-4 induced ectopic ossification by improving endochondral ossification.

Fluorescent microcopy results showed that LIPU treatment enhanced the innervation of CGRP-positive nerve fibers in ectopic bone tissues. Spatially, LIPU promoted the in-growth of CGRP-positive nerve fibers into the new bone forming tissues. On the sham LIPU side, CGRP-positive nerve fibers were observed only at the fibrous tissues which surrounded the new bone and cartilage tissues, and in the bone marrow of the new bone tissue. On the LIPU treated side, CGRP-positive nerve fibers were also observed in the new bone and cartilage tissues in addition to the presence in fibrous and bone marrow tissues. Temporally, LIPU increased the density of CGRP-positive nerve fibers in

fibrous and bone marrow tissues during the process of ectopic ossification. On the sham LIPU side, the density of CGRP-positive nerve fibers in fibrous tissues was of a low level at day 3 and week 1, and then increased markedly at week 3. On the LIPU treated side, LIPU treatment increased the density of CGRP-positive nerve fibers to a high level from day 3, suggesting that the promotion effect of LIPU on the in-growth of CGRP-positive nerve fibers into the ectopic bone was more effectively during the early stage of healing.

The present study revealed that LIPU could effectively enhance rhBMP-4 induced ectopic ossification, possibly by improving endochondral ossification. Moreover, LIPU treatment facilitated the invasion of CGRP-positive sensory fibers in ectopic ossification during the healing process, which contributes to the overall concept of mechanobiology and its application in augmenting repair of musculoskeletal tissues in conjunction with its associated regulatory system(s).

AWARDS AND PUBLICATIONS

Award

Silver Award. Bone Morphogenetic Protein (BMP) combing therapeutic ultrasound inducing fast ectopic ossification. Guo X, **Wang XY.** *The 1st Korea international women's invention exposition 2008, Seoul, Korea, 8-10 May 2008.*

Journal paper

Wang XY, Guo X. Occurrence of CGRP-positive nerve fibers during spinal fusion healing (submitted).

Wang XY, Guo X. Contribution of sensory nerve innervation to the promoting effect of LIPU on ectopic ossification: an *in vivo* study (prepared).

Wang XY, Guo X, Qian ZM. The distributions and physiological functions of the calcitonin gene-related peptide in bone tissues. *Chinese Journal of Orthopaedics*, 2005, 25(3): 185-188(*Chinese*).

Conference paper:

Wang XY, Guo X, Liu MQ, Cheng JYC. Mi YL. Collagen hydrogel delivery system for rhBMP-4 in Non-decorticated Posterior Spinal Fusion model. *The 4th world congress of the international society of physical and rehabilitation medicine, Seoul, Korea, June 10-14, 2007: Page 304.*

Wang XY, Guo X, Liu MQ, Cheng JYC, Mi YL. Low intensity pulsed ultrasound enhanced the healing of rhBMP-4 incorporated collagen hydrogel graft in spinal fusion. *The 4th world congress of the international society of physical and rehabilitation medicine, Seoul, Korea, June 10-14, 2007: Page 356.*

Wang XY (Presenter), Guo X, Liu MQ, Cheng JYC, Mi YL. The effect of low intensity pulsed ultrasound on osteogenesis in spinal fusion with rhBMP-4 incorporated collagen hydrogel graft. *The 1st inaugural Australia-China biomedical research conference, February 1-3, 2007: Page 14 (oral presentation).*

Wang XY, Guo X, Liu MQ, Cheng JYC, Mi YL. Collagen hydrogel delivery system for recombinant human bone morphogenetic protein-4. *The fifth Pan-Pacific conference on rehabilitation and the Pre-FIMS world congress of sports medicine, Hong Kong, June 9-11, 2006: Page 78.*

Guo X, **Wang XY(Presenter),** Kwong SC, Liu MQ, Qian ZM. Efficacy of low intensity pulsed ultrasound in the prevention of disuse osteoporosis in rats. *The fifth Pan-Pacific conference on rehabilitation and the Pre-FIMS world congress of sports medicine, Hong Kong, June 9-11, 2006: Page 29 (oral presentation).*

Ke Y, **Wang XY**, Guo X, Zhou HZ, Guo FY, Qian ZM. Hepcidin and bone mineralization: effects of hepcidin on iron and calcium uptake by cultured

osteoblasts *in vitro*. *The 12th national conference of Chinese society for pharmaceutical industry, and the 2nd national conference of Chinese society for applied pharmacology international symposium of biopharmacology and biotechnology, Hong Kong, August 4-10, 2006, Chinese Traditional and Herbal Drug, 37(suppl.): Page 177.*

Chapters in books:

Guo X, **Wang XY**, Lam WL. Neurogenic limb disuse animal Model (Chapter 29), 477-494, in *A practical manual for musculoskeletal research (editors: Leung et al.), 2008,* World Scientific: Singapore.

Guo X, **Wang XY.** Introduction of biomechanics (Chapter 1), 1-9; International system of units (Appendix 1), 10-13, in *Basic biomechanics of musculoskeletal system (translators: Kwong and Guo), 2008,* People's medical publishing house: Beijing *(in Chinese).*

ACKNOWLEDGEMENTS

First of all, I would like to thank my chief supervisor, Dr. Xia Guo, for her constructive guidance and support for this research. Without her encouragement, knowledge and perceptiveness I would never have finished my study. I must also thank Prof. YongLi Mi, my co-supervisor for his suggestions and inspirations on my study. I must also thank to my examiners, for managing to read the whole thing so thoroughly and providing all the advice and suggestions.

Thanks to Dr. Muqing Liu, Dr. Baoting Zhang, Dr. Qing Wang, Ms. Trish Wai-Ling Lam, Mr. Baosheng Guo, Dr. Chi-Keung Yeung, Mr. Zongkang Zhang, Mr. Roy Yuen-Chi Lau and all the other people that I have worked with, in the laboratory, during the course of my studies. Thanks also to all my friends in Hong Kong and elsewhere, for keeping me company and encouraging me through the difficult times that came my way.

I heartily thank my experimental animals. Their sacrifice is priceless in terms of the contribution to our understanding of the effect of therapeutic ultrasound in bone healing, which has undoubtedly formed the foundation for future human studies.

Most importantly, I would like to thank my husband, my parents and my sister, for their love, patience and continuous support during the whole PhD period.

The study summarized in this thesis was supported by the research grant from The Research Grants Council of Hong Kong (RGC ref No. PolyU5406/03M).

Wang Xiaoyun

Sep. 2008

TABLE OF CONTENTS

LIST OF ABBREVIATION

Absorbable collagen sponges (ACS)

Bone mineral density (BMD)

Bone mineral content (BMC)

Bone morphogenetic protein (BMP)

β-tricalcium phosphate (β-TCP)

Cyclic adenosine monophosphate (cAMP)

Calcitonin gene related peptide (CGRP)

40, 60-diamidino-2-phenylindole (DAPI)

Food and Drug Administration (FDA)

Fluorescein isothiocynate (FITC)

Hydroxyapatite (HA)

Insulin-like growth factor 1 (IGF-1)

Interleukin-6 (IL-6)

Low intensity pulsed ultrasound (LIPU)

Neuropeptide Y (NPY)

Poly (d,l-lactic acid) (PDLLA)

Poly (glycolic acid) (PGA)

Protein kinase C (PKC)

Poly (lactic acid) (PLA),

Poly (lactic-glycolic acid) (PLGA)

Peripheral quantitative computed tomography (pQCT)

Recombinant human bone morphogenetic protein-4 (RhBMP-4)

Runt-related transcription factor 2 (Runx2)

Spatial average and temporal average (SATA)

Substance P (SP)

Transforming growth factor-β (TGF-β)

Vasoactive intestinal peptide (VIP)

LIST OF FIGURES

LIST OF TABLES

Chapter 1

Introduction

Ultrasound, a form of mechanical energy that can be transmitted through and into biological tissues as an acoustical pressure waves at a frequency beyond human audible range, has been used widely in medicine as a diagnostic, operative, and therapeutic tool. Low intensity pulsed ultrasound (LIPU) has been proven to effectively enhance bone healing in fresh fracture, delayed-union or non-union, bone defect and bone distraction (Kristiansen et al., 1997). However, few studies have reported the effect of LIPU on ectopic ossification, which also often occurs clinically. Ectopic ossification can be induced experimentally by bone morphogenetic protein (BMP), which has remarkable ability to induce osteogenesis. It has also been regarded as the potent stimulator of ectopic ossification since it was named in 1965 (Urist, 1965).

Although it is well accepted that LIPU can promote bone repair, the precise cellular mechanisms underlying the effect of LIPU remain unclear. LIPU transfers mechanical energy into tissues. How this mechanical stimulation is “sensed” by the healing tissue and how it delivers its therapeutic effect is not clearly understood. The present study tried to relate the mechanical basis of ultrasound to the sensitivity of bone tissue through its sensory nerve fibers to mechanical stimuli. In the present study, several kinds of measurement methods

were performed to evaluate the effect of LIPU on rhBMP-4 induced ectopic ossification; immunofluorescence microscopy was used to investigate the role of sensory innervation in ectopic osteogenesis and its response to ultrasound stimulation.

Ectopic ossification often occurs clinically after skeletal injuries. The outcome of the present study will expand our knowledge on the effect of LIPU on bone healing. The present study also investigates the involvement of sensory nerve in ectopic ossification and its response to ultrasound stimulation during the healing process, which will provide novel insight into the mechanisms of promoting effect of LIPU on bone healing. The present study is of great significance to appropriate application of LIPU for the treatment on bone healing in clinical practice.

Chapter 2

Literature review

2.1 Bone morphogenetic proteins (BMPs)

2.1.1 Historical perspective

In 1965, Dr. Marshall Urist (Urist, 1965) showed that new bone formation could be induced with the use of demineralized bone matrix. By implanting demineralized bone particles intramuscularly in animals, he was able to observe the ectopic ossification. With these studies, he pioneered the concept that there is some substance naturally present in the bone, which is responsible for the regeneration and repair activity. He called this substance bone morphogenetic protein (BMP). Since then, BMPs have become a subject of intensive research aimed at developing treatment strategies for skeletal conditions resulting from trauma and degenerative diseases. In 1988, highly purified protein derived from bovine bone was found to be able to induce ectopic bone formation. The molecular clones of this protein as well as the amino acid sequence were characterized subsequently (Wozney et al., 1988). This led to the isolation and expression of human complementary DNAs which were recognized as members of the transforming growth factor-β (TGF-β) supergene family. In the past 15 years, investigators have determined the molecular genetics of BMP biology and have identified 15 individual human BMPs that possess varied degrees of bone

or cartilage inductive activities, which have led to the development of therapeutic preparations for specific clinical applications (Carlisle and Fischgrund, 2005).

2.1.2 Biological activities of BMPs

In embryogenesis, BMPs define embryo polarity and patterning. BMP-4, BMP-2 and BMP-7 have been shown to have ventralizing effects (Fainsod et al., 1994; Hawley et al., 1995; Hemmati-Brivanlou and Thomsen, 1995; Schmidt et al., 1995). Many studies have also demonstrated that BMPs are important factors in regulating chondrogenesis and skeletogenesis during normal embryonic development. BMP-4 is expressed in perichondrium, while BMP-2 is expressed in areas surrounding the initial cartilage condensations (Duprez et al., 1996). BMP-2 is also expressed in periosteal and osteogenic zones(Lyons et al., 1989). BMP-5 is expressed in initial cartilage condensations as well as in perichondrium and periosteum at later stages of bone development (King et al., 1994). Distinct expression patterns of individual BMPs indicated that different BMP molecules mediate specific events during skeletogenesis. For example, BMP-4 recruits periochondrial cells, while BMP-2 recruits mesenchymal cells surrounding the initial cartilage condensations into chondrogenic cells (Duprez et al., 1996).

In postnatal animals, BMPs act as potent bone regeneration factors, to recruit osteoblast precursors to a defined location in response to a specific need. The continued osteogenesis required for bone growth, bone remodeling, and bone repair can be regulated by the availability of a subset of BMPs. BMP-2 and BMP-7 are the most extensively studied for their ability to promote osteogenesis *In vivo*, preclinical studies demonstrated accelerated recovery of biomechanical strength or radiographic union by using rhBMP-2 and rhBMP-7 in rabbit, dog, goat, and nonhuman primate models of spontaneously healing osteotomy(Bouxsein et al., 2001; den Boer et al., 2002). *In vitro*, rhBMP-2 and rhBMP-7 have been shown to induce both chondrocyte and osteoblast differentiation in C3H10T1/2 cells(Wang et al., 1993; Asahina et al., 1996). It has been proposed that BMPs can induce both undifferentiated stem cells and more differentiated multipotent cells along chondrogenic or osteogenic pathway(Yamaguchi et al., 1991; Katagiri et al., 1994; Gimble et al., 1995).

BMP-4 can also increase new bone formation by both endochondral ossification and intramembrance ossification. Nakase indicated that BMP-4 could participate in endochondral ossification and was one of the main local contributing factors in callus formation in the early phase of fracture healing(Nakase et al., 1994). Shum showed BMP-4 enhanced cartilage maturation and induced ectopic chondrocyte hypertrophy in the cranial

base(Shum et al., 2003).*In vitro* studies have shown that like marrow derived mesenchymal cells, non-marrow derived mesenchymal stem cells can also undergo osteoblastic differentiation in response to rhBMP-4(Kanatani et al., 1995; Jortikka et al., 1998).Lin showed that BMP-4 induced osteoblastic differentiation and mineralization in adipose tissue derived from stromal cells(Lin et al., 2006).

2.1.3 BMPs signaling and regulation

As members of TGF-β superfamily, BMPs trigger cellular response mainly through the smad pathway(Massague, 1998). After binding to BMP receptors type I and II, BMPs activate intracellular transcription factors, including smad 1,smad5, and smad8, and proceed toward dimerization with smad4 before translocation into nucleus(Chen et al., 2004; Nohe et al., 2004; Miyazono et al., 2005). The complexes are then translocated into nucleus to regulate specific gene transcription. For example, the complex translocates into the nucleus where they interact with other transcription factors, such as runt-related transcription factor 2 (Runx2) in osteoblasts.

BMP signaling can be regulated at different molecular levels as follows (Figure 2.1): First, BMP antagonists, such as Noggin, bind with BMP and block signaling. Second, smad6 can bind with BMP receptor and prevent smad

proteins activation. Third, tob interacts specifically with BMP activated smad proteins. Fourth, smurf1 interacts with smad1 and smad5 for mediating the degradation of these proteins. Fifth, smurf1 mediate Runx2 degradation. Finally, smurf 1 form a complex combination with smad6 and target to the type I BMP receptor for their degradation(Chen et al., 2004).

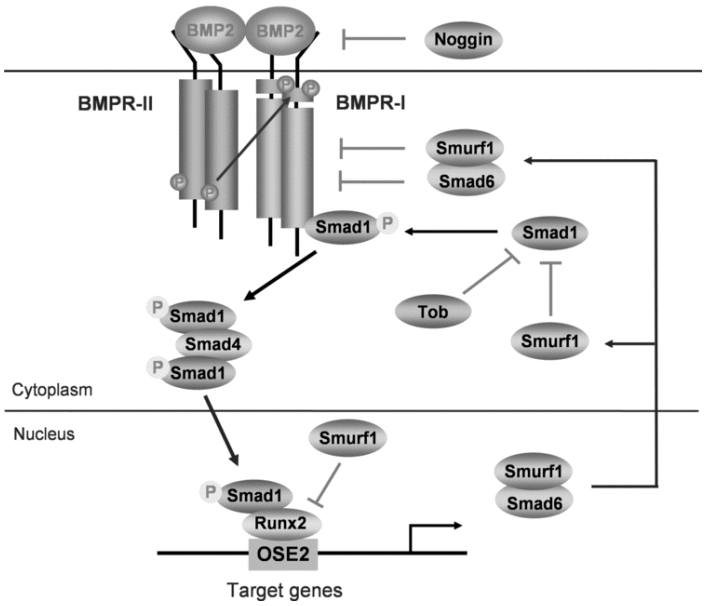

Figure 2.1 BMP signaling and its regulation(Chen et al., 2004).

2.1.4 BMPs induced ectopic ossification

Because of its remarkable ability to induce ectopic osteogenesis, BMP as potent stimulators of ectopic ossification is obvious. Wang demonstrated that BMPs induced ectopic ossification via endochondral ossification when implanted subcutaneously in rats. Histological results showed an early fibroproliferative phase followed by chondrocyte differentiation, vascularization, osteoblast differentiation with bone matrix formation, and subsequent mineralization of osteoid (Wang et al., 1990). Yoshida compared the osteoinduction capability of rhBMP-2 in the muscle and in the subcutaneous tissue in rats, and concluded that mesenchymal cells in the muscle could more easily differentiate into osteoblasts, leading to osteoinduction. The difference in osteoinduction could be related to the partial pressure of oxygen or the blood supply in the intramuscular and subcutaneous sites (Yoshida et al., 1998).

Presently rhBMP-2 and rhBMP-7 with various carriers are being used to induce ectopic ossification in spinal fusion. Many studies showed that rhBMP-2 enhance osteogenesis in spinal fusion models, whenever rhBMP-2/collagen composite (Sandhu et al., 2002) or rhBMP-2/tantalum (Sidhu et al., 2001) were used as graft. Boden proved that the effect of rhBMP-2 was dose-dependent. Bone formation associated with a higher concentration of rhBMP-2 was denser and quicker than that associated with a lower concentration (Boden et al., 1998).

Moreover, Hecht suggested the presence of rhBMP-2 accelerated not only the osteoblastic bone formation but also the osteoclastic remodeling (Hecht et al., 1999). On the other hand, rhBMP-7 has also been proven effective in spinal fusion by previous studies (Cook et al., 1994). Guo indicated that rhBMP-4 effectively enhanced new bone formation and accelerates fusion in the rabbit posterolateral posterior spinal fusion model. Moreover, the effective dose of rhBMP-4 is 10 times lower than the reported dosage of rhBMP-2 and rhBMP-7 (Guo et al., 2002). This is also the reason that we use rhBMP-4 in our study.

2.1.5 Carriers for BMPs

The ideal carrier materials must support bone formation through direct interaction with the target area and the cells by providing an attachment substrate and binding and delivering the BMPs to the local environment for "release" at the most opportune time. There are many kinds of materials as follows:

Collagen has a long history of use in surgical applications given its biocompatibility, ease of degradation, and interaction with other bioactive molecules including proteins. The association of rhBMP-2 and absorbable collagen sponges (ACS) allows retention of the active osteoinductive protein while minimizing immediate leaching of the agent (Damien et al., 2002; Geiger

et al., 2003). Bovine bone-derived type I collagen also serves as a carrier for rhBMP-7 and has been evaluated in numerous preclinical studies (Grauer et al., 2001; Bomback et al., 2004).

Calcium phosphate biomaterials closely resemble the mineral composition, properties, and microarchitecture of human cancellous bone. They also have a high affinity for binding proteins. Normal cortical bone has pore sizes ranging from 1μm to 1000 μm, whereas cancellous bone has pores from 200 μm to 400 μm. This microarchitecture of cancellous bone including the size, extent, and interconnectivity of the pores affects tissue ingrowth, cell attachment, and diffusion of nutrients into the area. Studies have suggested an optimum pore size for neovascularization of at least 50 μm and 200 μm for new bone appositional formation and ingrowth (Kuboki et al., 1998; Jahng et al., 2004). Calcium phosphate materials may be classified according to chemical composition and whether it is of natural or synthetic (ceramic) origin. These include hydroxyapatite (HA), β-tricalcium phosphate (β-TCP), biphasic calcium phosphate (combination of TCP and HA), and calcium deficient apatite forms (Tay et al., 1999). Ceramic composites may be more suited to function as a delivery vehicle for cells and BMPs based on composition and mechanical properties.

As a delivery system for BMPs, the combination of carriers, including collagen and biphasic calcium phosphate, may have at least theoretical advantages for the retention of appropriate concentrations at the site of the bone paucity. It has been evaluated in posterolateral rabbit fusion and subcutaneous bone formation models (Itoh et al., 2001; Minamide et al., 2004). A ceramic–collagen composite may also have compression-resistant mechanical properties that can improve the handling of the graft and maintain a larger space.

A new class of carrier material, the biodegradable polymers has recently received considerable attention. Poly (lactic acid) (PLA), Poly (glycolic acid) (PGA) and Poly (lactic-glycolic acid) (PLGA) are widely used to carry BMPs. Miyamoto synthesized PLA into several molecular weights and concluded that the PLA at 650 d was best suited as a carrier for BMP because of its material properties (Takaoka et al., 1988). Bessho evaluated a low-molecular-weight PLGA copolymer as a synthetic, biodegradable carrier for rhBMP-2 *in vivo*. A mixture of 2, 10, or 50 μg of rhBMP-2 and 10 mg of PLGA 50:50 copolymer was implanted into the calf muscles of rats. The results indicated that new bone formation occurred at all rhBMP-2 implanted sites within 3 weeks after implantation and that the amount of bone induction was correlative with the rhBMP-2 concentration (Bessho et al., 2002). Other studies have also demonstrated the effects of PLA-PGA microspheres or when used as a sponge

containing BMP-2 in ectopic bone formation assays, long bone defects or osteotomy models, and canine and rabbit posterior lumbar fusion models (Alpaslan et al., 1996; Fischgrund et al., 1997; Whang et al., 1998; Schrier and DeLuca, 2001; Saito and Takaoka, 2003; Kokubo et al., 2004).

2.2 Spinal fusion and ectopic ossification

2.2.1 Anatomy of lumbar spine of a rabbit

The lumbar spine of a rabbit is typically composed of seven vertebrae. In the sagittal plane, the thoracic and lumbar spines together form a single curve, which is dorsally convex. Each vertebra consists of an anterior body and a posterior neural arch, which together enclose the vertebral foramen. Processes arise from the neural arch, including spinous, mammillary, transverse, superior articular and inferior articular process (Figure 2.2). The intrinsic spinal muscles are bounded ventrally by the transverse processes and medially by the lumbar spinous processes and the intervening interspinous ligaments. Iliocostalis muscle inserts in a continuous mass onto the lateral two-thirds of the lumbar transverse process. Medially, the iliocostalis wraps over the lateral and dorsal surface of the longissimus muscle, attaches to the tips of the lumbar mammillary processes and is separated from the midline by the multifidus muscle. The longissimus muscle is applied to the lateral surface of the mammillary processes and the medial third

of the transverse processes. The iliocostalis and longissimus overlay the intertransverse ligament at each segmental level (Palumbo et al., 2004) (Figure 2.3).

At each segmental level of the lumbar spine, the intervertebral foramen transmits the associated spinal nerve. The lumbosacral plexus is formed from the L4-L7 and the S1-S4 spinal nerves, which can be conceptually separated into a lumbar portion that gives rise to the femoral nerve and a sacral component form, which originates the sciatic nerve. Within the L5-L6 intertransverse zone, the L5 spine nerve exits the neural foramen at a level just dorsal to the plane of the transverse processes. At this location, the dorsal ramus is closely associated with the posterior branch of the fifth lumbar segmental artery. The ventral ramus passes anteriorly, piercing the intertransverse ligament just cranial to the base of the L6 transverse process (Palumbo et al., 2004).

A

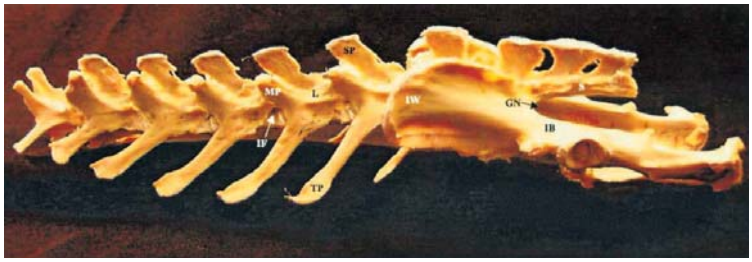

B

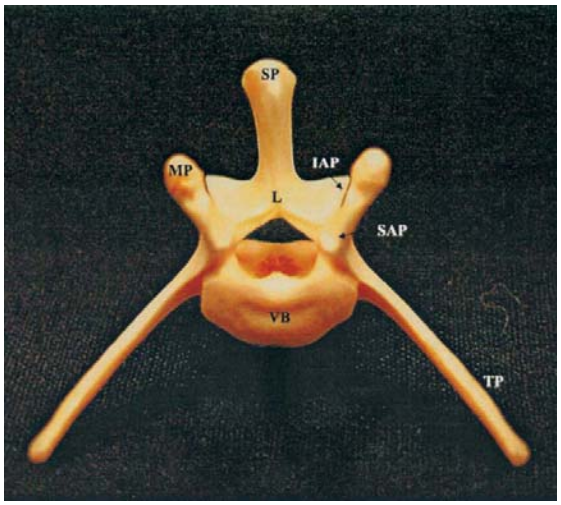

Figure 2.2 Osteology of the rabbit lumbar spine. (A) Whole specimen (posterolateral view). (B) Sixth lumbar vertebra (craniodorsal view). GN=greater sciatic notch; IAP=inferior articular process; IB=iliac body; IF=intervertebral foramen; IW=iliac wing; L=lamina; MP=mammillary process; S=sacrum; SAP=superior articular processes; SP=spinous process; TP=transverse process; VB=vertebral body (Palumbo et al., 2004).

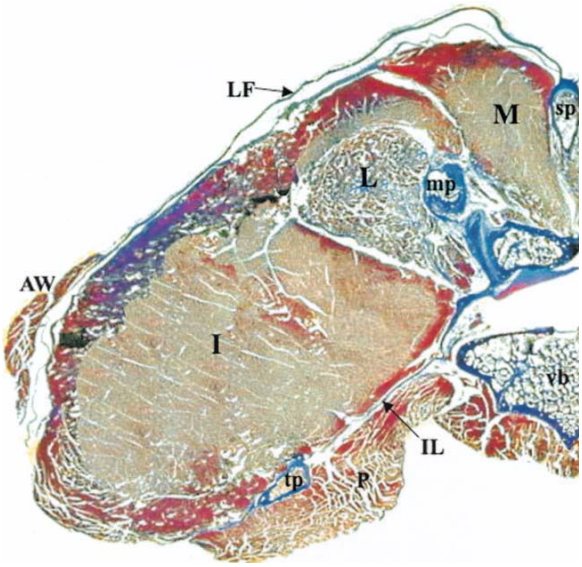

Figure 2.3 Intrinsic musculature of the rabbit lumbar spine. Cross section through the L5–L6 level (low-power photomicrograph). AW=anterior abdominal wall muscles; I=iliocostalis; IC=iliac crest; IL=intertransverse ligament; L=longissimus; LF=lumbodorsal fascia; M=multifidus; mp=mammillary process; P=psoas; sp=spinous process; tp=transverse process; vb=vertebral body (Palumbo et al., 2004).

2.2.2 Intertransverse process fusion model (decorticated spinal fusion model and non-decorticated spinal fusion model)

Spinal fusion is used to align and stabilize the axial skeleton. As a result, animal spinal fusion model is intended to disturb pathologic anatomy, to create a mechanically optimal arrangement. The rabbit model of intertransverse process fusion is the most commonly used. It requires the formation of an ectopic bone bridge across the intertransverse processes, allowing for comparisons of growth factors, bone graft substitutes, and microscopic changes in the fusion process. Typically, the ectopic bone bridge is produced by recreating conditions of skeletal injury along a “fusion site” and allowing the normal bone healing response to occur. The biological environment of the fusion site requires the presence of osteogenic or osteopotential cells, osteoinductive cytokines, adequate blood supply and sufficient inflammatory response.

It is well known that, decortication is required in preparing the local bone in spinal fusion model. Decortication is the process of removing the outer cortex of the local bone with a burr to induce the release of bone marrow which contains the osteoinductive cytokines and uncommitted mesenchymal stem cells. Consequently, these mesenchymal stem cells are directed by osteoinductive cytokines to differentiate into bone-forming cells, leading to osteogenesis. The technique of decortication was first reported by Hibbs in 1924. Hibbs

emphasized a thorough removal of the soft tissue, obliteration of the facet joints, and decortication of the lamina for a successful spinal arthrodesis (Hibbs, 1924). Since then, numerous articles describing the different techniques of spinal fusion all emphasized meticulous subperiosteal dissection with thorough decortication of the posterior elements (Kostuik et al., 1973; Edgar and Mehta, 1988). However, there are also some disadvantages in the process of decortication. The surgical procedure of decortication increases blood loss, operative exposure, operative time, postoperation pain and the chance of neurological damage.

The use of BMP, an osteoinductive cytokine makes it possible to develop the animal model without decortication. Previous studies indicated that BMPs can induce non-marrow derived mesenchymal stem cells to differentiate into osteogenic cells, resulting in cartilage and bone formation in ectopic sites (Wozney, 1992). Sanhu demonstrated that it was feasible, in the presence of rhBMP-2, to achieve an osseous bridge between the adjacent transverse processes (Sandhu et al., 1997). In a further study, the bilateral transverse processes of the rabbit at L5–L6 were surgically exposed and a HA-TCP block integrated with rhBMP-4 was implanted onto the transverse processes of each side. As a result, the interaction between rhBMP-4 and non-marrow derived mesenchymal cells successfully induced ectopic bone bridge without decortication (Guo et al., 2002). In general, the surgical procedures of the

non-decorticated spinal fusion model include exposing a portion of each of adjacent vertebrae requiring fusion, adding an osteoinductive cytokine to a carrier material and placing the carrier material between the portions of adjacent vertebrae in contact with the cortical bone of the portions.

2.2.3 Application in ectopic ossification study

Ectopic ossification is characterized by normal bone formation at ectopic sites in the body. BMPs have been regarded as the most effective agent for inducing ectopic ossification. In 1965, Urist induced ectopic ossification in the soft tissue adjacent to the site where he had implanted demineralized bone matrix containing BMP (Urist, 1965). Since then, the most commonly used animal model of ectopic ossification has been established by the surgical implantation of BMPs at ectopic sites to induce bone formation. Among them, the experimental BMPs induced ectopic ossification in intertransverse processes fusion model is the most useful tool in the study of the biological process of ectopic ossification.

The biological environment of the intertransverse processes is appropriate for BMPs induced ectopic ossification, which can be conductive to the continued production of ectopic bone. In the intertransverse processes fusion model, BMPs with carrier block is implanted into the muscles overlaying the

transverse processes with one surface of the block contacting the cortical bone of transverse processes and the intertransverse ligament. It has been proven that BMPs with the carrier block effectively induce ectopic bone formation after intramuscular implantation (Wurzler et al., 2004; Kakudo et al., 2006). Therefore, the intertransverse processes fusion model possesses the ability of inducing the ectopic ossification.

The outcomes of ectopic ossification in intertransverse processes fusion model can be well determined and analyzed. In this model, the new bone formation is confined to the intertransverse interval and the carrier block. Compared with ectopic bone induced at intramuscular and subcutaneous sites, the new bone formation between transverse processes are restricted more by the geometry of the implant. Moreover, the methods for evaluating the ectopic bone in the intertransverse fusion model are widely accepted. Radiography, mechanics and histology are all used to determine the fusion mass.

2.3 Low intensity pulsed ultrasound (LIPU)

2.3.1 Ultrasound in medicine

Ultrasound, a form of mechanical energy that can be transmitted through and into living tissues as acoustical pressure waves at a frequency beyond the audible range of humans, has been used widely in medicine as a diagnostic,

operative, and therapeutic tool. As diagnostic devices, ultrasound with an intensity of 50-1000mW/cm^2 could image fetuses (Papp and Fekete, 2003), peripheral blood flow, eye structures, and bone mass (Gonnelli and Cepollaro, 2002). The use of ultrasound as a surgical instrument requires even higher intensity levels (5-300W/cm^2) to fragment calculi, ablate disease tissues such as cataracts (Kelman, 1969). As therapeutic tools, ultrasound with low intensity of 30-100mW/cm^2 is used mainly in the treatment of soft tissue injuries and bone healing. Food and Drug Administration (FDA) of the Unite States had approved the use of LIPU for the treatment of fractures and other bone defects.

2.3.2 Property and signal characteristics of LIPU

Low intensity has been proven effective in bone repair and the frequency of 1.5 MHz has been more commonly used to stimulate osteogenesis experimentally and clinically. The parameters of LIPU are usually set as 1.5MHz, 30mW/cm^2 spatial average and temporal average (SATA) intensity and pulsed 200μs:800μs for 20 min daily, which are widely used to enhance bone healing.

2.3.3 Historical perspective of LIPU

In 1950, Maintz first investigated the effect of high intensity ultrasound treatment on fracture healing. He discovered that callus formation can be reduced when using the intensity of 1000, 1500, and 2500mW/cm^2 (Maintz, 1950). Early reports in the mid to late 1950s showed ultrasound treatment with very high intensities (5000-25000 mW/cm^2) led to delayed bone healing, necrosis and dense fibrous tissue formation in dog femora (Bender et al., 1954; Herrick et al., 1956; Ardan et al., 1957). In the 1980s, LIPU was initially reported to effectively facilitate bone healing. Duarte (Duarte, 1983) studied the stimulation of bone growth by ultrasound and found that pulsed ultrasound at low intensity of 49.6 mW/cm^2 and 57mW/cm^2 accelerated fibular osteotomy vertical bridging. Xavier and Duarte (Xavier and Duarte, 1983) reported that 70% of 26 non-unions healed after a brief exposure (20 min/day) to very low intensity ultrasound (30mW/cm^2). Several years later, Pilla (Pilla et al., 1990) showed that with LIPU (1.5MHz, 30mW/cm^2 SATA, pulsed 200us:800Us, 20 min daily) treatment, the strength of fractured rabbit fibulae returned to that of the intact bone in 17 days, whereas it took 28 days for the untreated control. Wang (Wang et al., 1994) compared the effect of 0.5 MHz and 1.5 MHz burst ultrasound at low intensity on femoral shaft fracture healing and found that 1.5 MHz burst was significantly greater in stiffness than 0.5 MHz burst. With all

these early efforts, the parameters of therapeutic LIPU were established as pulsed ultrasound of 200μs burst of 1.5 MHz sine wave, repeated at 1 kHz, delivering the intensity of 30mW/cm^2 with treatment duration of 20min per day.

2.3.4 Efficacy of ultrasound on bone repair (fresh fracture healing, delayed-union or non-union healing, bone distraction)

The FDA approved the use of LIPU for the accelerated healing of fresh fractures in October 1994 and for the treatment of established nonunion in February 2000. Two earlier double-blind, placebo-controlled clinical trials evaluated the use of LIPU for the treatment of fracture. In the fist study, Heckman (Heckman et al., 1994) reported a significant 38% reduction in the clinic and radiographic healing time of tibial fracture under LIPU treatment. In the second study, the effect of LIPU on the healing of fresh radial fracture was determined. The time duration of union was 38% shorter in the LIPU treatment compared to that in the control (Kristiansen et al., 1997). Furthermore, Mayr (Mayr et al., 2000b) discovered that LIPU effectively accelerated the healing of fresh scaphoid fracture. In concert with these clinical studies, substantial animal experiments were in an attempt to determine if the effect of LIPU was greatest at some specific stage of fracture healing. Azuma investigated the effect of the timing of LIPU treatment in the bilateral closed femoral fracture model in rats

(Azuma et al., 2001). The right femur was exposed to LIPUS and the left femur was used as a control. Rats were divided into four groups according to timing and duration of treatment (days 1-8; days 9-16; days 17-24; days 1-24 after the fracture) and were sacrificed on day 25. The results showed that the union was accelerated in each group regardless of the duration or timing of the treatment Moreover, the maximum torque to failure on the treated side was greater than that on the control side at all time-periods. Thus, LIPU positively influences three key stages of the fracture healing process (inflammation, repair, and remodeling).

LIPU was also evaluated for treatment of delayed-union or non-union. Mayr reported the use of LIPU on the treatment of 951 delayed unions and 366 non-unions. The overall success rate was 91% for delayed unions and 86% for non-unions (Mayr et al., 2000a). Frankel studied the registry database and assessed the healing rate of 404 non-unions at different bone sites. He showed a healing rate of 70% for the humerus, 86% for the femur, 81% for the metatarsals, 96% for the radius 86% for the scaphoid and 83% for the tibia (Frankel, 1998). These data suggest that LIPU has the potential to treat the delayed-union or non-union.

Many experimental studies investigated the possible role of LIPU in bone distraction. Three groups studied the influence of LIPU treatment on the

maturation period of the bone regeneration, using a rabbit's tibia distraction model (Shimazaki et al., 2000; Tis et al., 2002; Sakurakichi et al., 2004). They all found a larger callus formation in the LIPU treated animals. Moreover, a longer maturation time led to an increase in bone regeneration in the untreated control groups. This result demonstrated that LIPU treatment has only an acceleratory effect on the maturation of the newly formed bone.

In summary, LIPU treatment effectively enhances bone healing in bone repair. In fact, ectopic ossification also often occurs clinically with orthopedic injuries. For example, ectopic ossification appears following internal fixation or arthroplasty for displaced femoral neck fractures (Johansson et al., 2001). However, few experiments have reported the effect of LIPU on ectopic ossification.

2.3.5 Biophysical and biological mechanisms of LIPU on bone tissues

Many experimental studies in both *in vitro* and *in vivo* levels have been performed to explore the biophysical and biological mechanisms responsible for the ultrasound efficacy on the bone tissue.

As a form of mechanical stimulation, biophysical effects of LIPU, including thermal effects and nonthermal effects have been proposed to underlie its benefit effects observed on bone healing. Chang (Chang et al., 2002) indicated that the

heating effect from LIPU (20-50 mW/cm^2) was well below 1℃. Such minimal heating effect may affect some enzymes, such as collagenase. Collagenase has been shown to be exquisitely sensitive to small variations in temperature (Welgus et al., 1981; Welgus et al., 1985). The nonthermal effects produced by LIPU have attracted great attention.

Many studies suggest that LIPU may follow Wolff's law by serving as a noninvasive force stimulating the bone healing processes. Wolff's law stated that the form and architecture of bone adapt to the mechanical environment by remodeling to accommodate the magnitude and direction of the applied force. The acoustic pressure waves generated by LIPU may provide a surrogate for the force at work in Wolff's law influencing the process of bone healing.

Moreover, LIPU treatment may also be associated with generating the phenomena of stable cavitation and microstreaming. Cavitation refers to ultrasonically induced activity occurring in a liquid or liquid-like material that contains bubbles or pockets containing gas or vapor. Microstreaming is a small scale eddying of fluids near a vibration structure. During stable cavitation, gas accumulates in the medium and forms gas bubbles, with the cavity acting to enhance microstreaming (Watson, 2000). Sable cavitation and microstreaming can affect a biological system by virtue of a mechanical stress. They have been shown to affect diffusion rates and membrane permeability. Data from the

previous *in vitro* study suggest that LIPU may induce the changes in the cell membrane and thus alter ionic permeability (Chapman et al., 1980; Ryaby et al., 1989) and second messenger activity (Ryaby et al., 1992) These changes may then lead to downstream alteration in gene expression, resulting in the acceleration of the bone healing process by regulating bone cartilage and bone specific genes as well as others.

Despite the above biophysical mechanisms, many studies investigated the potential cellular processes influenced by LIPU. Many types of cells associated with bone healing processes have been shown to be directly affected by LIPU (Table 2.1). These studies indicate that LIPU has direct effects on the reparative processes of angiogenesis, chondrogenesis and osteogenesis. In concert with these studies, some tissue culture experiments also discussed the potential biological mechanisms. Korstjens indicated that LIPU increased bone collar and calcified cartilage volume through stimulation of bone cell differentiation and calcified matrix production respectively (Korstjens et al., 2004). Nolte suggested that LIPU stimulation caused an increase in the osteoblast activity or number and stimulated hypertrophic cartilage cells, which resulted in the increased calcified matrix (Nolte et al., 2001).

Table 2.1 Cellular processes influenced by LIPU

Cell/tissue type	results	implication	study
periosteal cells	cell proliferation, activity of ALP↑, osteocalcin secretion↑, VEGF production↑, calcium nodules formation↑	LIPUS stimulated periosteal cell proliferation and differentiation toward osteogenic lineage.	(Leung et al., 2004)
bone marrow-derived mesenchymal stem cells	IGF mRNA↑, osteocalcin ↑, and bone sialoprotein mRNA↑	LIPUS induced a direct anabolic reaction of osteogenic cells, leading to bone matrix formation.	(Naruse et al., 2000)
	Aggrecan deposition↑	LIPUS enhanced TGF-β-mediated chondrocyte differentiation of mesenchymal stem cells	(Ebisawa et al., 2004)
	proteoglycan↑,collagen↑ chondrogenic marker genes↑,	LIPUS enhanced chondrogenesis of mesenchymal stem cells in cell aggregates.	(Schumann et al., 2006)
osteoblast	cell proliferation, collagen↑, non-collagen protein↑, IL-1β↑, IL-8↑,bFGF↑, VEGF↑	LIPU induced cell proliferation and enhanced bone matrix formation.	(Doan et al., 1999)
	cfos↑, COX-2↑, ALPmRNA↑, osteocalcin mRNA↑	LIPU had a direct effect on bone formation.	(Warden et al., 2001)
	NO↑, PGE2↑	LIPU stimulated the production of NO and PGE_2, which were proved mediators in mechanically induced bone formation.	(Reher et al., 2002) (Li et al., 2002)

osteoblast	Cbfal/Runx2 mRNA ↑, osteocalcin mRNA↑, PTX-sensitive Galphai protein↑, ERK↑,	LIPUS activated membrane-bound Gαi protein and cytosolic ERK, which were involved in regulating US-promoted osteogenic transcription.	(Chen et al., 2003)
chondrocyte	aggrecan mRNA↑, proteoglycan synthesis↑	LIPU stimulated synthesis of extracellular matrix proteins in cartilage altering chondrocyte maturation and endochondral bone formation.	(Parvizi et al., 1999)
	Intracellular calcium↑ proteoglycan synthesis↑		(Parvizi et al., 2002)
	Chondrocyte proliferation	LIPU increased proliferation of chondrocytes.	(Zhang et al., 2003)
Endothelial	PDGF↑	LIPU stimulated growth factor secretion from endothelial cells.	(Ito et al., 2000)

2.4 Peripheral innervation involvement in ectopic ossification

The peripheral nervous system is made up of the sensory receptors, the nerves that link the sensory receptors with the central nervous system and the nerves that link the central nervous system with the effectors-the muscles and glands. The portion of the peripheral nervous system that keeps the body adjusted with the outside world is the somatic division. The nerves and receptors that maintain internal balance make up the autonomic division (Solomon, 2003).

2.4.1 Innervation of CGRP-positive nerve fibers in bone tissue

Previous studies have confirmed that CGRP-positive nerve fibers are widely distributed in bone tissue. They were found in the periosteum and bone marrow. In periosteum, a loose network of straight and varicose CGRP-positive nerve fibers was demonstrated (Irie et al., 2002).Moreover, different innervation pattern was found between the membranous bone and the long bones in the periosteum. In calvaria and mandible, CGRP-positive nerve fibers of varying caliber formed complex networks, with trunks followed by vascular elements. In tibia, the CGRP-positive nerve fibers followed a course parallel to the long axis of the bone, which were present around the nutrient artery. More CGRP-positive nerve fibers were observed at the epiphysis than in the diaphysis (Hill and Elde, 1991). In the bone marrow, CGRP-positive nerve fibers were richer in the

epiphysis region than in the cortical diaphysis. A dense CGRP-positive nerve fiber innervation was found in the epiphysis side of growth plate (Bjurholm et al., 1988; Bjurholm et al., 1989; Bjurholm, 1991; Hukkanen et al., 1992b; Hukkanen et al., 1992a; Hara-Irie et al., 1996), whereas subchondral regions facing the knee joint were less densely innervated(Imai et al., 1997a). CGRP-positive nerve fibers in the epiphysis and diaphysis were often associated with blood vessels.

2.4.2 Involvement of CGRP-positive nerve fibers in bone healing

Experimental studies suggest the involvement of CGRP-positive nerve fibers in bone healing. Hukkanen observed that CGRP-positive nerve fibers rapidly proliferated after initial degeneration distal to and in the vicinity of the fracture gap. The proliferation period of CGRP-positive nerve fiber coincided with callus formation and bone remodeling. This suggests that CGRP-positive nerve fiber has an active participation of the in the process of bone repair and remodeling (Hukkanen et al., 1993). Madsen demonstrated that femoral and sciatic nerve resection resulted in decreased stiffness and mineralization of the fracture callus (Madsen et al., 1998). Moreover, the peripheral innervation was found to be decreased or absent in delayed union or non-union of fractures (Aro et al., 1985; Santavirta et al., 1992).

CGRP-positive nerve fibers also appeared in the repair process of experimental bone defect. The CGRP-positive nerve fibers were located mainly in the dense fibrous tissue in close proximity to the new bone, and in some cases within the new forming bone. Moreover, the increase of CGRP-positive nerve fibers became evident in the later phases of bone repair and remodeling (Aoki et al., 1994; Madsen et al., 2000). Additionally, CGRP-positive nerve fibers degenerated in the infiltration of adjuvant-induced arthritics and reinnervated the postarthritic ossifying periosteum (Imai et al., 1997b).

2.4.3 The invasion of CGRP-positive nerve fibers in ectopic ossification

A previous study reported that when ectopic ossification was induced through the implantation of demineralized bone matrix in muscles, CGRP-positive nerve fibers appeared very early. One week after implantation, some weak CGRP-positive nerve fibers could be seen in the fibrous tissue surrounding the implant. The number and the intensity of CGRP-positive nerve fibers increased markedly in the following week. At two weeks, there were abundant, intense CGRP-positive nerve fibers in the fibrous tissue. In the marrow of ectopic bone, CGRP-positive nerve fibers were also observed, and its number increased until six weeks after implantation (Bjurholm et al., 1990). These observations suggest the involvement of CGRP-positive nerve fibers in the early

development of the bone. However, the answer as to which cells are responding and through what mechanisms is still unclear.

2.4.4 CGRP and bone cells

CGRP is a 37 amino acid peptide produced by tissue specific alternative processing of the primary RNA transcripts of the calcitonin gene. Two isoforms of CGRP, CGRP-1 and CGRP-2, differ only in three amino acids in humans and one amino acid in rats. CGRP-2 is produced by a separate gene thought to have arisen as a result of the exon duplication (Zaidi et al., 1987a).

CGRP secreted by the sensory nerve fibers has been shown to stimulate osteogenesis. A number of studies have found direct effects of CGRP on the osteoblasts through a CGRP receptor. CGRP have been shown to regulate cellular and autocrine activities of osteoblasts. An increase of cyclic adenosine monophosphate (cAMP) by CGRP has been demonstrated both in primary chicken, mouse, rat, and human osteoblasts (Crawford et al., 1986; Michelangeli et al., 1989), as well as cultured osteosarcoma cell lines(Bjurholm et al., 1992). Kawase (Kawase et al., 1995)demonstrated the effect of CGRP on intracellular calcium concentration in, as well as potassium efflux from, osteoblasts (Kawase and Burns, 1998). On the other hand, CGRP increased the production of insulin-like growth factor 1 (IGF-1)(Vignery and McCarthy,

1996), interleukin-6 (IL-6) (Sakagami et al., 1993) and reduced the production of tumor necrosis factor α (TNF-α) (Millet and Vignery, 1997). Moreover, CGRP has also been shown to stimulate osteogenesis either by activating stem cell mitosis or osteoprogenitor cell differentiation, or both (Shih and Bernard, 1997).

Since CGRP has a common origin and sequence homology with calcitonin, attention also focused on its effect on bone resorption. CGRP has been shown to inhibit osteoclastic resorption *in vitro* (D'Souza et al., 1986; Yamamoto et al., 1986; Zaidi et al., 1987b; Zaidi et al., 1987c). The action of CGRP on osteoclasts seems, in part, to involve inhibition of cell motility of calcitonin that is mediated by intracellular cAMP (Alam et al., 1991). CGRR also has an effect on osteoclast precursors via inhibition of differentiation and recruitment (Akopian et al., 2000).

The effect of CGRP on bone cells is mediated via $CGRP_1$ and $CGRP_2$ receptors. It has been shown that CGRP receptors activate the cAMP or the protein kinase C (PKC) pathways. These two transduction pathways required guanosine triphosphate (GTP)-binding proteins (G proteins) and led to the opposite biological response. Moreover, selective activation of one or the other pathway was cell cycle-dependent (Garcia-Castellano et al., 2000).

2.4.5 Relationship of neural involvement with ultrasound treatment

Evidence showed that ultrasound at low intensity promotes peripheral nerve regeneration. Hong et al (Hong et al., 1988) showed the application of low dose ultrasound for one minute in three days per week over one month enhanced the recovery of normal nerve conduction velocity after partial crush injury to the tibia nerve of rats. A further study confirmed that ultrasound can accelerate functional recovery after peripheral nerve damage. Mourad et al (Mourad et al., 2001) discovered that rats subjected to the ultrasound treatment showed a statistically significant acceleration of foot function recovery starting 14 days after injury versus 18 days for the control group. Full recovery of the ultrasound group occurred before full recovery of the control group. In 2002, Crisci and Ferreira suggested that the use of LIPU prompted a fast recuperation of the nerve after its neurotomy. In their study, they evaluated the effect of LIPU on the axotomy of the sciatic nerve in rats. After neurotomy, the proximal stump of the nerve was stimulated for 12 consecutive days with LIPU for the treatment group. Based on the morphological and morphometric analysis, they found that LIPU treatment led to a rapid regeneration of the nerve after axotomisation (Crisci and Ferreira, 2002).

2.5 Summary of literature review

The literature review reveals that LIPU can effectively enhance bone healing in bone repair. However, many areas on the effect of LIPU on bone healing still lack research. Moreover, the precise cellular mechanisms underlying the effect of LIPU remain unclear. How this mechanical stimulation is “sensed” by the healing tissue and delivers its therapeutic effect is not clearly understood.

It is necessary to carry out a study to fill in the missing areas in the research on the LIPU as a treatment for bone healing. It is important for researchers to explain how LIPU could promote the bone healing process and to know the underlying mechanisms behind it. These findings would be clinically significant as they could help us to determine the possibility of using LIPU as a form of treatment option or as a supplement to conservative/surgical treatment during the rehabilitation of patients with orthopedic injuries.

2.6 Hypothesis

It is hypothesized that LIPU may enhance rhBMP-4 induced ectopic ossification. It is also hypothesized that LIPU may improve the in-growth of CGRP-positive nerve fibers into the ectopic bone forming tissues.

2.7 Aims of thesis

This thesis aims to investigate the effect of LIPU on rhBMP-4 induced ectopic ossification and the relationship between the sensory nerve fibers and ectopic ossification and the response of the sensory nerve fibers to ultrasound stimulation during ectopic ossification.

With regards to the objective of this study, the coming chapters of this thesis present a detailed study. Chapter 3 lists the methodology used in this thesis. It explains how to establish the animal model, how to evaluate the osteogenesis induced by rhBMP-4, and how to detect the sensory nerve fibers in bone healing tissues. Chapter 4 demonstrates the results of the study. Chapter 5 illustrates the effect of LIPU on rhBMP-4 induced ectopic ossification and the relationship between the LIPU treatment and the innervation of the sensory nerve fibers in healing tissues. Chapter 6 summarizes the findings and leads to the conclusions of the present study.

Chapter 3

Materials and methodology

3.1 Animals

60 New Zealand white rabbits 30 weeks of age (around 4.5kg) were used as the experimental animals for this study. All animals were kept in the Centralized Animal Faculty of Hong Kong Polytechnic University at constant temperature (22℃) and on a regular 12-hour light/dark cycle. The surgical procedures and post-operation treatment were approved by the Ethics Committee of the Hong Kong Polytechnic University, and a license to conduct animal experiments was issued by the Department of Health of Hong Kong.

3.2 Experimental design

Each rabbit underwent a single level non-decorticated bilateral posterolateral intertransverse process fusion at L5–L6 through the implantation of porous polymer incorporated with rhBMP-4. LIPU treatment was applied unilaterally on the skin over the implantation site daily, starting at day 2 after operation. Rabbits were randomly allocated into 10 groups according to application of different dose of rhBMP-4 (low dose and high dose) and different treatment duration of LIPU (3 days, 1 week, 3 weeks, 7 weeks and 12 weeks), as illustrated in Table 3.1.

Animals were sacrificed after the LIPU treatment was completed. The process of new bone formation at the implantation site was assessed through radiography, peripheral quantitative computed tomography (pQCT) and histological methods. The innervation of CGRP expressing sensory nerves in the area of the new bone formation was detected with the use of the immunofluorescent staining method.

Table 3.1 Experimental group design

Groups	LIPU			No. of animals
	sham side	treated side	duration	
Low dose groups (PDLLA+1.25μg rhBMP-4 in PBS)	L	R	3 days	6
	L	R	1 week	6
	L	R	3weeks	6
	L	R	7 weeks	6
	L	R	12 weeks	6
High dose groups (PDLLA+5μg rhBMP-4 in PBS)	L	R	3 days	6
	L	R	1 week	6
	L	R	3weeks	6
	L	R	7 weeks	6
	L	R	12 weeks	6

3.3 Non-decorticated spinal fusion model

3.3.1 Preparation of graft

Porous poly (d,l-lactic acid) PDLLA blocks (2.3 x 1.1 x 0.8 cm^3) with a porosity of 85%, and pore size of 50–200 μm were supplied by Southwest Jiaotong University, China. At room temperature and 40 min before the implantation procedure, rhBMP-4 (R&D System Inc, USA) was diluted in PBS solution to achieve the final concentration of 3.125 μg/ml (solution 1) and 12.5 μg/ml (solution 2).The PDLLA blocks were loaded with 0.4 ml solution 1 (1.25 μg rhBMP-4) or 0.4 ml solution 2 (5 μg rhBMP-4) accordingly.

3.3.2 Operation procedure and surgical implantation

Operation was done under clean conditions. Rabbits were put under anesthesia using an intramuscular injection of ketamine-hydrochloride (10 mg/kg, Alfasan, Holland) combined with xylazine (3 mg/kg, Alfasan, Holland). The anesthesia was maintained through continuous slow infusion of pentobarbital solution (2.5% Sigma, Chemicals Co., St Louis Mo, USA) through the marginal ear vein (Figure 3.1 A). The shaved dorsal skins were washed with 70% ethanol. A midline longitudinal posterior approach was used (Figure 3.1 B). On both sides of the lumbar spine, the transverse processes of L5–L6 and the adjacent lateral surface of the facet joints were exposed subperiosteally with fine

periosteal elevator, and the interfacets and intertransverse processes tissues were cleaned down to the intertransverse ligament (Figure 3.1 C). A PDLLA block incorporated with rhBMP-4 was placed on the surfaces of the transverse processes of both left and right side L5-L6 (Figure 3.1 D). The dorsal muscles were sewn tight to the contralateral muscles with absorbable sutures to fix the implant in place (Figure 3.1 E). The skin was sutured with non-absorbable sutures(Figure 3.1 F).

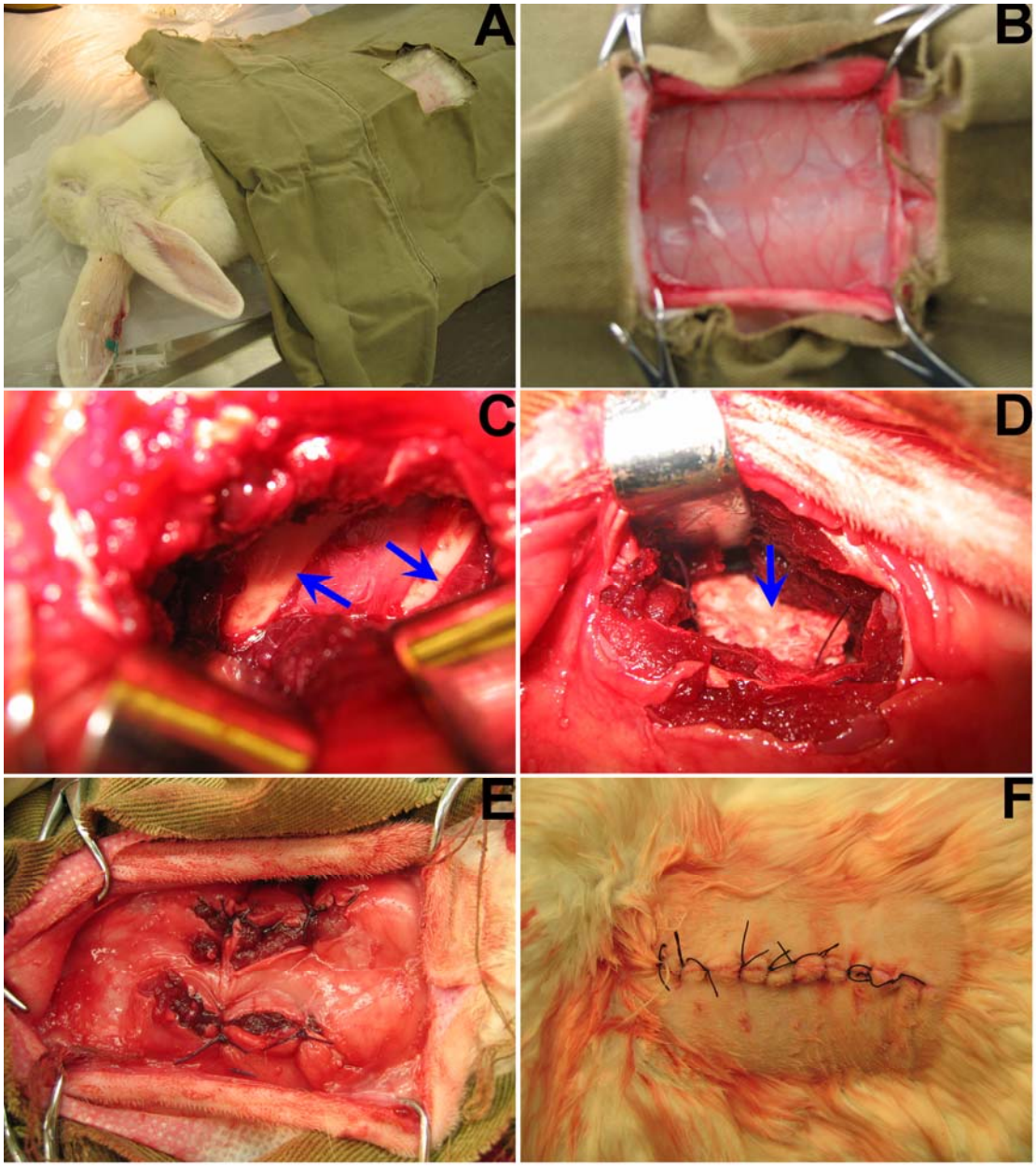

Figure 3.1 Operation procedures and surgical implantation. Arrows in C indicated the transverse processes and arrows in D indicated the PDLLA graft.

3.4 LIPU treatment

A LIPU machine (SAFHS, Exogen, Inc, West Calwell, NJ, USA) was used for this study. LIPU treatment was conducted under sedation of rabbit with ketamine/xylazine (i.m.). LIPU was delivered via a 2.5 cm diameter ultrasound transducer, which was placed lateral to the midline, directly over the implantation site and against the dorsal surface skin with the use of ultrasound coupling gel (Figure 3.2.). The ultrasound signal consisted of a 200us burst of 1.5 MHz sine wave repeating at 1.0 kHz and delivering 30.0 ± 5.0 mW/cm SATA (Table 3.2). The relatively low soft tissue attenuation of the ultrasound signal with a carrier frequency of 1.5 MHz allowed a significant portion of the signal to reach the desired fusion site(Glazer et al., 1998; Cook et al., 2001).The fusion site received a LIPU or sham exposure daily for 20-minutes. Application of LIPU/sham treatment started on the second day after the operation.

Figure 3.2 LIPU treatment applied to the rabbit.

Table 3.2 Ultrasound characteristics of LIPU

Frequency:	1.5 MHz	Off period:	800 µs
Wave shape:	Sine wave	Repetition rate:	1 kHz
Signal type:	Pulsed	Intensity:	30 mW/cm^2
Length of signal:	200 µs		

3.5 Postoperative assessment

3.5.1 Plain Radiography

Using Toshiba KXO-30R General Diagnostic X-ray machine (Japan), the anterior-posterior radiographs of the operated site were taken directly at 3 days, 1, 3 and 7 weeks postoperatively under general anesthesia and after animal sacrifice for 12 weeks groups. The whole rabbit anterior-posterior radiography was taken with the setting of 70 Kvp, 200 mA for 0.625 sec. For spinal samples obtained after animal sacrifice, radiography was taken at 60 Kvp, 80 mA for 0.25 sec. The change of bony status induced by implantation was observed.

3.5.2 pQCT measurement

After the lumbar vertebrae (L5-L6) were dissected en bloc out, the samples were fixed with 4% formaldehyde (Sigma, St Louis Mo, USA) for 24 hours and immersed in 70% ethanol. The bone mineral density (BMD) and bone area(BA) of composite graft, recipient transverse processes and their interface were determined for samples in all groups using a high resolution and multi-slice peripheral quantitative computed tomography (XCT 2000, Norland Stratec, Germany) (Figure 3.3). The high resolution of tomography was 0.2 mm. The calibrations were done using standard phantom daily and cone phantom at a 25-day interval. The precision error of the pQCT operation to measure the total

density of the bone (including repositioning of the specimens and independent analyses) was 0.38% (Lam, 2005).

The sample was positioned horizontally at the center of the scanning aperture on a wood support. The transverse images of specimens were then scanned at 2 mm interval and the scanning diameter of 140 mm. The reference line was set in the middle of the vertebral body, and five consecutive sections (totally 10mm thickness) were measured in both sides of the spine (Figure 3.4 and Figure 3.5), covering the whole graft, served for analysis of total BMD (cortical bone and trabecular bone), total bone volume, and total bone mineral content (BMC).

Figure 3.3 The pQCT equipment.

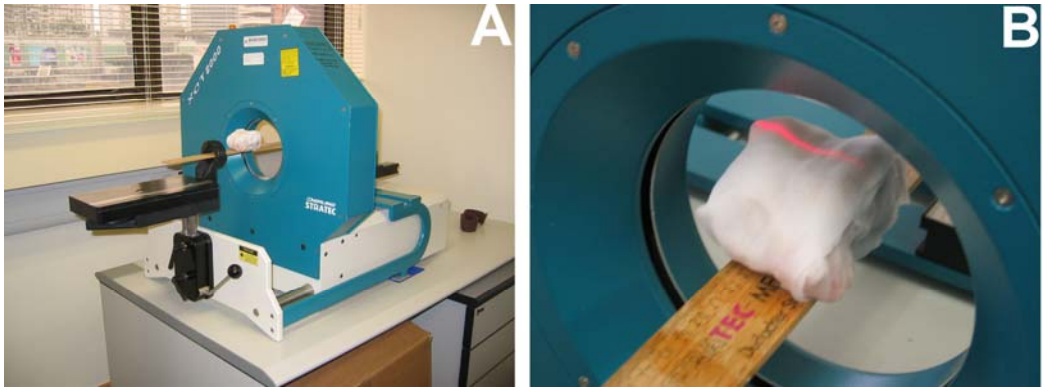

Figure 3.4 Evaluation of the samples on the pQCT equipment.

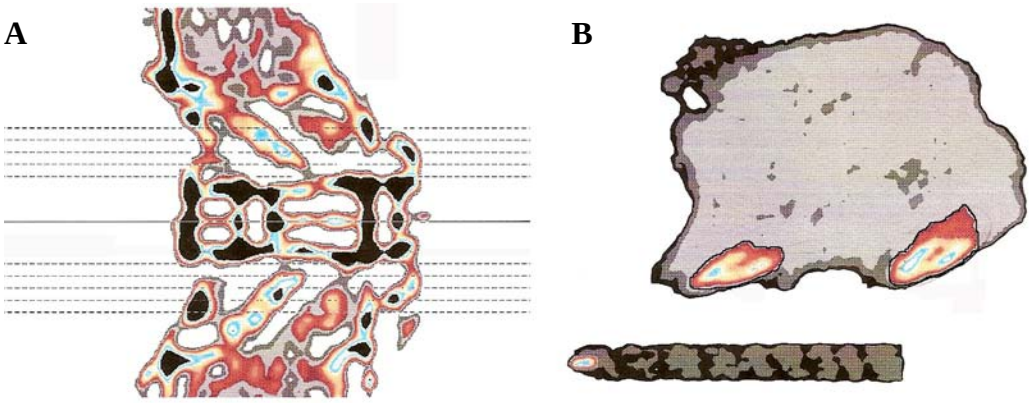

Figure 3.5 Scan images of the sample. A, showed the position of reference line (the middle one in the image) and measure lines (the other lines) B, showed one slice obtained by scanning.

3.5.3 Histology

3.5.3.1 Histology of decalcified bone specimen

The samples were decalcified with 10% ethylenediaminetetraacetic acid (EDTA) (Sigma, St Louis Mo, USA) for 3-4 weeks. After dehydration with 30% sucrose (Sigma, St Louis Mo, USA), all samples were embedded in Optimal Cutting Temperature (OCT) compound (Thermo Electron Corporation, USA) and cut sagittally into serial sections in a thickness of 12 µm using a freezing microtome (Model CM1900, Leica Instruments). Total thickness of 10 mm was included according to the dimension of PDLLA graft (Figure 3.6).

Sections were selected to constitute a section pool for each side of the animal with the following criterion: higher proportion of new bone formation area in tissue section.

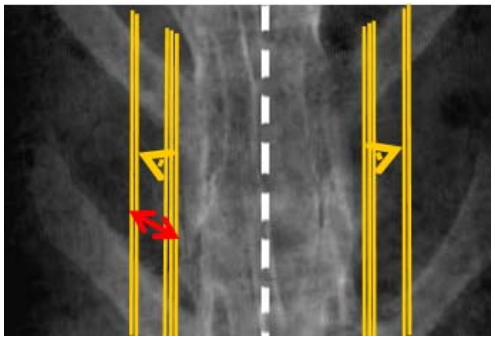

Figure 3.6 Diagram of vertebral body and transverse process; Serial sections were cut sagittally.

3.5.3.2 Haematoxylin & Eosin (HE) and saffranin O/ fast green staining.

Six sections from each section pool were selected randomly to stain with Haematoxylin (Sigma, St Louis Mo, USA)/ Eosin (Sigma, St Louis Mo, USA), and another six sections were stained with saffranin O (Sigma, St Louis Mo, USA) / fast green (Sigma, St Louis Mo, USA). The process of HE staining was used to show the general histology. With the saffranin O/ fast green staining, the proteoglycan rich cartilaginous tissue was stained with red coloration of saffranin O. The staining protocols are illustrated in Table 3.3 and Table 3.4.

Table 3.3 HE staining protocol

Rehydration	70% Ethanol	2mins
Haematoxylin staining	Harris' Haematoxylin	12mins
	distilled water	1min
	Acid alcohol	1min
	distilled water	1min
	Scotts tap water	3mins
	distilled water	2mins
Eosin staining	Eosin Y	5mins
Dehydration	70% Ethanol	10 sec
	80% Ethanol	10 sec
	90% Ethanol	10 sec
	100% Ethanol I	3mins
	100% Ethanol II	5mins
Mount the slide with DPX		

Table 3.4 Saffranin O/ fast green staining protocol

Rehydration	70% Ethanol	2mins
Fast Green staining	0.1%Fast Green	1min
	1% Acetic acid	1min
Saffranin O staining	0.1% Saffranin O	6mins
		2mins
Dehydration	70% Ethanol	10 sec
	80% Ethanol	10 sec
	90% Ethanol	10 sec
	100% Ethanol I	3mins
	100% Ethanol II	5mins
Mount the slide with DPX		

3.5.3.3 Histomorphometry

The percentage of the fusion area occupied by the bone, cartilage or fibrous tissue was calculated. All HE and saffranin O/fast green stained sections were digitized and analyzed using the software analysis® version 3.2 (Soft Imaging System GmbH, Germany). A rectangle grid centered in the intertransverse fusion area defined the analyzed area. The transverse processes defined the cephalocaudal dimension of the grid, and the dorsovental dimension is demarcated under the 4X objective of the microscope, equal to the size of the view field with the ventral margin of the transverse processes defining the ventral border (Figure 3.7). The newly formed bone, not including the original bone of the upper and the down transverse processes, was defined as the new bone tissue. Cartilage tissue was stained using saffranin O and proteoglycan rich cartilaginous tissue stained in red color was found clearly in saffranin O/fast green sections. The remaining area was summarized as fibrous tissue.

Figure 3.7 Grid area calculated in each section (saffranin O/fast green staining).

3.5.3.4 Immunofluorescent staining for localization and quantification of CGRP expressing nerve fibers.

3.5.3.4.1 Immunofluorescent staining protocol

The sections were washed in PBS to remove traces of fixatives. After incubation in normal bovine serum for 2 hours at room temperature to block non-specific binding of antibodies, the sections were incubated with the goat polyclonal CGRP primary antibody (Santa Cruz, USA; diluted 1:50) for 24 hours at 4 ℃. Following rinse in PBS, fluorescein isothiocynate (FITC)-conjugated bovine anti-goat secondary antibody (Santa Cruz, USA; diluted 1:100) was applied for 1 hour at 37 ℃. After a final rinse, the sections were then co-stained with 40, 60-diamidino-2-phenylindole (DAPI) in UltraCruz™ mounting medium (Santa Cruz, USA). All sections were examined under a Nikon eclipse 80i fluorescence microscope (Nikon, Japan) equipped with a mercury lamp and filter system. The excitation filter of this system is a band pass filter in the range of 330-380 nm and 450–490 nm, which could be applied to detect the fluorescent stains of DAPI and FITC separately.

3.5.3.4.2 Quantification of CGRP expressing nerve fibers.

The bone formation area was divided into three regions (fibrous tissue, new cartilage and bone tissue, and bone marrow of new bone) based on

morphological properties（Fig 3.8 A）. Owing to the dispersed distribution of the CGRP-positive nerve clusters along the relatively large area of the sections, the weighted length density (length of nerve per unit of area, wLa) was estimated to do the quantification of the CGRP immunohistological results. First, the CGRP-positive nerve clusters in the section were rated with numbers according to the relative density of clusters by estimation. Then, one to several representative sample regions (of middle rating numbers) were selected in order to calculate the length density, by dividing the total length of all CGRP-positive nerves by the sample area of the investigated tissue type (La) within a sample region. Each sample region was circumscribed with a rectangle that has a constant area of 0.5373 mm^2 along the orientation of the nerves (Figure 3.8 B and C). The exact number of the sample regions depends on the number of CGRP-positive nerve clusters per section, for instance, one sample area is used given only one nerve cluster present on the section. Finally, the weighted length density (wLa) of a section was measured by multiplying La by the weight, that is, the total number of the CGRP-positive nerve clusters per unit of area of the investigated tissue type.

Six sections were selected by random systematic sampling from the section pool of each side of animals.

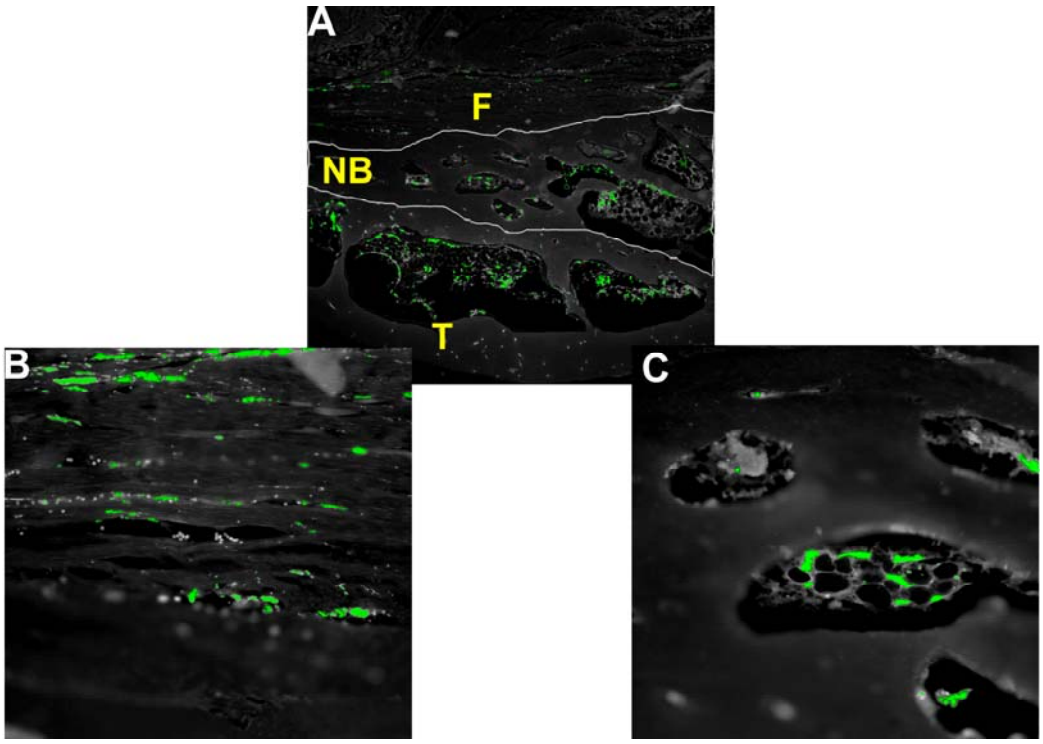

Figure 3.8 Quantification of the CGRP-positive nerve fiber. A showed an image of a section taken at the lowest magnification (40X);B showed one sample region for fibrous tissue from A (200X);C showed one sample region for bone marrow from A (200X). “NB”, new bone tissue; “F”, fibrous tissue; “T”, transverse process.

3.6 Statistical analysis

The statistical analyses were performed using SPSS. The outcome of pQCT was tested by paired t-test between the sham LIPU side and the LIPU treated side in all groups. The histomorphometric measurement was tested using paired t-test to determine the effect of LIPU, independent t-test to evaluate the effect of different dose of rhBMP-4 on enhancing new bone formation. The density of CGRP-positive nerve fibers was compared between the sham LIPU side and the LIPU treated side by using paired t-test. The density of CGRP-positive nerve fibers was also compared among different time points by using one-way ANOVA. Statistical significance was considered when $p<0.05$.

Chapter 4

Results

4.1. Plain Radiography

The anterior-posterior radiographs of the lumbar spine were taken at 3 days, 1, 3 and 7 weeks postoperatively and after animal sacrifice for week 12 group. The plain radiographs of different experimental groups at different time points are shown in Figure 4.1 to 4.2. The PDLLA blocks were not visible in the plain x-ray images for all the groups. Plain radiography showed visible new bone formation first at week 7 and this was located close to the transverse processes.

4.1.1 Low-dose rhBMP-4 groups (PDLLA +1.25μg rhBMP-4 in PBS)

On the sham LIPU side, a tiny new bone was found near the transverse process at week 7, and the new bone could be clearly observed at week 12 (Figure 4.1).

On the LIPU treated side, a little new bone was also observed at week 7, and its area increased as shown in the radiography taken at week 12**.** The gap between the transverse processes on the LIPU treated side was narrower than that on the side without LIPU treatment indicating more new bone formation on the LIPU treated side (Figure 4.1).

4.1.2 High-dose rhBMP-4 groups (PDLLA +5μg rhBMP-4 in PBS)

On the sham LIPU side, more new bone was formed close to the transverse process in high dose groups in comparison with the low dose groups at week 7 and week 12 (Figure 4.2).

On the LIPU treated side, it was also found that more new bone formed in the high-dose rhBMP-4 group when compared with the low dose group at week 7. An obviously large amount of new bone was observed at week 12 (Figure 4.2). Moreover, the gap of the transverse processes on the LIPU treated side was also obviously narrower when compared with the sham LIPU side at week 12 (Figure 4.2).

In summary, the results obtained from the observation of plain radiography indicated that 1) rhBMP-4 is able to induce new bone formation in this posterior intertransverse processes fusion model; 2) rhBMP-4 induced bone formation was in a positive dose-dependent manner on both LIPU and sham-LIPU sides; 3) LIPU could promote the bone formation induced by rhBMP4.

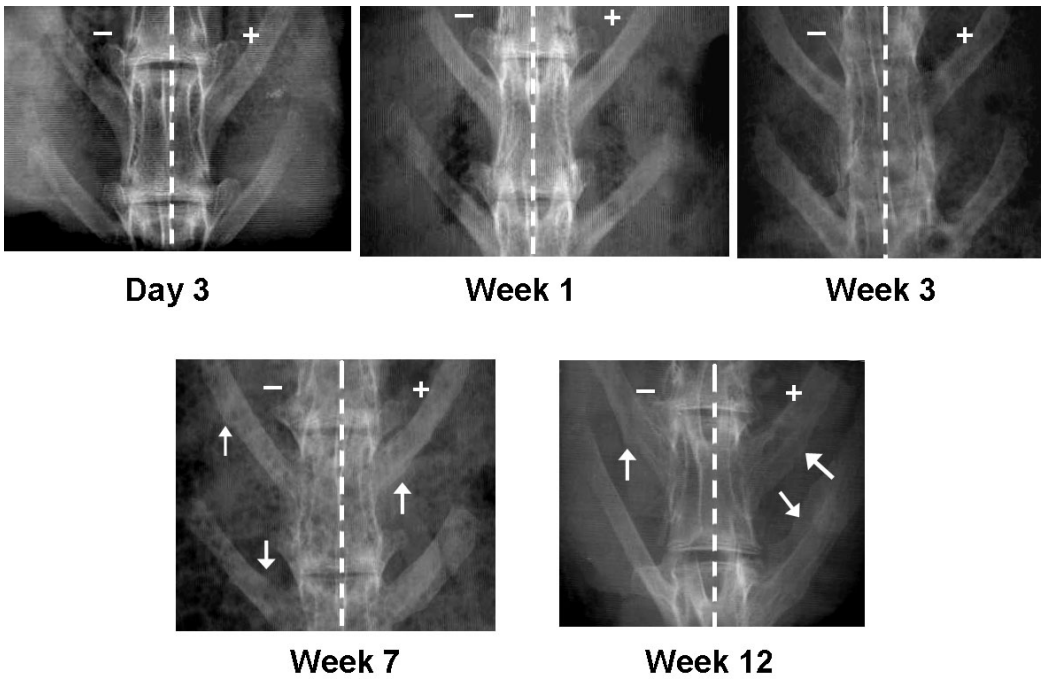

Figure 4.1 The plain x-ray image of low-dose rhBMP-4 groups. "+" showed the side with LIPU treatment, "-"showed the side without LIPU treatment. Arrows showed new bone.

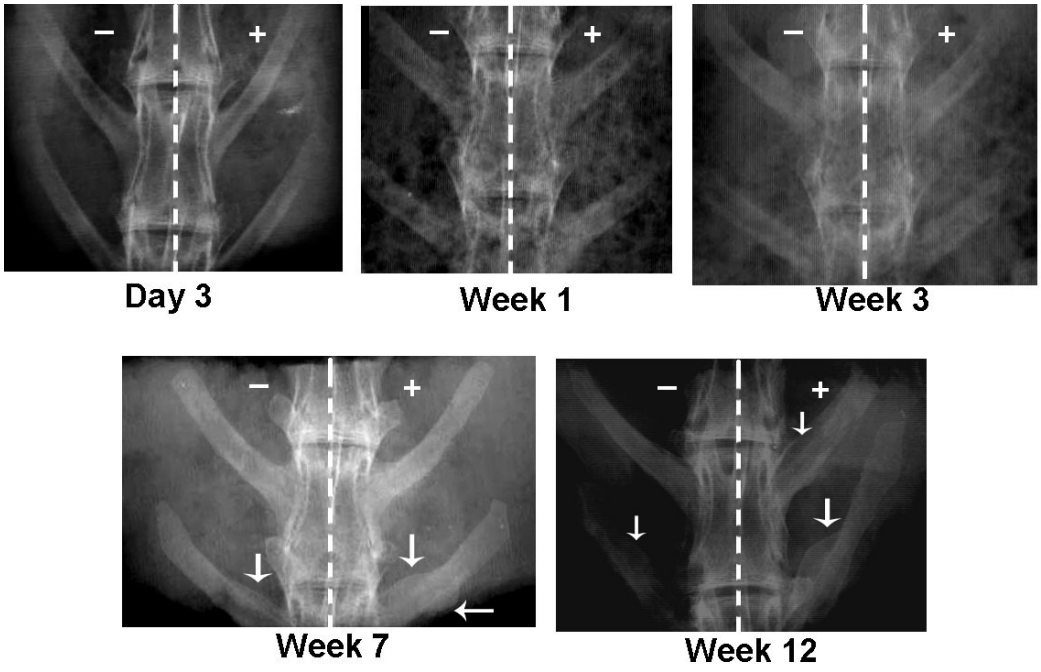

Figure 4.2 The plain x-ray image of high-dose rhBMP-4 groups. "+" showed the side with LIPU treatment, "-"showed the side without LIPU treatment. Arrows showed new bone.

4.2 The pQCT measurement

The total BMC, total bone volume and total BMD of composite graft, recipient transverse processes and their interface were measured by using pQCT. Results are summarized in Table 4.1 to 4.5.

4.2.1 Day 3, week 1 and week 3 postoperation

Tables 4.1 to 4.3 listed the results of pQCT at day 3, week 1 and week 3 postoperation respectively. The total BMC, total bone volume and total BMD were found to have no significant difference ($p>0.05$, paired t-test) in the LIPU treated side and the sham LIPU side in low-dose and high-dose rhBMP-4 groups at day 3, week 1 and week 3 postoperation.

The total BMC, total bone volume and total BMD on both LIPU treated and sham LIPU sides had no significant difference ($p>0.05$, t-test) in the low-dose and high-dose rhBMP-4 groups at day 3, week 1 and week 3 postoperation.

4.2.2 Week 7 postoperation

In all groups, both the total BMC and the total bone volume of the LIPU treated sides were significantly higher ($p<0.05$, paired t-test) compared to the sham LIPU side after 7 weeks postoperation, while the total BMD was significantly lower ($p<0.05$, paired t-test). This result indicated that LIPU

treatment resulted in a faster enlargement of bone volume than the increase of total BMC.

No significant differences in all pQCT measurements were found on either side between low-dose and high-dose rhBMP-4 groups at week 7 postoperation ($p>0.05$, t-test) (Table 4.4).

4.2.3 Week 12 postoperation

In low-dose and high dose rhBMP-4 groups, the total BMC on the LIPU treated side was significantly higher ($p<0.05$, paired t-test) than that on the sham LIPU side, and the total bone volume increased significantly ($p<0.05$, paired t-test) on the LIPU treated side when compared with that on the sham LIPU side. No significant difference was shown in total BMD between the LIPU treated side and the sham LIPU side ($p>0.05$ paired t-test).

Similarly, no significant differences of the total BMC, bone volume and total BMD were presented on either side between low-dose and high-dose rhBMP-4 groups at week 12 postoperation ($p>0.05$ t-test) (Table 4.5).

In summary, pQCT results showed that LIPU effectively enhanced rhBMP-4 induced ectopic ossification.

Table 4.1 pQCT results at day 3 postoperation

pQCT measurement	Low dose rhBMP-4 group		High dose rhBMP-4 group	
	Sham LIPU side	LIPU treated side	Sham LIPU side	LIPU treated side
total BMC(mg)	216.16 ±6.30	217.93± 10.53	231.48±24.24	239.13±14.23
total Volume(cm^3)	0.53±0.06	0.52±0.02	0.54±0.05	0.57±0.03
total BMD(mg/cm^3)	408.47±40.98	419.51±9.44	422.36±7.33	418.34±18.37

Data are shown as Mean±SD.

Table 4.2 pQCT results at week 1 postoperation

pQCT measurement	Low dose rhBMP-4 group		High dose rhBMP-4 group	
	Sham LIPU side	LIPU treated side	Sham LIPU side	LIPU treated side
total BMC(mg)	245.05 ±47.86	230.90± 70.99	242.92±38.81	242.52±30.89
total Volume(cm^3)	0.51±0.09	0.47±0.12	0.55±0.08	0.55±0.05
total BMD(mg/cm^3)	472.66±39.04	484.35±35.61	439.30±12.33	437.77±15.48

Data are shown as Mean±SD.

Table 4.3 pQCT results at week 3 postoperation

pQCT measurement	Low dose rhBMP-4 group		High dose rhBMP-4 group	
	Sham LIPU side	LIPU treated side	Sham LIPU side	LIPU treated side
total BMC(mg)	229.89±9.25	247.48±9.75	263.06±34.0	263.84±31.31
total Volume(cm^3)	0.55±0.05	0.61±0.02	0.66±0.04	0.63±0.04
total BMD(mg/cm^3)	419.22±29.36	401.9±8.57	401.25±71.46	415.63±54.55

Data are shown as Mean±SD.

Table 4.4 pQCT results at week 7 postoperation

pQCT measurement	Low dose rhBMP-4 group		High dose rhBMP-4 group	
	Sham LIPU side	LIPU treated side	Sham LIPU side	LIPU treated side
total BMC(mg)	231.77±30.01	285.18±56.99*	254.79±94.33	278.56±103.17*
total Volume(cm^3)	0.60±0.13	0.76±0.13*	0.62±0.20	0.71±0.17*
total BMD(mg/cm^3)	397.35±43.21	374.10±35.60*	411.39±50.05	386.12±55.60*

Data are shown as Mean±SD; *, $p<0.05$, by paired t-test between sham LIPU side and LIPU treated side.

Table 4.5 pQCT results at week 12 postoperation

pQCT measurement	Low dose rhBMP-4 group		High dose rhBMP-4 group	
	Sham LIPU side	LIPU treated side	Sham LIPU side	LIPU treated side
total BMC(mg)	311.76±44.84	371.49±8.89*	286.15±26.99	339.36±71.21*
total Volume(cm^3)	0.81±0.17	0.88±0.10*	0.77±0.09	0.88±0.17*
total BMD(mg/cm^3)	420.13±38.28	434.35±48.80	365.87±26.66	369.96±53.98

Data are shown as Mean±SD; *, $p<0.05$, by paired t-test between sham LIPU side and LIPU treated side.

4.3 Light microscopy

4.3.1 Day 3 postoperation

There were abundant mesenchymal cells and fibroblasts surrounding the implant and contacting the transverse processes in all groups three days after implantation. No newly formed cartilage or bone tissue was observed at this stage (Figure 4.3).

4.3.2 Week 1 postoperation

At week 1, new cartilage and bone tissues were observed against the transverse process on both LIPU treated and sham LIPU sides in low-dose and high-dose rhBMP-4 groups (Figure 4.4). The bone forming tissue looked like islands encapsulated by fibrous tissues. There was no obvious difference in morphological structure of the LIPU treated side and the sham LIPU side. It seemed that the cartilage and bone were forming from different pathways concurrently at this stage, since chondrocytes aligned in multiple parallel columns in the new cartilage tissue (Figure 4.4 C, E) while new bone was formed directly through intramembranous ossification (Figure 4.4 B, D).

4.3.3 Week 3 postoperation

After implantation, the PDLLA block was progressively absorbed and replaced by fibrous tissue, cartilage, and new bone. At week 3, the new cartilage and bone tissues were formed along the ventral surface of the PDLLA block on bilateral sides of both low-dose and high-dose rhBMP-4 groups (Figure 4.5 A, C). Spaces inside the PDLLA block and at the dorsal side of PDLLA block in all groups were filled by fibrous tissue without the presence of cartilage or bone (Figure 4.5 A, B).

Percentage of the fusion area occupied by cartilage, bone or fibrous tissue for all groups at week 3 postoperation was calculated and is summarized in Table 4.6.

New cartilage tissue

There was significant higher percentage of cartilage occupied area ($p<0.05$ paired t-test) on the LIPU treated side compared to the sham LIPU side in low-dose and high-dose rhBMP-4 groups (Figure 4.6, 4.7). This suggests that LIPU treatment significantly enhanced cartilage formation. Moreover, there was significantly higher percentage of cartilage in high dose rhBMP-4 groups than in low dose rhBMP-4 groups ($p<0.01$ t-test) (Figure 4.6, 4.7). The results indicated

that the application of rhBMP-4 may stimulate and facilitate the formation of cartilage and this effect is dose-dependent.

New bone tissue

No significant difference in percentage of the new bone that occupied fusion area was found between low-dose rhBMP-4 and high-dose rhBMP-4 groups (P>0.05, t-test), as well as between LIPU treated and sham LIPU sides (P>0.05 paired t-test) at week 3.

Bone formation mode

At week 3, active endochondral ossification was observed. New cartilage tissues were distributed as islands in the fibrous tissue containing the spindle-shaped mesenchymal cells. New cartilage tissues comprised undifferentiated chondrocytes and hypertrophic chondrocytes (Figure 4.7, 4.8). On the LIPU treated sides of low-dose and high-dose rhBMP-4 groups, new cartilage tissues contained more undifferentiated chondrocytes (Figure 4.7, 4.8). Moreover, blood vessels were observed in the new cartilage tissues on the LIPU treated side of high-dose rhBMP-4 group (Figure 4.8 C D).

Active intramembranous ossification was also observed in all groups (Figure 4.9) at week 3 postoperation. New bone was formed directly by

osteoblast, which was differentiated from the mesenchymal cells in the fibrous tissue. The new bone tissue was trabecular form which originated from woven bone. The irregular medullary cavity contained bone marrow-like cells.

4.3.4 Week 7 postoperation

Biodegradation of PDLLA was not completed by the end of week 7 (Figure 4.10). At this stage, cartilage tissue was still observable on the LIPU treated side of low-dose and high-dose rhBMP-4 groups while no cartilage was found on the sham LIPU side of low-dose and high-dose rhBMP-4 groups.

New cartilage tissue

There was no cartilage on the sham LIPU treated side while there was still presence of cartilage on the LIPU treated side at week 7. Therefore, the percentage of cartilage was absolutely higher on the LIPU treated side than on the sham LIPU side, in both low-dose and high-dose rhBMP-4 groups ($p<0.05$, paired t-test, Table 4.7 Figure 4.11, 4.13). Moreover, more cartilage tissues were observed on high-dose rhBMP-4 group when compared with the low-dose rhBMP-4 group ($p<0.01$, t-test Figure 4.11, 4.13) on the LIPU treated side. These results indicated that LIPU treatment could prolong rhBMP-4 induced cartilage formation and the effect is also rhBMP-4 dose-dependent.

New bone tissue

The percentage of new bone was significantly higher on the LIPU treated side ($p<0.05$, paired t-test) or in the groups of high dose rhBMP-4 ($p<0.01$, t-test) (Table 4.7 Figure 4.12, 4.14). This suggests that LIPU treatment or the application of high-dose rhBMP-4 could enhance new bone formation.

Bone formation mode

At week 7, endochondral ossification was observed on the LIPU treated side of low-dose and high-dose rhBMP-4 groups. Intramembranous ossification was not found at week 7 postoperation on both sides of low-dose and high-dose rhBMP-4 groups. At this stage, few chondrocytes and osteoblasts remained at the sham LIPU side, suggesting that the osteogenetic activity almost ceased on the side without LIPU treatment at week 7 postoperation.

Woven bone became more mature, characterized by a well defined and highly organized lamellar cortical bone matrix and an enlarged medullary cavity on both sides of low-dose and high-dose rhBMP-4 groups.

4.3.5 Week 12 postoperation

At week 12 postoperation, the biodegradation of PDLLA was almost completed. Fusion area was fully occupied by new bone and fibrous tissue.

The percentage of new bone was significantly higher on the LIPU treated side ($p<0.01$, paired t-test) or in the groups of high dose rhBMP-4 ($p<0.01$, t-test) (Table 4.8, Figure 4.15, 4.16). Neither endochondral ossification nor intramembranous ossification was on-going in all groups, suggesting that osteogenetic activity had ceased at week 12 postoperation.

In summary, the light microscopy can deepen our understanding about the effect of LIPU on rhBMP-4 induced ectopic ossification from the following aspects: 1) New bone formation was observed via intramembranous ossification and endochondral ossification on the sham LIPU side of low-dose and high-dose rhBMP-4 groups (Table 4.11), indicating that application of rhBMP-4 could effectively induce ectopic ossification. Moreover, more new bone tissues were found in high dose rhBMP-4 groups than in low dose rhBMP-4 groups at week 7 and week 12 postoperation (Table 4.10), suggesting the apparent dose-dependent effect of rhBMP-4 on inducing and promoting ectopic ossification. 2) LIPU treatment effectively enhanced rhBMP-4 induced ectopic ossification. The pQCT results showed that BMC and bone volume were significantly higher in

the LIPU treated side than in the sham LIPU side at week 7 and week 12 postoperation in both low-dose and high-dose rh-BMP-4 groups. Histological results also showed that the percentage of new cartilage tissue was significantly higher on the LIPU treated side than on the sham LIPU side at week 3 and 7 postoperation (Table 4.9), suggesting that LIPU could enhance rhBMP-4 induced ectopic ossification by improving endochondral ossification.

Day 3

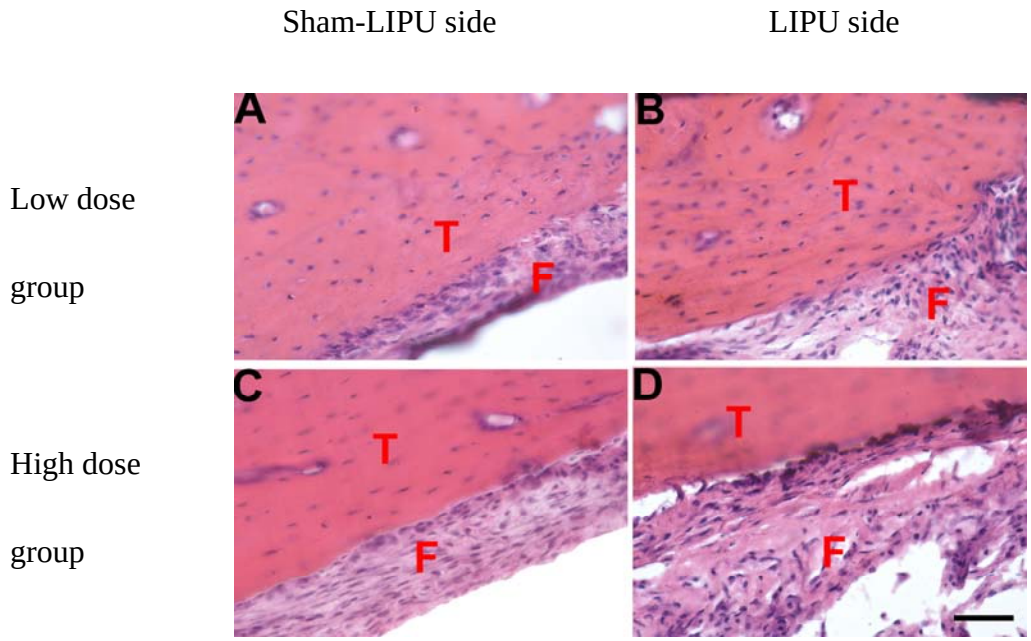

Figure 4.3 Fibrous tissues at day 3 postoperation (HE staining). A, B: low dose group; C, D: high dose group. “F”, fibrous tissue; “T”, transverse process; Scale bar is 50μm.

Week 1

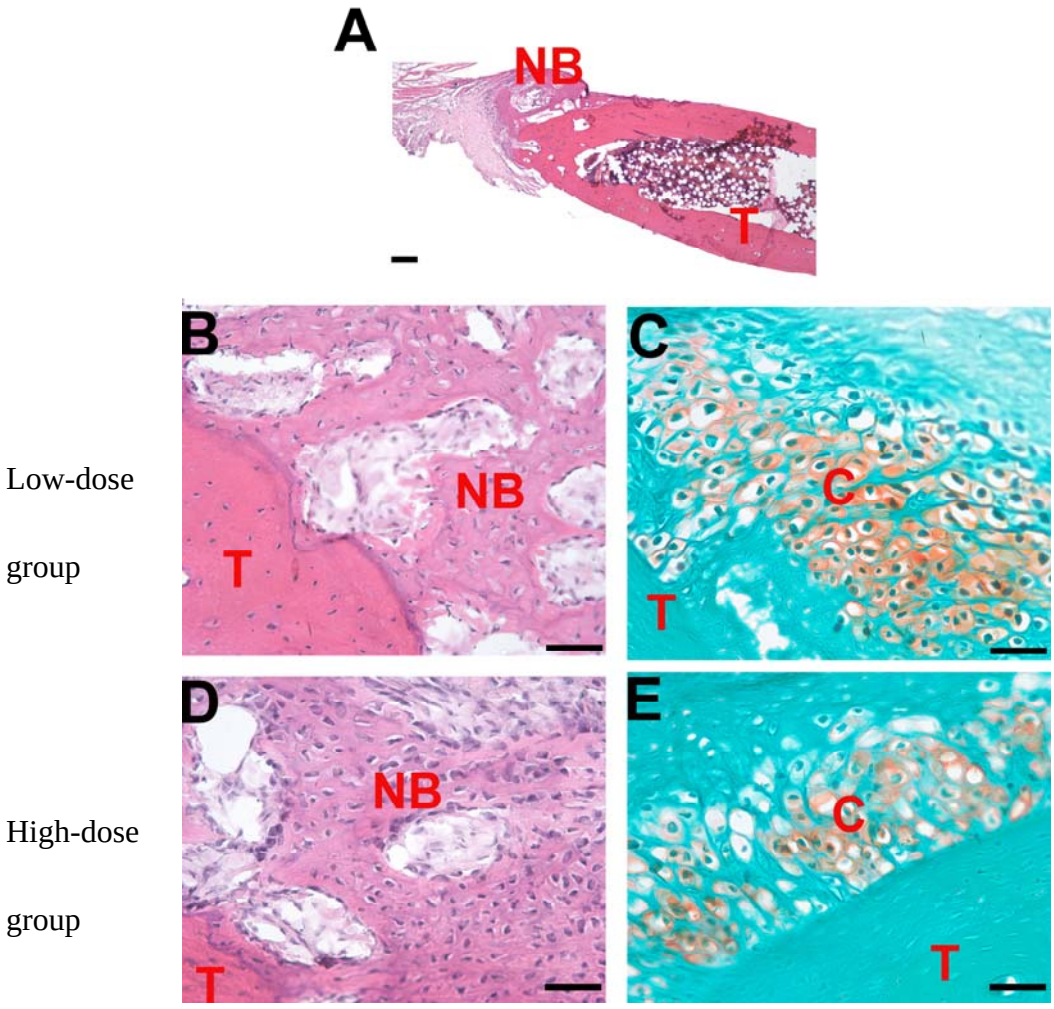

Figure 4.4 New cartilage and bone tissues at week 1 postoperation. BC showed low-dose rhBMP-4 group; DE showed high-dose rhBMP-4 group. BD, HE staining; CE, saffranin O/fast green staining; “NB”, new bone tissue; “C”, new cartilage tissue; “F”, fibrous tissue; “T”, transverse process; Scale bar is 100μm.

Week 3

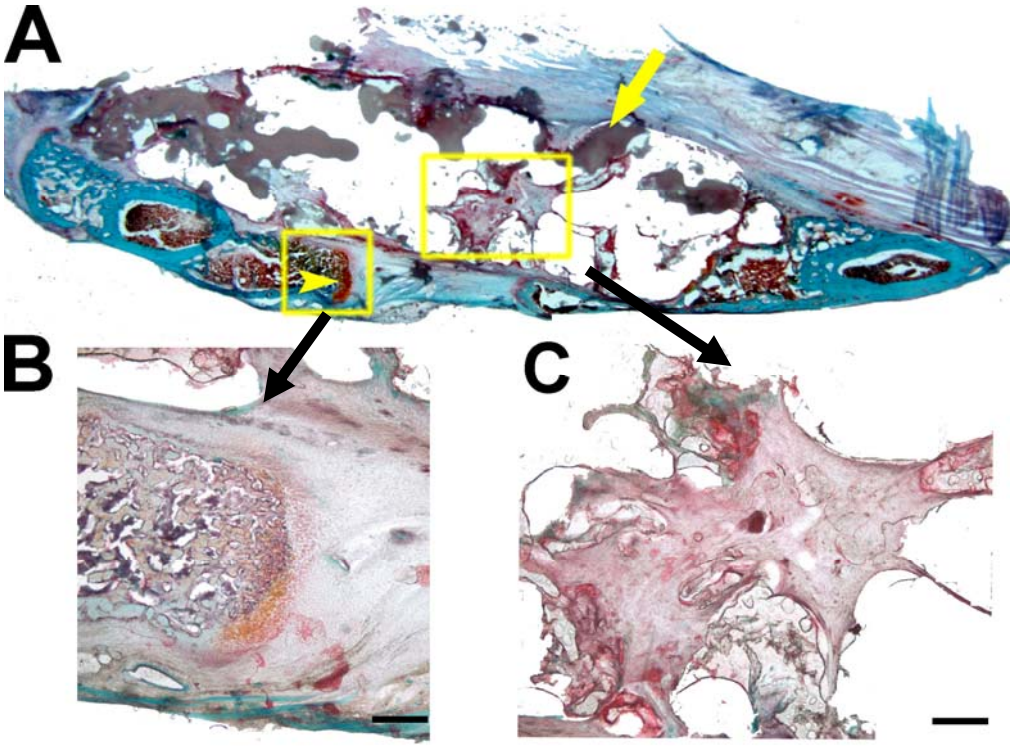

Figure 4.5 PDLLA block implantation at week 3 postoperation (saffranin O/fast green staining).Rectangular areas were illustrated in B and C, respectively. B showed the new cartilage and bone tissue; C showed fibrous tissue inside the PDLLA block. Arrow in A showed PDLLA; Scale bar is 200μm.

Table 4.6 Percentage of new bone, cartilage and fibrous tissue at week 3 postoperation

Tissue	Low dose rhBMP-4 group		High dose rhBMP-4 group	
	Sham LIPU side	LIPU treated side	Sham LIPU side	LIPU treated side
New Bone (%)	2.25±0.35	2.99±0.52	3.85±0.24	5.51±1.41
Cartilage (%)	0.39±0.05	0.71±0.29	0.48±0.16	3.06±0.65
Fibrous tissue (%)	97.75±0.15	97.01±0.53	96.15±0.24	94.49±1.40

Data are shown as Mean±SD.

Week 3, percentage of cartilage

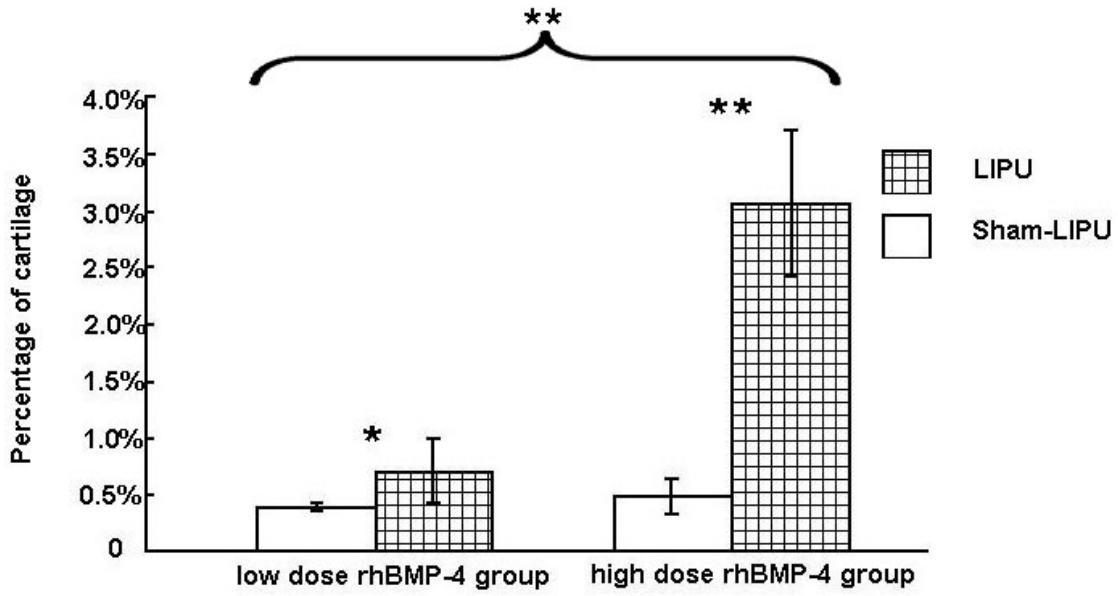

Figure 4.6 Percentage of cartilage at week 3 * $p<0.05$ ** $p<0.01$.

Week 3

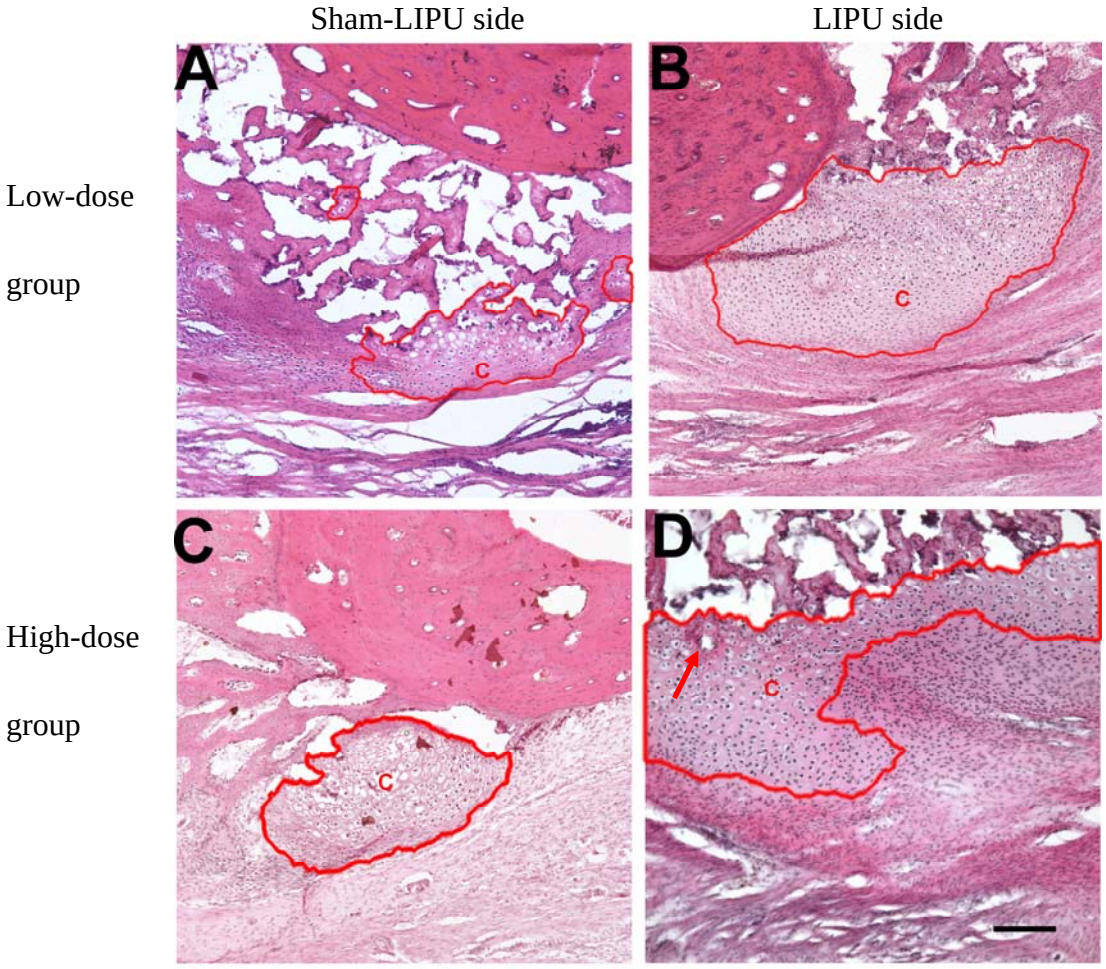

Figure 4.7 New cartilage tissues at week 3 postoperation (HE staining). A, B: low-dose rhBMP-4 group; C, D: high dose rhBMP-4 group. “C”, new cartilage tissue; Arrow showed blood vessel; Scale bar is 200μm.

Week 3

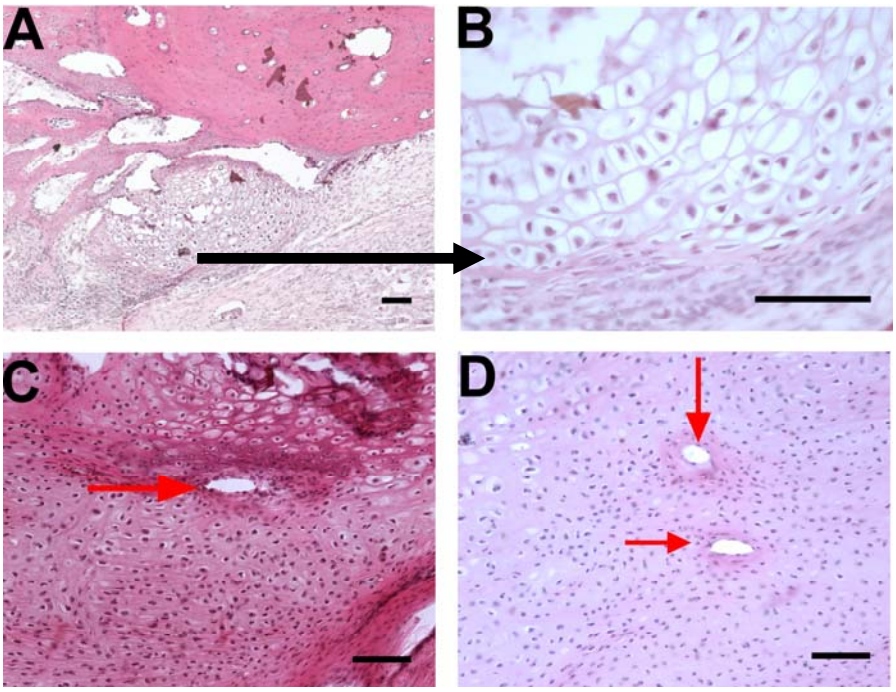

Figure 4.8 Endochondral ossification at week 3 postoperation in high dose rhBMP-4 groups (HE staining). A, B: showed sham LIPU side; C, D: showed LIPU treated side. Arrow in C D, showed blood vessels; Scale bar is 100μm.

Week 3

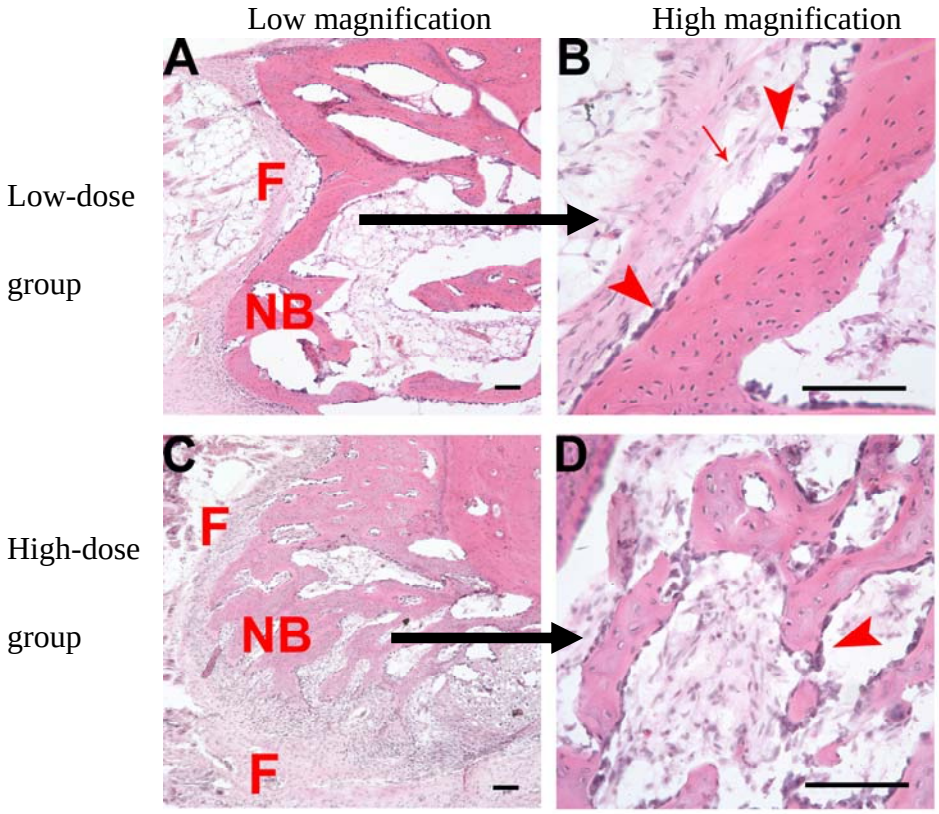

Figure 4.9 Intramembranous ossification at week 3 postoperation (HE staining). AB: low-dose rhBMP-4 group. CD: high-dose rhBMP-4 group. Arrow in B showed mesenchymal cell; Arrow head in B and D showed osteoblasts; “F” fibrous tissue; “NB” new bone tissue; Scale bar is 100μm.

Week 7

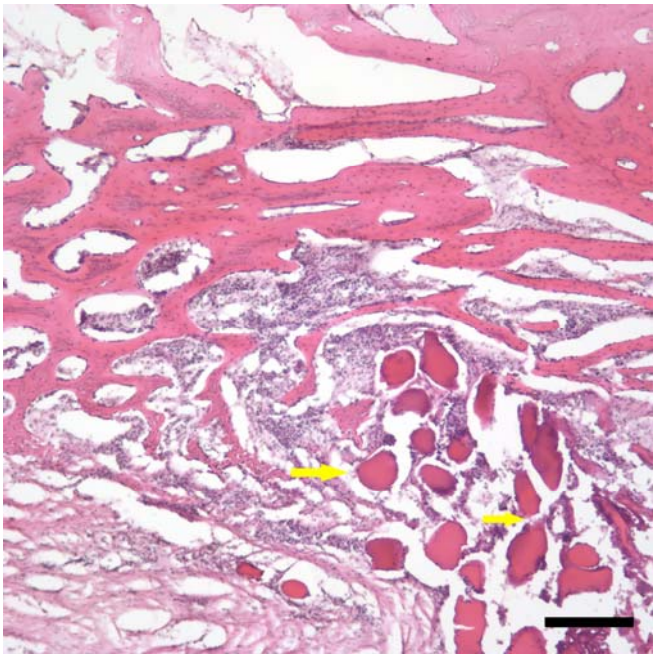

Figure 4.10 Residua of the PDLLA biodegradation at week 7 postoperation (HE staining). Arrows showed the residua; Scale bar is 200μm.

Table 4.7 Percentage of new bone, cartilage and fibrous tissue at week 7 postoperation

Tissue	Low dose rhBMP-4 group		High dose rhBMP-4 group	
	Sham LIPU side	LIPU treated side	Sham LIPU side	LIPU treated side
New Bone (%)	4.98±0.41	5.43±0.30	16.50±0.73	23.85±1.50
Cartilage (%)	0	0.09±0.02	0	0.7±0.06
Fibrous tissue (%)	95.02±0.41	94.48±0.28	83.50±0.73	75.46±1.44

Data are shown as Mean±SD.

Week 7, percentage of cartilage

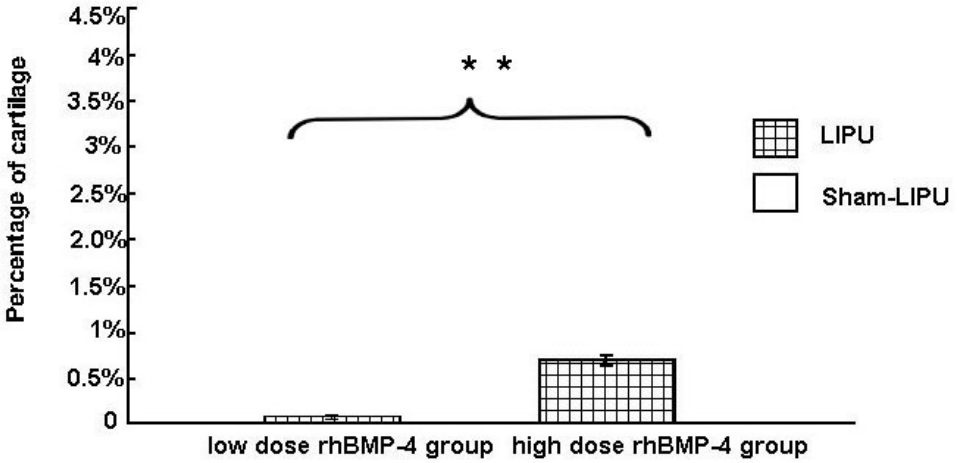

Figure 4.11 Percentage of cartilage at week 7 * * p<0.01.

Week 7, percentage of bone

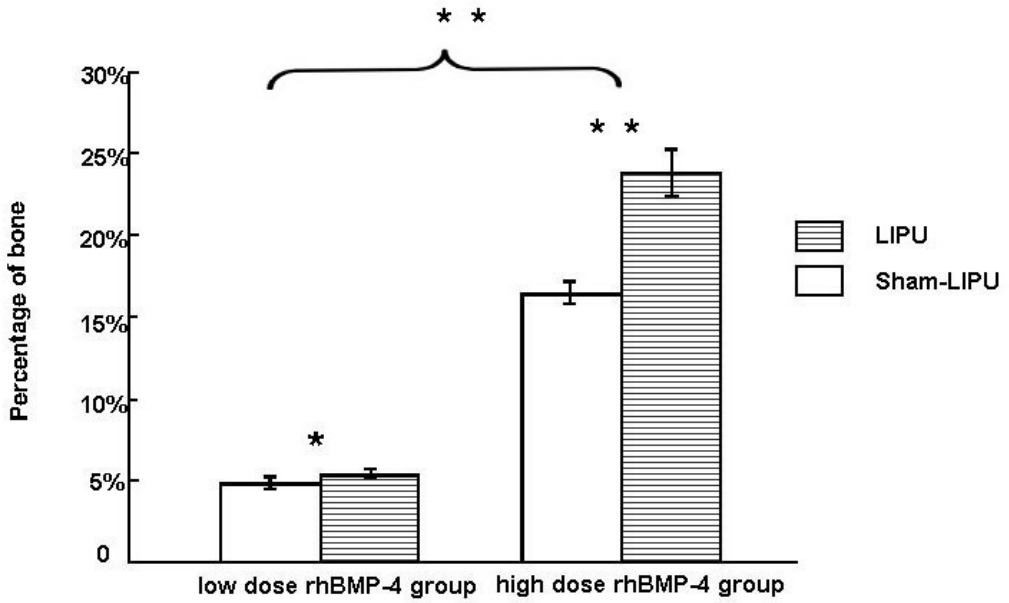

Figure 4.12 Percentage of bone at week 7 * p<0.05, ** p<0.01.

Week 7,

Sham-LIPU side LIPU side

Low- dose group

High-dose group

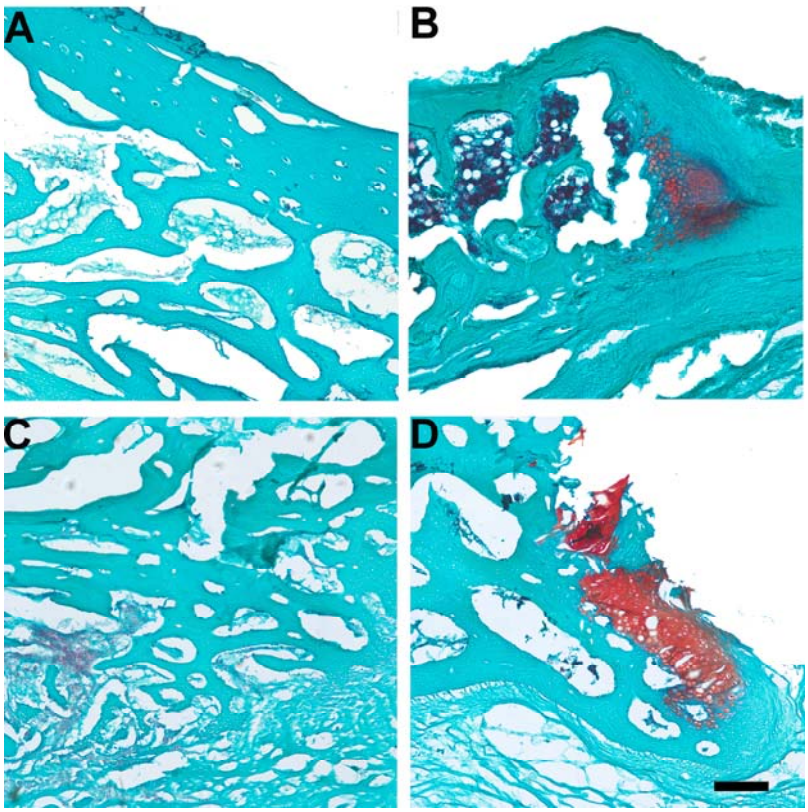

Figure 4.13 New cartilage tissues at week 7 postoperation (saffranin O/fast green staining). A, B: low-dose rhBMP-4 group; C, D: high-dose rhBMP-4 group. Red color showed new cartilage tissue. Scale bar is 200μm.

Week 7

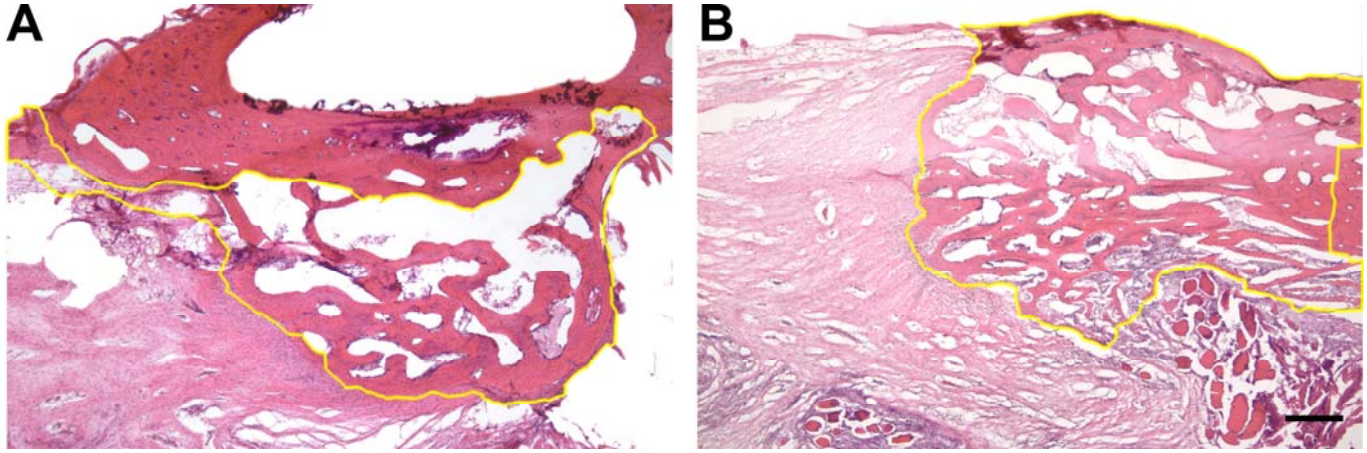

Figure 4.14 New bone tissues at week 7 postoperation (HE staining). A, low-dose rhBMP-4 group; B, high-dose rhBMP-4 group; Scale bar is 400μm.

Table 4.8 Percentage of new bone, cartilage and fibrous tissue at week 12 postoperation

Tissue	Low dose rhBMP-4 group		High dose rhBMP-4 group	
	Sham LIPU side	LIPU treated side	Sham LIPU side	LIPU treated side
New Bone (%)	13.94±0.38	15.22±0.17	23.07±0.57	27.31±0.48
Cartilage (%)	0	0	0	0
Fibrous tissue (%)	86.06±0.66	84.78±0.29	76.93±0.99	72.69±0.82

Data are shown as Mean±SD.

Week 12, percentage of bone

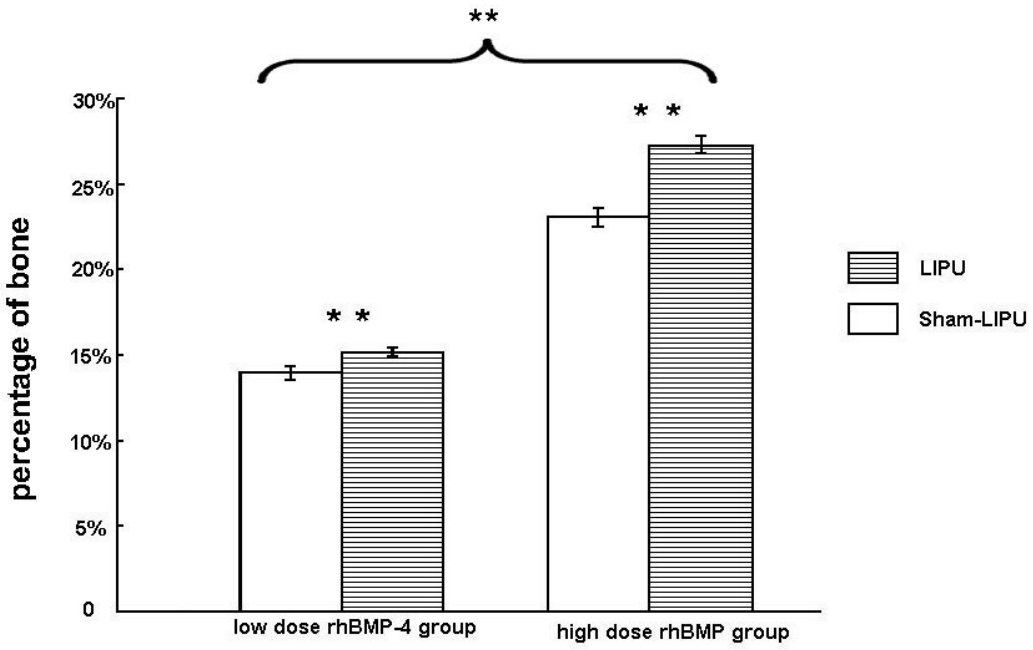

Figure 4.15 Percentage of bone at week 7 postoperation * $p<0.05$, ** $p<0.01$.

Week 12

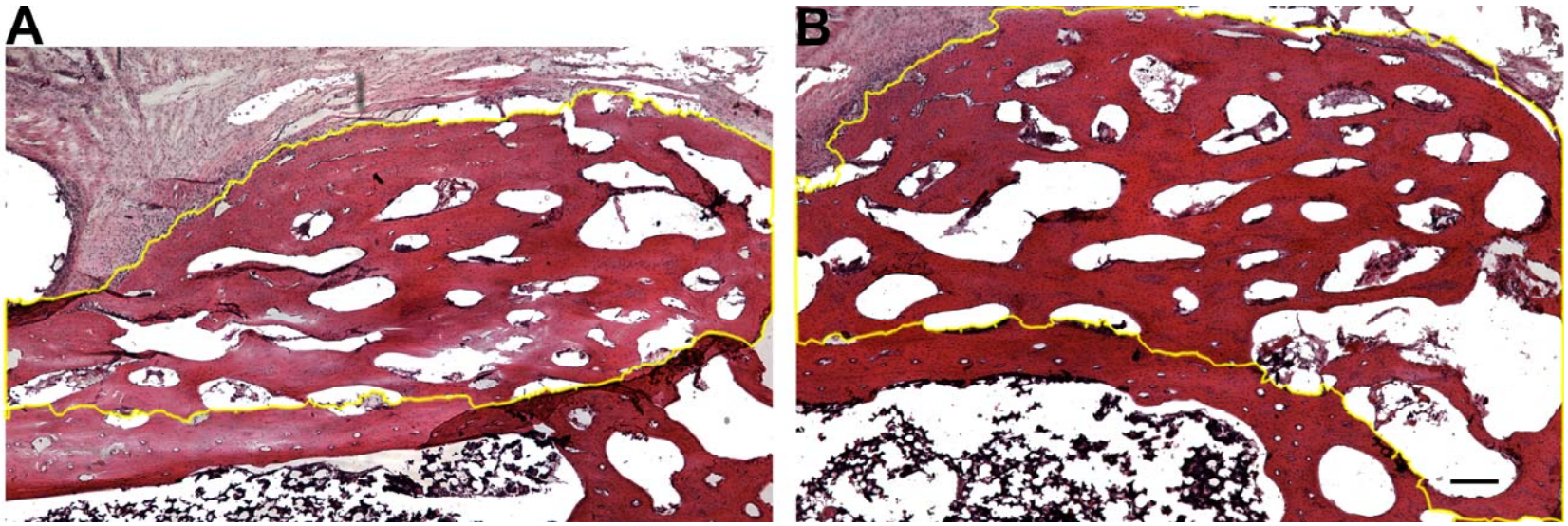

Figure 4.16 New bone tissues at week 12 postoperation. A low dose group; B: high dose group; Scale bar is 400μm.

Table 4.9 New cartilage tissues

	Day 3	Week 1	Week 3	Week 7	Week
High dose LIPU	-	++	3.1	0.7	-
High dose sham LIPU	-	++	0.5	0	-
Low dose LIPU	-	++	0.7	0.1	-
Low dose sham LIPU	-	++	0.4	0	-

Numeric value is the percent area; -: no cartilage tissue; +: find cartilage tissue.

Table 4.10 New bone tissues

	Day 3	Week 1	Week 3	Week 7	Week
High dose LIPU	-	+	5.5	23.9	27.9
High dose sham LIPU	-	+	3.9	16.5	23.4
Low dose LIPU	-	+	3.0	5.4	15.2
Low dose sham LIPU	-	+	2.3	5.0	13.9

Numeric value is the percent area; -: no bone tissue; +: find bone tissue.

Table 4.11 Bone formation mode

		Day 3	Week 1	Week 3	Week 7	Week 12
High dose sham LIPU	IO	-	+	+	-	-
	EO	-	+	+	+	-
High dose sham LIPU	IO	-	+	+	-	-
	EO	-	+	+	-	-
Low dose LIPU	IO	-	+	+	-	-
	EO	-	+	+	+	-
Low dose sham LIPU	IO	-	+	+	-	-
	EO	-	+	+	-	-

IO, intramembranous ossification; EO, endochondral ossification.

4.4 Fluorescence microscopy

CGRP immunostaining and fluorescence microscopy were used to investigate the innervation of CGRP-positive nerve fibers in the fusion area.

4.4.1 Day 3 postoperation

CGRP-positive nerve fibers were already visible in the fibrous tissue of both LIPU treated and sham sides in low-dose and high-dose rhBMP-4 groups (Figure 4.17). Co-staining with DAPI showed that the CGRP-positive nerve fiber was in contact with mesenchymal cells in the fibrous tissue (Figure 4.17). At this time point, CGRP-positive nerve fibers were thin and short. The density of CGRP-positive nerve fibers on the LIPU treated side were significantly higher than that on the sham LIPU side ($P<0.01$, paired t-test).

4.4.2 Week 1 postoperation

At week 1 postoperation, an increased number of CGRP-positive nerve fibers were observed in the fibrous tissue of the low-dose and high-dose rhBMP-4 groups (Figure 4.18). Furthermore, a few CGRP-positive nerve fibers were observed in the new bone on the LIPU treated side. CGRP-positive nerve fibers in the new bone tissue were found to be in contact with the osteoblasts (Figure 4.18).

The density of CGRP-positive nerve fibers was significantly higher on the LIPU treated side than on the sham-LIPU side ($P<0.01$, paired t-test). This was found to be always true during the whole observation period from day 3 to week 12 postoperation.

4.4.3 Week 3 postoperation

At this time point, CGRP-positive nerve fibers were longer compared to those of day 3 and week 1. CGRP-positive nerve fibers were found in the fibrous tissue and immature bone marrow of the low-dose and high-dose rhBMP-4 groups at week 3 postoperation (Figure 4.19). On the LIPU treated side, CGRP-positive nerve fibers were observed close to the blood vessels in the fibrous tissue. Such association was not observed in the bone marrow (Figure 4.19). Furthermore, CGRP-positive nerve fibers were found to be in contact with the chondrocyte in the cartilage tissue (Figure 4.20).

4.4.4 Week 7 postoperation

At week 7 postoperation, CGRP-positive nerve fibers were visible in fibrous tissue and bone marrow of low-dose and high-dose rhBMP-4 groups (Figure 4.21). Compared with other time points, the CGRP-positive nerve fibers at week 7 postoperation were thicker (Figure 4.21). On the LIPU treated side,

CGRP-positive nerve fibers were found close to the blood vessels in bone marrow, which was different from that of week 3.

4.4.5 Week 12 postoperation

CGRP-positive nerve fibers became obviously thinner and shorter at week 12 postoperation than that of week 7 (Figure 4.22).

4.4.6 Quantification of CGRP expressions across various time points

One way ANOVA was used to compare the density of CGRP-positive nerve fibers across various time points in the fibrous tissue (Figure 4.23) and bone marrow (Figure 4.24), respectively.

In the fibrous tissue, as mentioned in Section 4.2.4.1, CGRP positive nerve fibers innervated already at day 3 after surgery on both the LIPU treated and sham LIPU sides. On the sham LIPU side, the density of CGRP-positive nerve fibers was in a relatively lower level within the first 1 week. It increased noticeably in the following 2 weeks, peaking at week 3 postoperation ($P<0.01$, one way ANOVA with multiple comparisons test), and decreased after that. On the LIPU treated side, the density of CGRP-positive nerve fibers was detected in a high level from the very beginning (day 3). The high density of CGRP-positive nerve fibers was maintained until week 3 postoperation ($P>0.05$, one way

ANOVA with multiple comparisons test), and then decreased from week 7 onwards ($P<0.05$, one way ANOVA with multiple comparisons test).

In the bone marrow, CGRP immunoreactivity was not detected until week 3 postoperation for both LIPU treated and sham LIPU sides. Unlike that in the fibrous tissue, the LIPU treated and sham LIPU sides showed similar CGRP expression curves during the experimental period. The density of CGRP positive fibers peaked at week 7 and decreased at week 12 postoperation ($P<0.01$, one way ANOVA with multiple comparisons test).

In summary, CGRP immunofluorescence results demonstrated that LIPU treatment enhanced the innervation of CGRP-positive nerve fibers in ectopic bone tissues. 1) Spatially, LIPU promoted the in-growth of CGRP-positive nerve fibers into the new bone forming tissues. On the sham LIPU side, CGRP-positive nerve fibers were observed only at the fibrous tissues which surrounded the new bone and cartilage tissues, and in the bone marrow of the new bone tissue. On the LIPU treated side, CGRP-positive nerve fibers were also observed in the new bone and cartilage tissues in addition to their presence in the fibrous and bone marrow tissues. 2) Temporally, LIPU increased the density of CGRP-positive nerve fibers in fibrous and bone marrow tissues during the process of ectopic ossification. On the sham LIPU side, the density of

CGRP-positive nerve fibers was of a low level at the beginning, and then increased markedly. On the LIPU treated side, LIPU treatment increased the density of CGRP-positive nerve fibers to a high level from the beginning, suggesting that the promotion effect of LIPU on the in-growth of CGRP-positive nerve fibers into the ectopic bone was more effectively during the early healing stage.

Day 3

Sham LIPU side

LIPU treated side

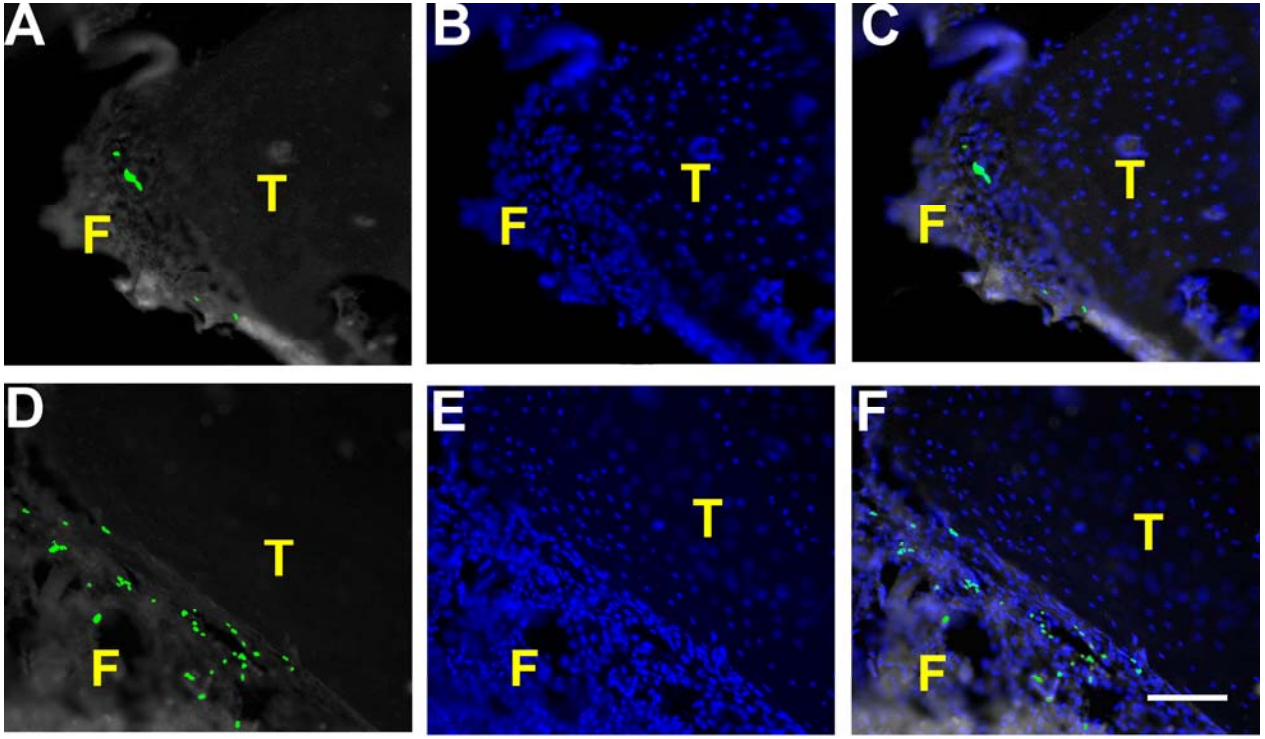

Figure 4.17 CGRP-positive nerve fibers at day 3 postoperation. (immunofluorescent staining) AD, CGRP staining, BE, DAPI staining, CF, double staining by CGRP and DAPI. F", fibrous tissue; "T", transverse process; Scale bar is 100μm.

Week 1

Sham

LIPU

side

LIPU

treated

side

LIPU

treated

Side

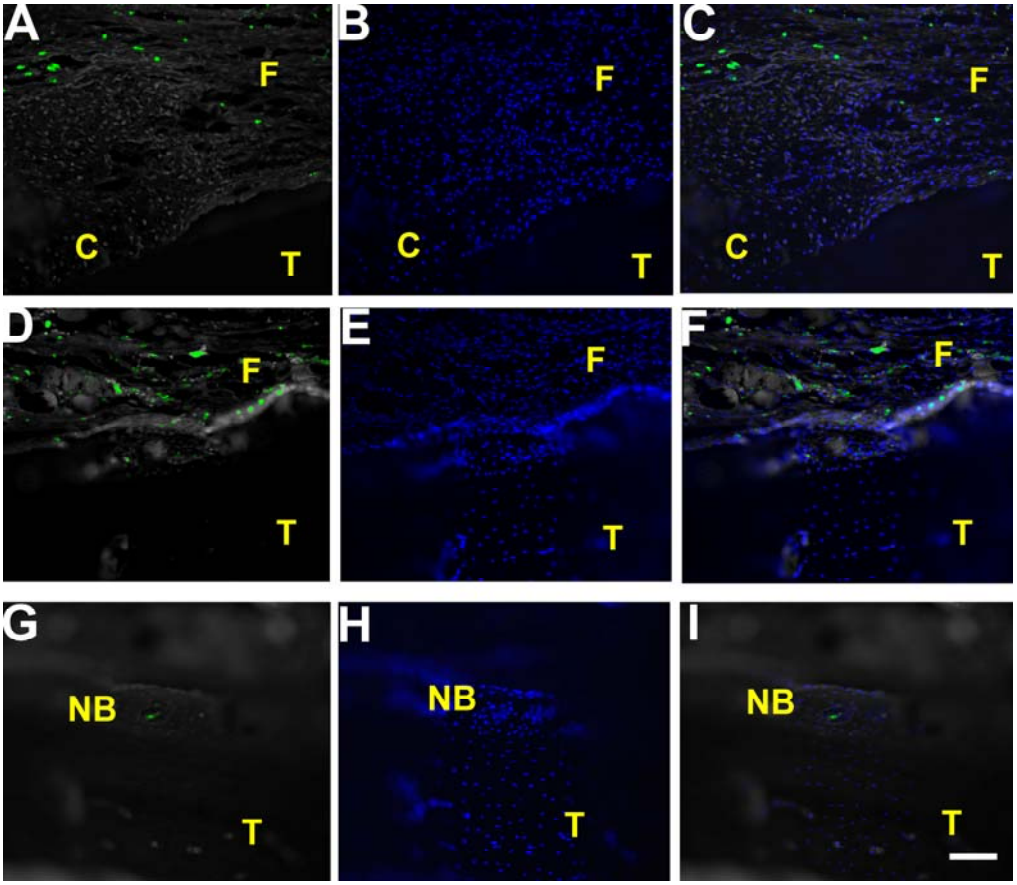

Figure 4.18 CGRP-positive nerve fibers at week 1 postoperation. (immunofluorescent staining) AD and G, CGRP staining, BEH, DAPI staining, CFI, double staining by CGRP and DAPI. F", fibrous tissue; "T", transverse process; "C" cartilage tissue; "NB" new bone tissue; Scale bar is 50μm.

Week 3

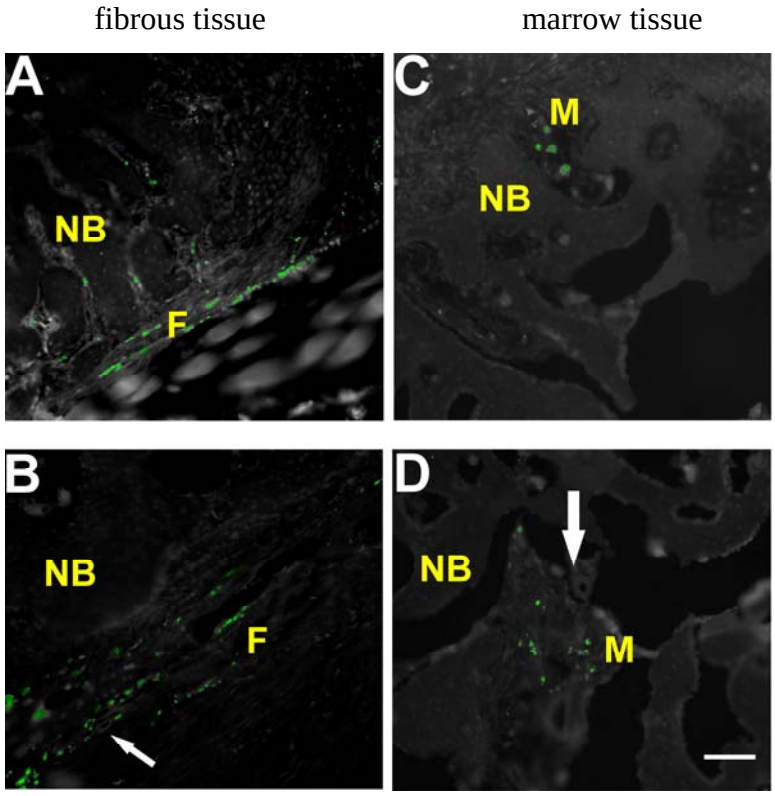

Figure 4.19 CGRP-positive nerve fibers at week 3 postoperation. (immunofluorescent staining) “F”, fibrous tissue; “NB”, new bone tissue; “M” new bone marrow; “Arrow” blood vessel; Scale bar is 100μm.

Week 3, CGRP-positive nerve fibers in cartilage tissue on LIPU treated sides

Low magnification

High magnification

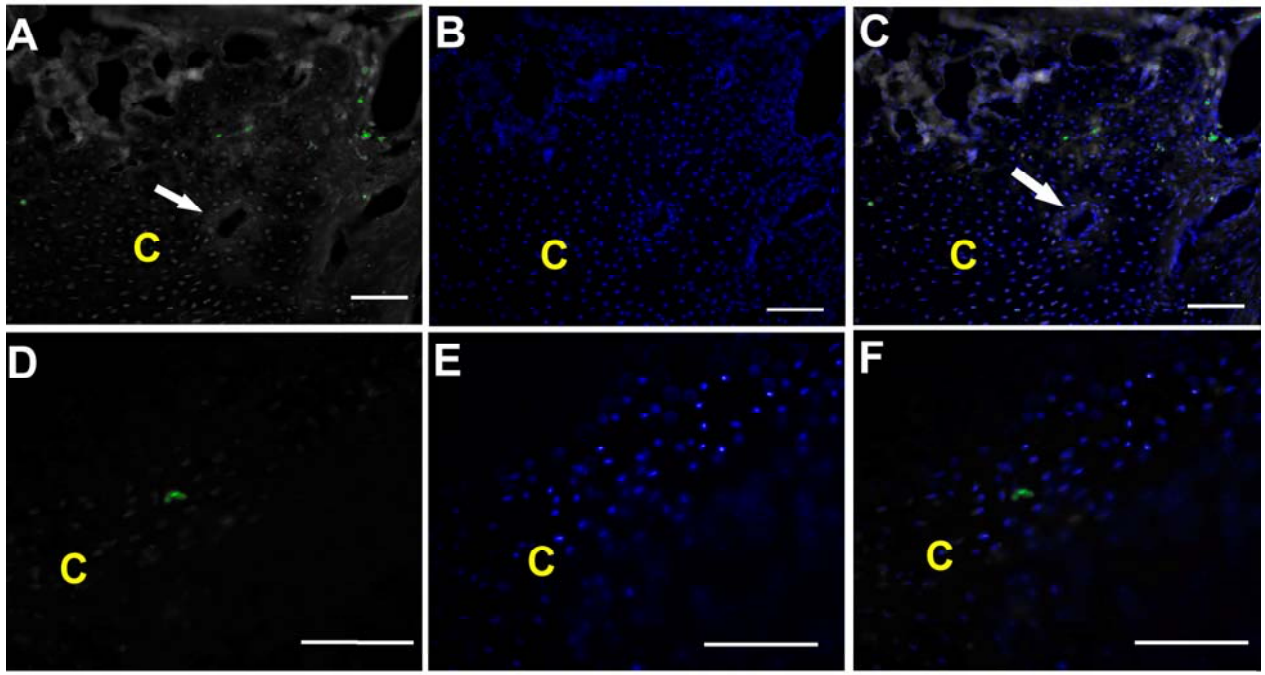

Figure 4.20 CGRP-positive nerve fibers at week 3 postoperation. (immunofluorescent staining) AD, CGRP staining, BE, DAPI staining, CF, double staining by CGRP and DAPI. “C”, cartilage tissue “Arrow”, blood vessel; Scale bar is 100μm.

Week 7

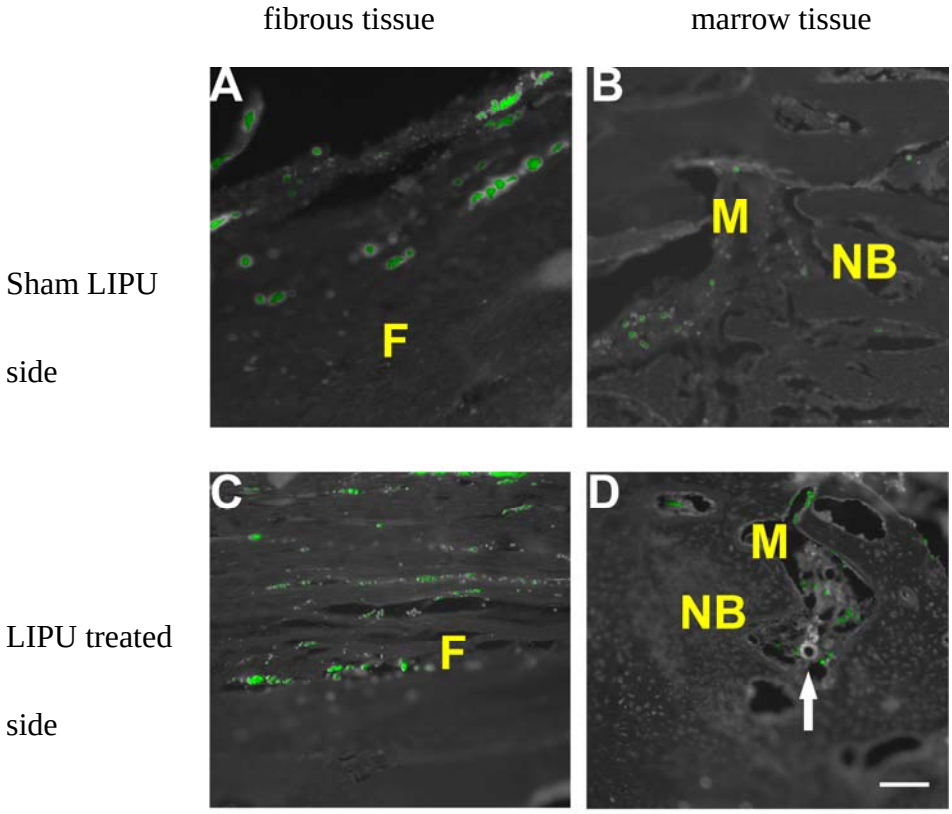

Figure 4.21 CGRP-positive nerve fibers at week 7 postoperation. (immunofluorescent staining) “F”, fibrous tissue; “NB”, new bone tissue; “M” new bone marrow “Arrow”, blood vessel; Scale bar is 100μm.

Week 12

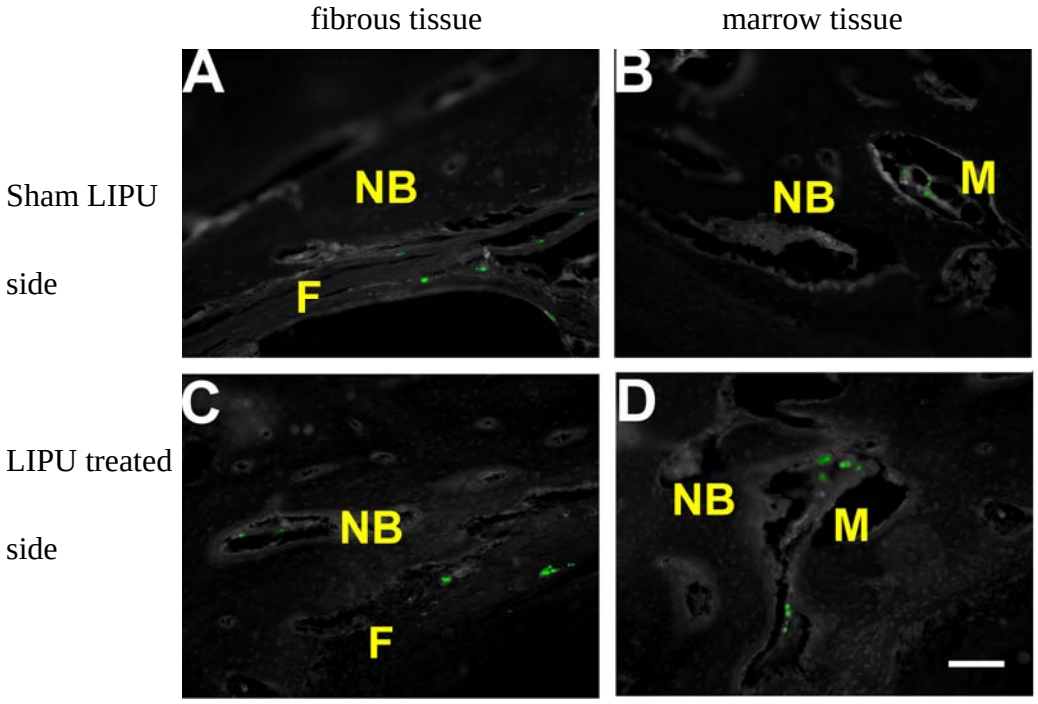

Figure 4.22 CGRP-positive nerve fibers at week 12 postoperation (immunofluorescent staining). “F”, fibrous tissue; “NB”, new bone tissue; “M” new bone marrow; Scale bar is 100μm.

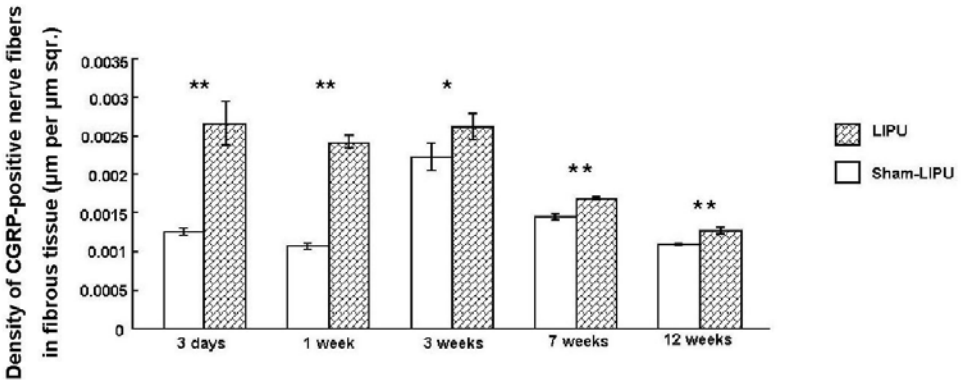

Figure 4.23 Density of CGRP-positive nerve fibers in the fibrous tissue.

* p<0.05, ** p<0.01

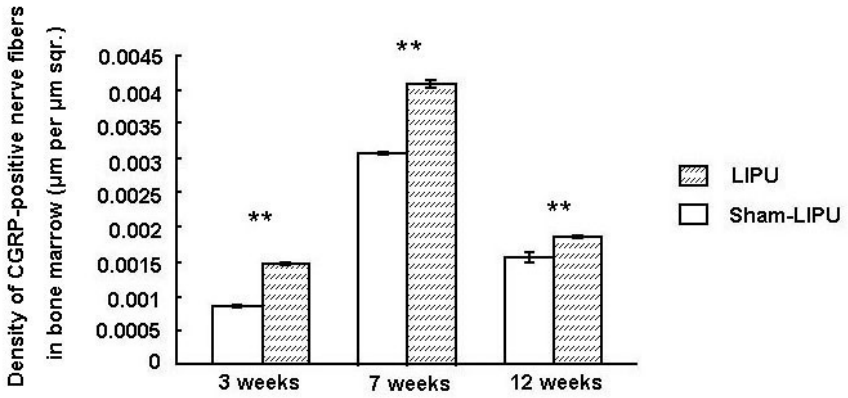

Figure 4.24 Density of CGRP-positive nerve fibers in the bone marrow tissue.

* p<0.05, ** p<0.01

Chapter 5

Discussion

5.1 RhBMP-4 induced ectopic ossification in spinal fusion model

The rhBMP-4 used in the present study served as the potent stimulator to induce ectopic ossification. The results showed that only abundant mesenchymal cells were observed at day 3 postoperation, surrounding the implant and contacting the transverse processes. One week after implantation, new cartilage and bone tissues were observed to be present for the first time, occupying the place where mesenchymal cells were previously situated. These results suggest that the mesenchymal cells could further differentiate into osteogenetic cells in response to rhBMP-4. Previous studies that were performed *in vivo* and *in vitro* have also shown that non-marrow derived mesenchymal stem cells can undergo osteogenetic differentiation induced by rhBMP-4 (Jortikka et al., 1998; Guo et al., 2002).

Ectopic bone was formed via both intramembranous ossification and endochondral ossification in the present study. It has been well accepted that rhBMP-4 can induce ectopic ossification via endochondral ossification. BMP-4 plays an important role in promoting the chondrogenic differentiation of non-marrow derived mesenchymal stem cells (Kuroda et al., 2006) and enhancing chondrocyte proliferation and matrix deposition (Minina et al., 2001;

Shum et al., 2003). It is also noted that BMP-4 could induce the newly formed cartilage to be replaced by bone, particularly in the presence of multipotent progenitor cells (Goldring, 2006). In the present study, endochondral ossification was observed in both low-dose and high-dose rhBMP-4 groups without LIPU treatment at week 1 and week 3 postoperation, proving the promoting effect of rhBMP-4 on endochondral ossification *in vivo*.

There are few reports on intramembranous ossification induced by local admission of rhBMP-4. In fact, most previous studies used BMP-4 as a potent stimulator to induce multipotent mesenchymal stem cells differentiating into chondrogenetic cells (Nakayama et al., 2003; Steinert et al., 2003). In the present study, more new bone formed via intramembranous ossification appeared at week 1 postoperation in both low-dose and high-dose rhBMP-4 groups, suggesting that rhBMP-4 could induce ectopic bone through intramembranous ossification at the very early stage. The *in vivo* results confirmed that non-marrow derived mesenchymal stem cells can also undergo osteoblastic differentiation in response to rhBMP-4. Moreover, active intramembranous ossification was observed at week 3 postoperation and no intramembranous ossification was found at week 7 and week 12 in both low-dose and high-dose rhBMP-4 groups. Similarly, endochondral ossification peaked at week 3 and discontinued at week 7 and week 12 for low-dose and high-dose rhBMP-4

groups without LIPU treatment. The results suggest that these two pathways of new bone formation are of the same important value on the ectopic ossification induced by rhBMP-4.

The effective dose of rhBMP-2 and rhBMP-7 for enhancing posterior spinal fusion in the rabbit model is reported to be 50 to 3000μg (Cook et al., 1994; Boden et al., 1995; Boden et al., 1996; Sandhu et al., 1996; Itoh et al., 1999). Our previous study demonstrated that the effective dose of rhBMP-4 to induce and promote posterior spinal fusion is 5μg, which is found in significantly lower levels than either BMP-2 or BMP-7 (Cheng et al., 2002). Thus 5μg and 1.25μg were designed as the threshold for high dose and low dose respectively in the present study. It has also been well documented that the effect of rhBMP-4 on osteogenesis is dose-dependent (Guo et al., 2002). In the present study, plain x-ray, pQCT and microscopy results showed that more new bone tissues were found in high-dose rhBMP-4 groups than in low-dose rhBMP-4 groups at week 7 and week 12, suggesting the apparent dose-dependent effect of rhBMP-4 on inducing and promoting ectopic ossification.

5.2 Effect of LIPU on rhBMP-4 induced ectopic ossification

Previous studies revealed that LIPU can promote osteogenesis in bone healing. LIPU treatment accelerated callus formation in fracture healing and increased bone formation inside the femoral cortical bone defects and at a rabbit fibulae osteotomy site (Duarte, 1983). Also, LIPU accelerated the bone formation and remodeling in distraction osteogenesis (Chan et al., 2006). In the present study, plain x-ray and pQCT results showed that more new bones were formed on the LIPU treated side in both low-dose and high-dose rhBMP-4 groups. This was demonstrated by significantly higher BMC and bone volume on the LIPU treated side than on the sham LIPU side at week 7 and week 12 postoperation. These results suggest that LIPU effectively enhanced ectopic ossification induced by rhBMP-4.

The underlying mechanisms of larger bone mass formation on the LIPU treated side can be explained by histological findings. In the present study, the ectopic bone induced by rhBMP-4 was formed via both endochondral ossification and intramembranous ossification at the initial stage. Histological results showed that the percentage of the new cartilage tissue was significantly higher on the LIPU treated side than on the sham LIPU side at week 3, suggesting that LIPU enhanced ectopic bone formation by boosting up chondrogenesis at the early stage of endochondral ossification.

Previous studies have revealed the effects of LIPU on the process of chondrogenesis and endochondral ossification. *In vitro* studies demonstrated that LIPU can stimulate chondrocyte proliferation (Zhang et al., 2003) and chondrocyte-associated gene expression (Yang et al., 1996) in the process of chondrogenesis, as well as increase intracellular concentration of the second messenger, which is calcium, in chondrocytes (Parvizi et al., 2002). On the other hand, LIPU can stimulate the process of ossification of the cartilage. It was demonstrated that LIPU can activate ossification in the process of endochondral ossification through a direct effect on ossifying cartilage (Nolte et al., 2001). The influence of LIPU on chondrocytes hypertrophy has been reported in controversy. It was reported by Wiltink et al. (1995) that LIPU can stimulate the proliferation of chondrocytes without influencing chondrocyte hypertrophy, while another study revealed that LIPU inhibited chondrocyte hypertrophy by decreasing the expression of type X collagen (Zhang et al., 2003). Our histological results support the finding by Wiltink, since chondrocyte hypertrophy was observed unaltered quantitatively and morphologically between the LIPU treated side and the sham LIPU side. The histological results also demonstrated that the cartilage tissue could be observed continuously till week 7 on the LIPU treated side while it disappeared before week 7 on the sham LIPU

side. This finding further indicates that LIPU can also prolong chondrogenesis activity during ectopic osteogenesis.

Intramembranous ossification was observed during the early stage of ectopic osteogenesis in the present study. It was reported that LIPU can promote intramembranous ossification during fracture healing (Kristiansen et al., 1997; Azuma et al., 2001). However, there was no significant difference in intramembranous ossification in rhBMP-4 induced ectopic osteogenesis between the presence or absence of LIPU.

5.3 Peripheral innervation involved in rhBMP-4 induced ectopic ossification

Many evidences have revealed the importance of peripheral nerve innervation in fracture healing (Hukkanen et al., 1993; Madsen et al., 1998; Li et al., 2007);(Aro et al., 1985; Santavirta et al., 1992). The neuropeptides, which are secreted by sensory nerve fibers in fracture callus, may play a key role in the facilitating effect. Among these neuropeptides, CGRP has been attracting more and more attention because of its active participation in the bone metabolism. Previous studies *in vitro* revealed that CGRP stimulated osteogenesis via receptors on the osteogenetic cells (Shih and Bernard, 1997).

Experimental studies have demonstrated the involvement of CGRP-positive nerve fibers in bone repair, such as fractures (Hukkanen et al., 1993) and bone

defects (Aoki et al., 1994; Madsen et al., 2000). CGRP-positive nerve fibers also have been proven to participate in ectopic ossification. In a study investigating the potential involvement of CGRP-positive nerve fibers in ectopic ossification induced by demineralized bone matrix in muscles, the authors showed that CGRP-positive nerve fibers could be seen in the fibrous tissue surrounding the implant and bone marrow during the healing process. Moreover, the number of CGRP-positive nerve fibers in the fibrous tissue reached the peak when the new bone formation could be discerned. In the bone marrow it increased as osteogenetic activity decreased (Bjurholm et al., 1990).

In the present study, CGRP-positive nerve fibers could also be found at fibrous tissue surrounding the implant and bone marrow, consistent with the former study. Additionally, CGRP-positive nerve fibers appeared in fibrous tissue as early as day 3 after implantation with appearance of abundant mesenchymal cells when the osteogenetic cells could not yet be identified. Co-staining with DAPI showed that CGRP-positive nerve fibers in fibrous tissue contacted with the mesenchymal cells. The result suggested that CGRP-positive nerve fibers may participate in the osteogenetic differentiation of mesenchymal cells in response to rhBMP-4 in the present study. An *in vitro* study was designed to test whether CGRP has an osteogenetic potential. The light density bone marrow white cells, consisting of monocytes, lymphocytes, blast cells and

stem cells were prepared and seeded on a previously prepared fibroblast layer in Petri dishes. 0.01, 0.1, and 1 μg/ml CGRP or calcitonin in BGJb medium was added daily to the dishes. The results showed that after 7 days, the number and size of bone colonies formed in the CGRP (0.1 or 1μg/ml) added group was significantly greater than that of the control group. This study suggested that CGRP has an osteogenic stimulating effect, either by stimulating stem cell mitosis or osteoprogenitor cell differentiation (or both). However, how CGRP acts on the stem cell and influences cell function remains unclear.

Changes of density and the morphology of CGRP-positive nerve fibers during the healing process were also investigated in the present study. Contrary to the former study, the density of CGRP-positive nerve fibers in the fibrous tissue reached the peak when active endochondral ossification and intramembranous ossification were observed. Morphologically, CGRP-positive nerve fibers in the fibrous tissue were shown to be long and varicose at that time. The results indicated that with the increasing of CGRP expression the osteogenetic activity also enhanced. The CGRP secreted by the nerve fibers plays an important role in promoting the ectopic ossification. Moreover, the density of CGRP-positive nerve fibers in the fibrous tissue was at a low level when the osteogenetic activity almost ceased. The results suggested that CGRP may not be involved in the remolding stage in ectopic ossification.

The present results also showed that the density of CGRP-positive nerve fibers in marrow increased when the osteogenetic activity decreased at week 7. This is consistent with the former study. Although bone marrow contains stem cells, the physiological function of CGRP in the bone marrow may not be relevant to the bone induction process. In fact, neuropeptides expressed in the bone marrow have been shown to be important in leukocyte trafficking and wound healing as well as hemopoiesis. Broome and Miyan revealed that neuropeptide input to the bone marrow is vital to normal granulopoiesis and that deletion of the neuropeptides, substance P, and CGRP, with the neurotoxin, capsaicin, abrogates normal blood cell production (Broome and Miyan, 2000).

Since ectopic ossification is different from bone repair which occurred normally inside the skeleton, the difference of CGRP-positive nerve fibers innervation during the healing process between two such cases should also be considered. In ectopic ossification, CGRP-positive nerve fibers were observed at the fibrous tissue surrounding the implant and bone marrow. However, positive nerve fibers were also observed in the middle of the callus interspersed with inflammatory cells and penetrating into secondary minor fractures in fracture healing (Hukkanen et al., 1993). Furthermore, CGRP-positive nerve fibers were observed close to the blood vessels in the fibrous tissues and bone marrow, during the processes of normal growth and bone repair healing (Hukkanen et al.,

1993; Aoki et al., 1994). Such was not apparent in ectopic ossification. The findings may suggest that CGRP has more potential in regulating local blood flow in bone repair than in ectopic ossification.

In ectopic ossification, the density of CGRP-positive nerve fibers in the fibrous tissue increased as the osteogenetic activity enhanced. Similarly, the quantitative changes of CGRP-positive nerve fibers were associated with the development and decay of callus tissues in bone repair (Aoki et al., 1994). The results suggested that CGRP-positive nerve fibers could have a potential importance in osteogenesis during the healing process.

5.4 Effect of LIPU on peripheral nerve fibers in-growth into rhBMP-4 induced ectopic ossification

LIPU treatment has been reported to promote peripheral nerve recovery in many kinds of injures, such as enhancing the recovery of normal nerve conduction velocity after partial crush injury (Hong et al., 1988) and prompting fast recuperation of the nerve after neurotomy (Crisci and Ferreira, 2002). In the present study, the results indicated that LIPU enhanced the innervation of CGRP-positive nerve fibers in ectopic bone healing tissues spatially and temporally.

Spatially, LIPU promoted the in-growth of CGRP-positive nerve fibers into the new bone forming tissues. On the sham LIPU side, CGRP-positive nerve fibers were observed at the fibrous tissues surrounding the new bone and cartilage tissues, and were also found in the bone marrow of the new bone tissue. However, on the LIPU treated side, CGRP-positive nerve fibers were visible not only in fibrous and bone marrow tissues, but also in the new bone and cartilage tissues. At week 1 postoperation, CGRP-positive nerve fibers were found in the new bone tissue. Co-staining with DAPI showed that CGRP-positive nerve fiber was in contact with osteoblast in intramembranous ossification. Moreover, CGRP-positive nerve fibers were found contacting undifferentiated chondrocytes in endochondral ossification. These findings directly indicated that LIPU could promote CGRP-positive nerve fibers in-growth into the new bone and cartilage tissues in rhBMP-4 induced ectopic ossification. In fact, CGRP has been demonstrated to regulate cellular (Crawford et al., 1986; Michelangeli et al., 1989) and autocrine activities (Vignery and McCarthy, 1996) of osteoblast, through a CGRP receptor. Thus, LIPU may accelerate the osteogenesis by promoting the in-growth of CGRP-positive nerve fibers into the new bone forming tissues.

Previous studies showed that no nerve fibers appeared at cartilage tissues which also did not contain blood vessels in bone repair (Aoki et al., 1994; Li et

al., 2001; Li et al., 2007). In the present study, CGRP-positive nerve fibers and blood vessels were found in the cartilage tissues on the LIPU treated side. The results undoubtedly proved the promoting effect of LIPU on vascular regeneration on bone healing. Moreover, CGRP-positive nerve fibers found in cartilage tissue were not close to the blood vessels, suggesting that CGRP participated in the regulation of chondrocyte, not in the regulation of blood flow in the cartilage tissue. In deed, an *in vitro* study showed that application of CGRP caused a distinctly increased level of cAMP, that was absent when CGRP was applied together with the CGRP receptor antagonist in cultured chondrocytes (Edoff and Hildebrand, 2003). The result indicated that terminals of primary sensory neurons present in developing cartilage may influence chondrocytes via local release of CGRP and the effect should be mediated by its receptor. Thus LIPU could influence endochondral ossification by promoting the CGRP-positive nerve fibers in-growth into the cartilage tissues in ectopic ossification.

In addition, on the LIPU treated side, CGRP-positive nerve fibers were also observed close to the blood vessels in fibrous tissues and bone marrow. This pattern is similar to the normal healing of bone repair. The observations together with those mentioned above revealed that LIPU could have osteogenetic, angiogenetic and vasodilator effects on bone healing in ectopic ossification and

the effects may be achieved by promoting the peripheral nerve fibers in-growth into the bone healing tissues.

Temporally, LIPU increased the density of CGRP-positive nerve fibers in fibrous and bone marrow tissues during the process of bone healing. On the sham LIPU side, the density of the CGRP-positive nerve fibers was of a low level at the beginning, and then increased markedly. While on the LIPU treated side, LIPU treatment increased the density of the CGRP-positive nerve fibers to a high level from the beginning, suggesting that the promotion effect of LIPU on the CGRP-positive nerve fibers in-growth was more effective during the early healing stage.

5.5 Limitations

Since the results were based on morphologic observations, it is hard to directly show how the peripheral nerve fibers secret neuropeptides in response to mechanical stimulation and how the neuropeptides in the local environment act on the target cells. Moreover, whether the activity of the neuropeptides receptors on related cells could be influenced by LIPU, should also be considered. In fact, the present study relates the mechanical basis of ultrasound to the sensitivity of the bone tissue through its sensory nerve fibers to mechanical stimuli, which provides a novel insight into the mechanisms of promoting the effect of LIPU on

bone healing. Thus, how the peripheral nerve fibers sense the mechanical stimuli and accelerate bone healing should be investigated in the further studies.

Bone healing is a complicated process, including of angiogenesis, neurogenesis and osteogenesis. In deed, many kinds of peripheral nerve fibers secreting neuropeptides such as CGRP, substance P (SP), neuropeptide Y (NPY) as well as vasoactive intestinal peptide (VIP), may actively participate in the bone healing process. However, we only chose CGRP, the most active neuropeptide involved in the bone metabolism, to be used in the present study. So the further study could deeply investigate the role of different kinds of neuropeptides containing nerve fibers in bone healing and their relationships.

5.6 Implications of this study

The present study proved the promoting effect of LIPU on rhBMP-4 induced ectopic ossification. The findings expand our knowledge on the effect of LIPU on bone healing. When we plan to apply LIPU to enhance the healing of orthopedic injuries, we also should consider the possible influence of the mechanical stimuli on ectopic ossification. More importantly, the present study relates neural components and mechanical stimuli to the bone healing. This may imply the possibility of using a neural mediator, such as CGRP, as another form

of treatment for bone healing, done through injection or incorporation with LIPU.

Chapter 6

Summary of findings and conclusions

As mentioned in Chapter 2, the present study aimed to

(1) Investigate the effect of LIPU on rhBMP-4 induced ectopic ossification;

(2) Investigate the involvement of peripheral nerve fibers in ectopic ossification;

(3) Investigate the interaction between sensory nerve fibers and the mechanical stimuli in ectopic ossification.

6.1 Effect of LIPU on rhBMP-4 induced ectopic ossification

As potent stimulator, rhBMP-4 induced ectopic ossification was via intramembranous ossification and endochondral ossification in the present study. The radiographic and histomorphological results revealed that LIPU could significantly enhance rhBMP-4 induced ectopic ossification. It was also found that the percentage of new cartilage tissues was significantly higher on the LIPU treated side than on the sham LIPU side. These findings suggest that LIPU could enhance ectopic ossification by improving endochondral ossification.

6.2 The involvement of peripheral nerve fibers in ectopic ossification

Fluorescence microcopy results showed that CGRP-positive nerve fibers were observed at fibrous tissue surrounding the implant and bone marrow of the new bone tissue in rhBMP-4 induced ectopic ossification. Moreover, CGRP-positive nerve fibers appeared in fibrous tissue as early as at day 3 after implantation with appearance of abundant mesenchymal cells. Also, the density of CGRP-positive nerve fibers in fibrous tissue increased as the osteogenetic activity enhanced. These findings revealed that CGRP-positive nerve fibers could have a potential importance in osteogenesis during the healing process. Peripheral nerve fibers in-growth into the healing tissue could be a key regulatory factor to ectopic ossification.

6.3 Interaction between LIPU and peripheral nerve fibers in ectopic ossification

In the present study, LIPU enhanced the invasion of CGRP-positive nerve fibers in ectopic bone tissues spatially and temporally.

Spatially, LIPU promoted the in-growth of CGRP-positive nerve fibers into the new bone forming tissues. On the sham LIPU side, CGRP-positive nerve fibers were observed at the fibrous tissues surrounding the new bone and cartilage tissues, and were also found in the bone marrow of the new bone tissue.

However, on the LIPU treated side, CGRP-positive nerve fibers were visible not only on the fibrous and bone marrow tissues, but also in the new bone and cartilage tissues.

Temporally, LIPU increased the density of CGRP-positive nerve fibers in the fibrous and bone marrow tissues during the process of bone healing. On the sham LIPU side, the density of CGRP-positive nerve fibers was of a low level at the beginning, and then increased markedly. While on the LIPU treated side, LIPU treatment increased the density of CGRP-positive nerve fibers to a high level from the beginning, suggesting that the promotional effect of LIPU on the CGRP-positive nerve fibers in-growth was more effective during the early healing stage.

These findings indicate that LIPU could promote CGRP-positive nerve fibers in-growth into the new bone and cartilage tissues in rhBMP-4 induced ectopic ossification. LIPU could have osteogenetic, angiogenetic and vasodilator effects on bone healing and the effects may be achieved via promoting the peripheral nerve fibers in-growth into the healing tissues.

6.4 Conclusions

The present study revealed that LIPU enhanced rhBMP-4 induced ectopic ossification effectively, possibly by improving endochondral ossification. These

findings expand our knowledge on the effect of LIPU on bone healing. Moreover, these attract more attention on the possible influence of the mechanical stimuli on ectopic ossification during the healing of orthopedic injuries with LIPU treatment. Moreover, the present study also indicated that CGRP-positive nerve fibers could have a potential importance in osteogenesis during healing process. Peripheral nerve fibers in-growth into the healing tissue could be a key regulatory factor to bone healing.

More importantly, the present study investigated the relationship between sensory nerve fibers and the mechanical stimuli on ectopic ossification. It has been proven in our study that LIPU could facilitate the invasion of sensory nerve fibers into the ectopic bone forming tissues during the healing process, which might explain how LIPU acted on the bone forming tissues. LIPU could have osteogenetic, angiogenetic and vasodilator effects on bone healing and the effects may show by promoting the peripheral nerve fibers in-growth into the bone healing tissues. This may imply to the possibility of using a neural mediator, such as CGRP, as another form of treatment for bone healing, for instance via injection or by incorporating with LIPU.

Reference:

Akopian A, Demulder A, Ouriaghli F, Corazza F, Fondu P, Bergmann P (2000) Effects of CGRP on human osteoclast-like cell formation: a possible connection with the bone loss in neurological disorders? Peptides 21:559-564.

Alam AS, Moonga BS, Bevis PJ, Huang CL, Zaidi M (1991) Selective antagonism of calcitonin-induced osteoclastic quiescence (Q effect) by human calcitonin gene-related peptide-(Val8Phe37). Biochem Biophys Res Commun 179:134-139.

Alpaslan C, Irie K, Takahashi K, Ohashi N, Sakai H, Nakajima T, Ozawa H (1996) Long-term evaluation of recombinant human bone morphogenetic protein-2 induced bone formation with a biologic and synthetic delivery system. Br J Oral Maxillofac Surg 34:414-418.

Aoki M, Tamai K, Saotome K (1994) Substance P- and calcitonin gene-related peptide-immunofluorescent nerves in the repair of experimental bone defects. Int Orthop 18:317-324.

Ardan NI, Jr., Janes JM, Herrick JF (1957) Ultrasonic energy and surgically produced defects in bone. J Bone Joint Surg Am 39-A:394-402.

Aro H, Eerola E, Aho AJ (1985) Development of nonunions in the rat fibula after removal of periosteal neural mechanoreceptors. Clin Orthop Relat Res:292-299.

Asahina I, Sampath TK, Hauschka PV (1996) Human osteogenic protein-1 induces chondroblastic, osteoblastic, and/or adipocytic differentiation of clonal murine target cells. Exp Cell Res 222:38-47.

Azuma Y, Ito M, Harada Y, Takagi H, Ohta T, Jingushi S (2001) Low-intensity pulsed ultrasound accelerates rat femoral fracture healing by acting on the various cellular reactions in the fracture callus. J Bone Miner Res 16:671-680.

Bender LF, Janes JM, Herrick JF (1954) Histologic studies following exposure of bone to ultrasound. Arch Phys Med Rehabil 35:555-559.

Bessho K, Carnes DL, Cavin R, Ong JL (2002) Experimental studies on bone induction using low-molecular-weight poly (DL-lactide-co-glycolide) as a carrier for recombinant human bone morphogenetic protein-2. J Biomed Mater Res 61:61-65.

Bjurholm A (1991) Neuroendocrine peptides in bone. Int Orthop 15:325-329.

Bjurholm A, Kreicbergs A, Schultzberg M (1989) Fixation and demineralization of bone tissue for immunohistochemical staining of neuropeptides. Calcif Tissue Int 45:227-231.

Bjurholm A, Kreicbergs A, Brodin E, Schultzberg M (1988) Substance P- and CGRP-immunoreactive nerves in bone. Peptides 9:165-171.

Bjurholm A, Kreicbergs A, Dahlberg L, Schultzberg M (1990) The occurrence of neuropeptides at different stages of DBM-induced heterotopic bone formation. Bone Miner 10:95-107.

Bjurholm A, Kreicbergs A, Schultzberg M, Lerner UH (1992) Neuroendocrine regulation of cyclic AMP formation in osteoblastic cell lines (UMR-106-01, ROS 17/2.8, MC3T3-E1, and Saos-2) and primary bone cells. Journal of Bone & Mineral Research 7:1011-1019.

Boden SD, Schimandle JH, Hutton WC (1995) An experimental lumbar intertransverse process spinal fusion model. Radiographic, histologic, and biomechanical healing characteristics. Spine 20:412-420.

Boden SD, Moskovitz PA, Morone MA, Toribitake Y (1996) Video-assisted lateral intertransverse process arthrodesis. Validation of a new minimally invasive lumbar spinal fusion technique in the rabbit and nonhuman primate (rhesus) models. Spine 21:2689-2697.

Boden SD, Martin GJ, Jr., Horton WC, Truss TL, Sandhu HS (1998) Laparoscopic anterior spinal arthrodesis with rhBMP-2 in a titanium interbody threaded cage. J Spinal Disord 11:95-101.

Bomback DA, Grauer JN, Lugo R, Troiano N, Patel T, Friedlaender GE (2004) Comparison of posterolateral lumbar fusion rates of Grafton Putty and OP-1 Putty in an athymic rat model. Spine 29:1612-1617.

Bouxsein ML, Turek TJ, Blake CA, D'Augusta D, Li X, Stevens M, Seeherman HJ, Wozney JM (2001) Recombinant human bone morphogenetic protein-2 accelerates healing in a rabbit ulnar osteotomy model. J Bone Joint Surg Am 83-A:1219-1230.

Broome CS, Miyan JA (2000) Neuropeptide control of bone marrow neutrophil production. A key axis for neuroimmunomodulation. Ann N Y Acad Sci 917:424-434.

Carlisle E, Fischgrund JS (2005) Bone morphogenetic proteins for spinal fusion. Spine J 5:240S-249S.

Chan CW, Qin L, Lee KM, Zhang M, Cheng JC, Leung KS (2006) Low intensity pulsed ultrasound accelerated bone remodeling during consolidation stage of distraction osteogenesis. J Orthop Res 24:263-270.

Chang WH, Sun JS, Chang SP, Lin JC (2002) Study of thermal effects of ultrasound stimulation on fracture healing. Bioelectromagnetics 23:256-263.

Chapman IV, MacNally NA, Tucker S (1980) Ultrasound-induced changes in rates of influx and efflux of potassium ions in rat thymocytes in vitro. Ultrasound Med Biol 6:47-58.

Chen D, Zhao M, Mundy GR (2004) Bone morphogenetic proteins. Growth Factors 22:233-241.

Chen YJ, Wang CJ, Yang KD, Chang PR, Huang HC, Huang YT, Sun YC, Wang FS (2003) Pertussis toxin-sensitive Galphai protein and ERK-dependent pathways mediate ultrasound promotion of osteogenic transcription in human osteoblasts. FEBS Lett 554:154-158.

Cheng JC, Guo X, Law LP, Lee KM, Chow DH, Rosier R (2002) How does recombinant human bone morphogenetic protein-4 enhance posterior spinal fusion? Spine 27:467-474.

Cook SD, Dalton JE, Tan EH, Whitecloud TS, 3rd, Rueger DC (1994) In vivo evaluation of recombinant human osteogenic protein (rhOP-1) implants as a bone graft substitute for spinal fusions. Spine 19:1655-1663.

Cook SD, Salkeld SL, Mse, Patron LP, Ryaby JP, Whitecloud TS (2001) Low-intensity pulsed ultrasound improves spinal fusion. Spine J 1:246-254.

Crawford A, Evans DB, Skjodt H, Beresford JN, Maclntyre I, Russell RGG (1986) Effect of human calcitonin gene-related peptide on human bone-derived cells in culture. Bone 7:157-158.

Crisci AR, Ferreira AL (2002) Low-intensity pulsed ultrasound accelerates the regeneration of the sciatic nerve after neurotomy in rats. Ultrasound Med Biol 28:1335-1341.

D'Souza SM, MacIntyre I, Girgis SI, Mundy GR (1986) Human synthetic calcitonin gene-related peptide inhibits bone resorption in vitro. Endocrinology 119:58-61.

Damien CJ, Grob D, Boden SD, Benedict JJ (2002) Purified bovine BMP extract and collagen for spine arthrodesis: preclinical safety and efficacy. Spine 27:S50-58.

Den Boer FC, Bramer JA, Blokhuis TJ, Van Soest EJ, Jenner JM, Patka P, Bakker FC, Burger EH, Haarman HJ (2002) Effect of recombinant human osteogenic protein-1 on the healing of a freshly closed diaphyseal fracture. Bone 31:158-164.

Doan N, Reher P, Meghji S, Harris M (1999) In vitro effects of therapeutic ultrasound on cell proliferation, protein synthesis, and cytokine production by human fibroblasts, osteoblasts, and monocytes. J Oral Maxillofac Surg 57:409-419; discussion 420.

Duarte LR (1983) The stimulation of bone growth by ultrasound. Arch Orthop Trauma Surg 101:153-159.

Duprez D, Bell EJ, Richardson MK, Archer CW, Wolpert L, Brickell PM, Francis-West PH (1996) Overexpression of BMP-2 and BMP-4 alters the size and shape of developing skeletal elements in the chick limb. Mech Dev 57:145-157.

Ebisawa K, Hata K, Okada K, Kimata K, Ueda M, Torii S, Watanabe H (2004) Ultrasound enhances transforming growth factor beta-mediated chondrocyte differentiation of human mesenchymal stem cells. Tissue Eng 10:921-929.

Edgar MA, Mehta MH (1988) Long-term follow-up of fused and unfused idiopathic scoliosis. J Bone Joint Surg Br 70:712-716.

Edoff K, Hildebrand C (2003) Neuropeptide effects on rat chondrocytes and perichondrial cells in vitro. Neuropeptides 37:316-318.

Fainsod A, Steinbeisser H, De Robertis EM (1994) On the function of BMP-4 in patterning the marginal zone of the Xenopus embryo. Embo J 13:5015-5025.

Fischgrund JS, James SB, Chabot MC, Hankin R, Herkowitz HN, Wozney JM, Shirkhoda A (1997) Augmentation of autograft using rhBMP-2 and

different carrier media in the canine spinal fusion model. J Spinal Disord 10:467-472.

Frankel VH (1998) Results of Prescription Use of Pulse Ultrasound Therapy in Fracture Management. Surg Technol Int VII:389-393.

Garcia-Castellano JM, Diaz-Herrera P, Morcuende JA (2000) Is bone a target-tissue for the nervous system? New advances on the understanding of their interactions. Iowa Orthopaedic Journal 20:49-58.

Geiger M, Li RH, Friess W (2003) Collagen sponges for bone regeneration with rhBMP-2. Adv Drug Deliv Rev 55:1613-1629.

Gimble JM, Morgan C, Kelly K, Wu X, Dandapani V, Wang CS, Rosen V (1995) Bone morphogenetic proteins inhibit adipocyte differentiation by bone marrow stromal cells. J Cell Biochem 58:393-402.

Glazer PA, Heilmann MR, Lotz JC, Bradford DS (1998) Use of ultrasound in spinal arthrodesis. A rabbit model. Spine 23:1142-1148.

Goldring MB (2006) Are bone morphogenetic proteins effective inducers of cartilage repair? Ex vivo transduction of muscle-derived stem cells.[comment]. Arthritis & Rheumatism 54:387-389.

Gonnelli S, Cepollaro C (2002) The use of ultrasound in the assessment of bone status. J Endocrinol Invest 25:389-397.

Grauer JN, Patel TC, Erulkar JS, Troiano NW, Panjabi MM, Friedlaender GE (2001) 2000 Young Investigator Research Award winner. Evaluation of OP-1 as a graft substitute for intertransverse process lumbar fusion. Spine 26:127-133.

Guo X, Lee KM, Law LP, Chow HK, Rosier R, Cheng CY (2002) Recombinant human bone morphogenetic protein-4 (rhBMP-4) enhanced posterior spinal fusion without decortication. J Orthop Res 20:740-746.

Hara-Irie F, Amizuka N, Ozawa H (1996) Immunohistochemical and ultrastructural localization of CGRP-positive nerve fibers at the epiphyseal trabecules facing the growth plate of rat femurs. Bone 18:29-39.

Hawley SH, Wunnenberg-Stapleton K, Hashimoto C, Laurent MN, Watabe T, Blumberg BW, Cho KW (1995) Disruption of BMP signals in embryonic Xenopus ectoderm leads to direct neural induction. Genes Dev 9:2923-2935.

Hecht BP, Fischgrund JS, Herkowitz HN, Penman L, Toth JM, Shirkhoda A (1999) The use of recombinant human bone morphogenetic protein 2 (rhBMP-2) to promote spinal fusion in a nonhuman primate anterior interbody fusion model. Spine 24:629-636.

Heckman JD, Ryaby JP, McCabe J, Frey JJ, Kilcoyne RF (1994) Acceleration of tibial fracture-healing by non-invasive, low-intensity pulsed ultrasound. J Bone Joint Surg Am 76:26-34.

Hemmati-Brivanlou A, Thomsen GH (1995) Ventral mesodermal patterning in Xenopus embryos: expression patterns and activities of BMP-2 and BMP-4. Dev Genet 17:78-89.

Herrick JF, Janes JM, Ardan NI, Jr. (1956) Experimental studies relative to the therapeutic use of ultrasound. J Am Vet Med Assoc 128:571-577.

Hibbs RA (1924) Scoliosis treated by fusion operation. J Bone Joint Surg Am 6:3-37.

Hill EL, Elde R (1991) Distribution of CGRP-, VIP-, D beta H-, SP-, and NPY-immunoreactive nerves in the periosteum of the rat. Cell Tissue Res 264:469-480.

Hong CZ, Liu HH, Yu J (1988) Ultrasound thermotherapy effect on the recovery of nerve conduction in experimental compression neuropathy. Arch Phys Med Rehabil 69:410-414.

Hukkanen M, Konttinen YT, Rees RG, Santavirta S, Terenghi G, Polak JM (1992a) Distribution of nerve endings and sensory neuropeptides in rat synovium, meniscus and bone. Int J Tissue React 14:1-10.

Hukkanen M, Konttinen YT, Rees RG, Gibson SJ, Santavirta S, Polak JM (1992b) Innervation of bone from healthy and arthritic rats by substance P and calcitonin gene related peptide containing sensory fibers. J Rheumatol 19:1252-1259.

Hukkanen M, Konttinen YT, Santavirta S, Paavolainen P, Gu XH, Terenghi G, Polak JM (1993) Rapid proliferation of calcitonin gene-related peptide-immunoreactive nerves during healing of rat tibial fracture suggests neural involvement in bone growth and remodelling. Neuroscience 54:969-979.

Imai S, Tokunaga Y, Maeda T, Kikkawa M, Hukuda S (1997a) Calcitonin gene-related peptide, substance P, and tyrosine hydroxylase-immunoreactive innervation of rat bone marrows: an immunohistochemical and ultrastructural investigation on possible efferent and afferent mechanisms. J Orthop Res 15:133-140.

Imai S, Rauvala H, Konttinen YT, Tokunaga T, Maeda T, Hukuda S, Santavirta S (1997b) Efferent targets of osseous CGRP-immunoreactive nerve fiber before and after bone destruction in adjuvant arthritic rat: an ultramorphological study on their terminal-target relations. J Bone Miner Res 12:1018-1027.

Irie K, Hara-Irie F, Ozawa H, Yajima T (2002) Calcitonin gene-related peptide (CGRP)-containing nerve fibers in bone tissue and their involvement in bone remodeling. Microsc Res Tech 58:85-90.

Ito M, Azuma Y, Ohta T, Komoriya K (2000) Effects of ultrasound and 1,25-dihydroxyvitamin D3 on growth factor secretion in co-cultures of osteoblasts and endothelial cells. Ultrasound Med Biol 26:161-166.

Itoh H, Ebara S, Kamimura M, Tateiwa Y, Kinoshita T, Yuzawa Y, Takaoka K (1999) Experimental spinal fusion with use of recombinant human bone morphogenetic protein 2. Spine 24:1402-1405.

Itoh S, Kikuchi M, Takakuda K, Koyama Y, Matsumoto HN, Ichinose S, Tanaka J, Kawauchi T, Shinomiya K (2001) The biocompatibility and osteoconductive activity of a novel hydroxyapatite/collagen composite biomaterial, and its function as a carrier of rhBMP-2. J Biomed Mater Res 54:445-453.

Jahng TA, Fu TS, Cunningham BW, Dmitriev AE, Kim DH (2004) Endoscopic instrumented posterolateral lumbar fusion with Healos and recombinant human growth/differentiation factor-5. Neurosurgery 54:171-180; discussion 180-171.

Johansson T, Risto O, Knutsson A, Wahlstrom O (2001) Heterotopic ossification following internal fixation or arthroplasty for displaced

femoral neck fractures: a prospective randomized study. Int Orthop 25:223-225.

Jortikka L, Laitinen M, Wiklund J, Lindholm TS, Marttinen A (1998) Use of myoblasts in assaying the osteoinductivity of bone morphogenetic proteins. Life Sciences 62:2359-2368.

Kakudo N, Kusumoto K, Wang YB, Iguchi Y, Ogawa Y (2006) Immunolocalization of vascular endothelial growth factor on intramuscular ectopic osteoinduction by bone morphogenetic protein-2. Life Sci 79:1847-1855.

Kanatani M, Sugimoto T, Kaji H, Kobayashi T, Nishiyama K, Fukase M, Kumegawa M, Chihara K (1995) Stimulatory effect of bone morphogenetic protein-2 on osteoclast-like cell formation and bone-resorbing activity. J Bone Miner Res 10:1681-1690.

Katagiri T, Yamaguchi A, Komaki M, Abe E, Takahashi N, Ikeda T, Rosen V, Wozney JM, Fujisawa-Sehara A, Suda T (1994) Bone morphogenetic protein-2 converts the differentiation pathway of C2C12 myoblasts into the osteoblast lineage. J Cell Biol 127:1755-1766.

Kawase T, Burns DM (1998) Calcitonin gene-related peptide stimulates potassium efflux through adenosine triphosphate-sensitive potassium

channels and produces membrane hyperpolarization in osteoblastic UMR106 cells. Endocrinology 139:3492-3502.

Kawase T, Howard GA, Roos BA, Burns DM (1995) Diverse actions of calcitonin gene-related peptide on intracellular free Ca2+ concentrations in UMR 106 osteoblastic cells. Bone 16:379S-384S.

Kelman CD (1969) Physics of ultrasound in cataract removal. Int Ophthalmol Clin 9:739-744.

King JA, Marker PC, Seung KJ, Kingsley DM (1994) BMP5 and the molecular, skeletal, and soft-tissue alterations in short ear mice. Dev Biol 166:112-122.

Kokubo S, Mochizuki M, Fukushima S, Ito T, Nozaki K, Iwai T, Takahashi K, Yokota S, Miyata K, Sasaki N (2004) Long-term stability of bone tissues induced by an osteoinductive biomaterial, recombinant human bone morphogenetic protein-2 and a biodegradable carrier. Biomaterials 25:1795-1803.

Korstjens CM, Nolte PA, Burger EH, Albers GH, Semeins CM, Aartman IH, Goei SW, Klein-Nulend J (2004) Stimulation of bone cell differentiation by low-intensity ultrasound--a histomorphometric in vitro study. J Orthop Res 22:495-500.

Kostuik JP, Israel J, Hall JE (1973) Scoliosis surgery in adults. Clin Orthop Relat Res:225-234.

Kristiansen TK, Ryaby JP, McCabe J, Frey JJ, Roe LR (1997) Accelerated healing of distal radial fractures with the use of specific, low-intensity ultrasound. A multicenter, prospective, randomized, double-blind, placebo-controlled study. J Bone Joint Surg Am 79:961-973.

Kuboki Y, Takita H, Kobayashi D, Tsuruga E, Inoue M, Murata M, Nagai N, Dohi Y, Ohgushi H (1998) BMP-induced osteogenesis on the surface of hydroxyapatite with geometrically feasible and nonfeasible structures: topology of osteogenesis. J Biomed Mater Res 39:190-199.

Kuroda R, Usas A, Kubo S, Corsi K, Peng H, Rose T, Cummins J, Fu FH, Huard J (2006) Cartilage repair using bone morphogenetic protein 4 and muscle-derived stem cells.[see comment]. Arthritis & Rheumatism 54:433-442.

Lam WL (2005) Effect of Acoustic Pressure Waves on Callus Innervation. In: Department of Rehabilitation Sciences. Hong Kong: The hong kong Polytechnic University.

Leung KS, Cheung WH, Zhang C, Lee KM, Lo HK (2004) Low intensity pulsed ultrasound stimulates osteogenic activity of human periosteal cells. Clin Orthop Relat Res:253-259.

Li J, Ahmad T, Spetea M, Ahmed M, Kreicbergs A (2001) Bone reinnervation after fracture: a study in the rat. J Bone Miner Res 16:1505-1510.

Li J, Kreicbergs A, Bergstrom J, Stark A, Ahmed M (2007) Site-specific CGRP innervation coincides with bone formation during fracture healing and modeling: A study in rat angulated tibia. J Orthop Res 25:1204-1212.

Li JG, Chang WH, Lin JC, Sun JS (2002) Optimum intensities of ultrasound for PGE(2) secretion and growth of osteoblasts. Ultrasound Med Biol 28:683-690.

Lin L, Fu X, Zhang X, Chen LX, Zhang JY, Yu CL, Ma KT, Zhou CY (2006) Rat adipose-derived stromal cells expressing BMP4 induce ectopic bone formation in vitro and in vivo. Acta Pharmacol Sin 27:1608-1615.

Lyons KM, Pelton RW, Hogan BL (1989) Patterns of expression of murine Vgr-1 and BMP-2a RNA suggest that transforming growth factor-beta-like genes coordinately regulate aspects of embryonic development. Genes Dev 3:1657-1668.

Madsen JE, Hukkanen M, Aspenberg P, Polak J, Nordsletten L (2000) Time-dependent sensory nerve ingrowth into a bone conduction chamber. Acta Orthop Scand 71:74-79.

Madsen JE, Hukkanen M, Aune AK, Basran I, Moller JF, Polak JM, Nordsletten L (1998) Fracture healing and callus innervation after peripheral nerve resection in rats. Clin Orthop Relat Res:230-240.

Maintz G (1950) [Animal experiments in the study of the effect of ultrasonic waves on bone regeneration.]. Strahlentherapie 82:631-638.

Massague J (1998) TGF-beta signal transduction. Annu Rev Biochem 67:753-791.

Mayr E, Frankel V, Ruter A (2000a) Ultrasound--an alternative healing method for nonunions? Arch Orthop Trauma Surg 120:1-8.

Mayr E, Rudzki MM, Rudzki M, Borchardt B, Hausser H, Ruter A (2000b) Beschleunigt niedrig intensiver, gepulster Ultraschall die Heilung von Skaphoidfrakturen? Handchirurgie, Mikrochirurgie, Plastische Chirurgie 32:115-122.

Michelangeli VP, Fletcher AE, Allan EH, Nicholson GC, Martin TJ (1989) Effects of calcitonin gene-related peptide on cyclic AMP formation in chicken, rat, and mouse bone cells. Journal of Bone & Mineral Research 4:269-272.

Millet I, Vignery A (1997) The neuropeptide calcitonin gene-related peptide inhibits TNF-alpha but poorly induces IL-6 production by fetal rat osteoblasts. Cytokine 9:999-1007.

Minamide A, Kawakami M, Hashizume H, Sakata R, Yoshida M, Tamaki T (2004) Experimental study of carriers of bone morphogenetic protein used for spinal fusion. J Orthop Sci 9:142-151.

Minina E, Wenzel HM, Kreschel C, Karp S, Gaffield W, McMahon AP, Vortkamp A (2001) BMP and Ihh/PTHrP signaling interact to coordinate chondrocyte proliferation and differentiation. Development 128:4523-4534.

Miyazono K, Maeda S, Imamura T (2005) BMP receptor signaling: transcriptional targets, regulation of signals, and signaling cross-talk. Cytokine Growth Factor Rev 16:251-263.

Mourad PD, Lazar DA, Curra FP, Mohr BC, Andrus KC, Avellino AM, McNutt LD, Crum LA, Kliot M (2001) Ultrasound accelerates functional recovery after peripheral nerve damage. Neurosurgery 48:1136-1140; discussion 1140-1131.

Nakase T, Nomura S, Yoshikawa H, Hashimoto J, Hirota S, Kitamura Y, Oikawa S, Ono K, Takaoka K (1994) Transient and localized expression of bone morphogenetic protein 4 messenger RNA during fracture healing. J Bone Miner Res 9:651-659.

Nakayama N, Duryea D, Manoukian R, Chow G, Han CY (2003) Macroscopic cartilage formation with embryonic stem-cell-derived mesodermal progenitor cells. J Cell Sci 116:2015-2028.

Naruse K, Mikuni-Takagaki Y, Azuma Y, Ito M, Oota T, Kameyama K, Itoman M (2000) Anabolic response of mouse bone-marrow-derived stromal cell clone ST2 cells to low-intensity pulsed ultrasound. Biochem Biophys Res Commun 268:216-220.

Nohe A, Keating E, Knaus P, Petersen NO (2004) Signal transduction of bone morphogenetic protein receptors. Cell Signal 16:291-299.

Nolte PA, Klein-Nulend J, Albers GH, Marti RK, Semeins CM, Goei SW, Burger EH (2001) Low-intensity ultrasound stimulates endochondral ossification in vitro. J Orthop Res 19:301-307.

Palumbo M, Valdes M, Robertson A, Sheikh S, Lucas P (2004) Posterolateral intertransverse lumbar arthrodesis in the New Zealand White rabbit model: I. Surgical anatomy. Spine J 4:287-292.

Papp Z, Fekete T (2003) The evolving role of ultrasound in obstetrics/gynecology practice. Int J Gynaecol Obstet 82:339-346.

Parvizi J, Parpura V, Greenleaf JF, Bolander ME (2002) Calcium signaling is required for ultrasound-stimulated aggrecan synthesis by rat chondrocytes. J Orthop Res 20:51-57.

Parvizi J, Wu CC, Lewallen DG, Greenleaf JF, Bolander ME (1999) Low-intensity ultrasound stimulates proteoglycan synthesis in rat chondrocytes by increasing aggrecan gene expression. J Orthop Res 17:488-494.

Pilla AA, Mont MA, Nasser PR, Khan SA, Figueiredo M, Kaufman JJ, Siffert RS (1990) Non-invasive low-intensity pulsed ultrasound accelerates bone healing in the rabbit. J Orthop Trauma 4:246-253.

Reher P, Harris M, Whiteman M, Hai HK, Meghji S (2002) Ultrasound stimulates nitric oxide and prostaglandin E2 production by human osteoblasts. Bone 31:236-241.

Ryaby JT, Matthew J, Duarte-Alves A (1992) Low intensity pulsed ultrasound affects adenylate cyclase activity and TGF-β synthesis in osteoblastic cells. Trans Orthop Res Soc 17:590-594

Ryaby JT, Bachner EJ, Bendo JA, Dalton PF, Tannenbaul S, Pilla AA (1989) Low intensity pulsed ultrasound increases calcium incorporation in both differentiating cartilage and bone cell cultures. Trans Orthop Res Soc 14 15-20.

Saito N, Takaoka K (2003) New synthetic biodegradable polymers as BMP carriers for bone tissue engineering. Biomaterials 24:2287-2293.

Sakagami Y, Girasole G, Yu XP, Boswell HS, Manolagas SC (1993) Stimulation of interleukin-6 production by either calcitonin gene-related peptide or parathyroid hormone in two phenotypically distinct bone marrow-derived murine stromal cell lines. Journal of Bone & Mineral Research 8:811-816.

Sakurakichi K, Tsuchiya H, Uehara K, Yamashiro T, Tomita K, Azuma Y (2004) Effects of timing of low-intensity pulsed ultrasound on distraction osteogenesis. J Orthop Res 22:395-403.

Sandhu HS, Kanim LE, Toth JM, Kabo JM, Liu D, Delamarter RB, Dawson EG (1997) Experimental spinal fusion with recombinant human bone morphogenetic protein-2 without decortication of osseous elements. Spine 22:1171-1180.

Sandhu HS, Toth JM, Diwan AD, Seim HB, 3rd, Kanim LE, Kabo JM, Turner AS (2002) Histologic evaluation of the efficacy of rhBMP-2 compared with autograft bone in sheep spinal anterior interbody fusion. Spine 27:567-575.

Sandhu HS, Kanim LE, Kabo JM, Toth JM, Zeegen EN, Liu D, Delamarter RB, Dawson EG (1996) Effective doses of recombinant human bone morphogenetic protein-2 in experimental spinal fusion. Spine 21:2115-2122.

Santavirta S, Konttinen YT, Nordstrom D, Makela A, Sorsa T, Hukkanen M, Rokkanen P (1992) Immunologic studies of nonunited fractures. Acta Orthop Scand 63:579-586.

Schmidt JE, Suzuki A, Ueno N, Kimelman D (1995) Localized BMP-4 mediates dorsal/ventral patterning in the early Xenopus embryo. Dev Biol 169:37-50.

Schrier JA, DeLuca PP (2001) Porous bone morphogenetic protein-2 microspheres: polymer binding and in vitro release. AAPS PharmSciTech 2:E17.

Schumann D, Kujat R, Zellner J, Angele MK, Nerlich M, Mayr E, Angele P (2006) Treatment of human mesenchymal stem cells with pulsed low intensity ultrasound enhances the chondrogenic phenotype in vitro. Biorheology 43:431-443.

Shih C, Bernard GW (1997) Calcitonin gene related peptide enhances bone colony development in vitro. Clinical Orthopaedics & Related Research:335-344.

Shimazaki A, Inui K, Azuma Y, Nishimura N, Yamano Y (2000) Low-intensity pulsed ultrasound accelerates bone maturation in distraction osteogenesis in rabbits. J Bone Joint Surg Br 82:1077-1082.

Shum L, Wang X, Kane AA, Nuckolls GH (2003) BMP4 promotes chondrocyte proliferation and hypertrophy in the endochondral cranial base. Int J Dev Biol 47:423-431.

Sidhu KS, Prochnow TD, Schmitt P, Fischgrund J, Weisbrode S, Herkowitz HN (2001) Anterior cervical interbody fusion with rhBMP-2 and tantalum in a goat model. Spine J 1:331-340.

Solomon EP (2003) Introduction to Human Anatomy and Physiology, second edition Edition.

Steinert A, Weber M, Dimmler A, Julius C, Schutze N, Noth U, Cramer H, Eulert J, Zimmermann U, Hendrich C (2003) Chondrogenic differentiation of mesenchymal progenitor cells encapsulated in ultrahigh-viscosity alginate. Journal of Orthopaedic Research 21:1090-1097.

Takaoka K, Nakahara H, Yoshikawa H, Masuhara K, Tsuda T, Ono K (1988) Ectopic bone induction on and in porous hydroxyapatite combined with collagen and bone morphogenetic protein. Clin Orthop Relat Res:250-254.

Tay BK, Patel VV, Bradford DS (1999) Calcium sulfate- and calcium phosphate-based bone substitutes. Mimicry of the mineral phase of bone. Orthop Clin North Am 30:615-623.

Tis JE, Meffert CR, Inoue N, McCarthy EF, Machen MS, McHale KA, Chao EY (2002) The effect of low intensity pulsed ultrasound applied to rabbit tibiae during the consolidation phase of distraction osteogenesis. J Orthop Res 20:793-800.

Urist MR (1965) Bone formation by autoinduction. Science 150:893-899.

Vignery A, McCarthy TL (1996) The neuropeptide calcitonin gene-related peptide stimulates insulin-like growth factor I production by primary fetal rat osteoblasts. Bone 18:331-335.

Wang EA, Israel DI, Kelly S, Luxenberg DP (1993) Bone morphogenetic protein-2 causes commitment and differentiation in C3H10T1/2 and 3T3 cells. Growth Factors 9:57-71.

Wang EA, Rosen V, D'Alessandro JS, Bauduy M, Cordes P, Harada T, Israel DI, Hewick RM, Kerns KM, LaPan P, et al. (1990) Recombinant human bone morphogenetic protein induces bone formation. Proc Natl Acad Sci U S A 87:2220-2224.

Wang SJ, Lewallen DG, Bolander ME, Chao EY, Ilstrup DM, Greenleaf JF (1994) Low intensity ultrasound treatment increases strength in a rat femoral fracture model. J Orthop Res 12:40-47.

Warden SJ, Favaloro JM, Bennell KL, McMeeken JM, Ng KW, Zajac JD, Wark JD (2001) Low-intensity pulsed ultrasound stimulates a bone-forming

response in UMR-106 cells. Biochem Biophys Res Commun 286:443-450.

Watson T (2000) The role of electrotherapy in contemporary physiotherapy practice. Man Ther 5:132-141.

Welgus HG, Jeffrey JJ, Eisen AZ (1981) Human skin fibroblast collagenase. Assessment of activation energy and deuterium isotope effect with collagenous substrates. J Biol Chem 256:9516-9521.

Welgus HG, Jeffrey JJ, Eisen AZ, Roswit WT, Stricklin GP (1985) Human skin fibroblast collagenase: interaction with substrate and inhibitor. Coll Relat Res 5:167-179.

Whang K, Tsai DC, Nam EK, Aitken M, Sprague SM, Patel PK, Healy KE (1998) Ectopic bone formation via rhBMP-2 delivery from porous bioabsorbable polymer scaffolds. J Biomed Mater Res 42:491-499.

Wozney JM (1992) The bone morphogenetic protein family and osteogenesis. Mol Reprod Dev 32:160-167.

Wozney JM, Rosen V, Celeste AJ, Mitsock LM, Whitters MJ, Kriz RW, Hewick RM, Wang EA (1988) Novel regulators of bone formation: molecular clones and activities. Science 242:1528-1534.

Wurzler KK, Emmert J, Eichelsbacher F, Kubler NR, Sebald W, Reuther JF (2004) [Evaluation of the osteoinductive potential of genetically modified BMP-2 variants]. Mund Kiefer Gesichtschir 8:83-92.

Xavier CAM, Duarte LR. (1983) [stimulation of bone callus by ultrasound] Rev Brasil Ortop 18:73-80.

Yamaguchi A, Katagiri T, Ikeda T, Wozney JM, Rosen V, Wang EA, Kahn AJ, Suda T, Yoshiki S (1991) Recombinant human bone morphogenetic protein-2 stimulates osteoblastic maturation and inhibits myogenic differentiation in vitro. J Cell Biol 113:681-687.

Yamamoto I, Kitamura N, Aoki J, Shigeno C, Hino M, Asonuma K, Torizuka K, Fujii N, Otaka A, Yajima H (1986) Human calcitonin gene-related peptide possesses weak inhibitory potency of bone resorption in vitro. Calcified Tissue International 38:339-341.

Yang KH, Parvizi J, Wang SJ, Lewallen DG, Kinnick RR, Greenleaf JF, Bolander ME (1996) Exposure to low-intensity ultrasound increases aggrecan gene expression in a rat femur fracture model. J Orthop Res 14:802-809.

Yoshida K, Bessho K, Fujimura K, Kusumoto K, Ogawa Y, Tani Y, Iizuka T (1998) Osteoinduction capability of recombinant human bone

morphogenetic protein-2 in intramuscular and subcutaneous sites: an experimental study. J Craniomaxillofac Surg 26:112-115.

Zaidi M, Breimer LH, MacIntyre I (1987a) Biology of peptides from the calcitonin genes. Quarterly Journal of Experimental Physiology 72:371-408.

Zaidi M, Chambers TJ, Gaines Das RE, Morris HR, MacIntyre I (1987b) A direct action of human calcitonin gene-related peptide on isolated osteoclasts. Journal of Endocrinology 115:511-518.

Zaidi M, Fuller K, Bevis PJ, GainesDas RE, Chambers TJ, MacIntyre I (1987c) Calcitonin gene-related peptide inhibits osteoclastic bone resorption: a comparative study. Calcified Tissue International 40:149-154.

Zhang ZJ, Huckle J, Francomano CA, Spencer RG (2003) The effects of pulsed low-intensity ultrasound on chondrocyte viability, proliferation, gene expression and matrix production. Ultrasound Med Biol 29:1645-1651.

THE HONG KONG POLYTECHNIC UNIVERSITY
香港理工大學

MEMO

To : Dr Guo Xia, Department of Rehabilitation Sciences

From : Mrs Maureen Boost, Chairman, Animal Subjects Ethics Sub-committee

Ref. : _____ Your Ref. : _____

Tel. No. : Ext. 6391 Date : - 7 APR 2003

Application for Ethical Review for the Use of Animals in Teaching or Research
[Effect of ultrasound for improving tendon healing and prevention of bone loss in disused limbs] (ASESC No. 03/6)
[Combination of extracorporeal shock wave therapy and low intensity ultrasound for inducing healing in a rabbit model] (ASESC No. 03/8)
[Effect of low intensity pulsed ultrasound on PhBMP-4 induced osteogenesis in an spinal fusion model] (ASESC No. 03/9)

Your applications for ethics review for the use of animals in the above projects have been approved for a period of two years from the date of this memo.

You are required to inform the Animal Subjects Ethics Sub-committee if at any time the conditions under which the animals are kept and cared for no longer fully meet the requirements of the Procedures for the Care of Laboratory Animals. If you are keeping animals in the University's animal holding room, you should state the full title of the approved project and the ASESC no. on the cage cards of the cages holding the animals. The members of the Sub-committee may visit the animal holding room unannounced at any reasonable time.

I would like to draw your attention to the University requirement that holders of licences under Cap. 340 must provide the Animal Subjects Ethics Sub-committee with a copy of their licences and a copy of their annual returns to the Licensing Authority. These must be kept up to date for the duration of the above work.

Mrs Maureen Boost
Chairman
Animal Subjects Ethics Sub-committee

c.c. Chairman, DRC (RS)

THE HONG KONG
POLYTECHNIC UNIVERSITY
香港理工大學

MEMO

To : Dr Guo Xia, Department of Rehabilitation Sciences

From : Dr Maureen Boost, Chairman, Animal Subjects Ethics Sub-committee

Ref. : _____ Your Ref. : _____

Tel. No. : Ext. 6391 Date : 14 APR 2005

Ethical approval granted for teaching / research projects using animals
[Effect of low intensity pulsed ultrasound on PhBMP-4 induced osteogenesis in an spinal fusion model]
(ASESC No. 03/9)

I am pleased to inform you that approval has been given to extend the approval validity period for the above project up to 6 April 2006 on condition of a valid license for the project being issued by the Licensing Authority. You should **not commence or continue** with your animal work unless you are holding a valid license and have forwarded a copy of it to the Sub-committee. You will be invited to advise on the status of your project by the end of the approval validity period.

You are required to inform the Animal Subjects Ethics Sub-committee if at any time the conditions under which the animals are kept and cared for no longer fully meet the requirements of the Procedures for the Care of Laboratory Animals. If you are keeping animals in the University's animal holding room, you should state the full title of the approved project and the ASESC no. on the cage cards of the cages holding the animals. The member of the Sub-committee may visit the animal holding room unannounced at any reasonable time.

I would like to draw your attention to the University requirement that holders of licences under Cap. 340 must provide the Animal Subjects Ethics Sub-committee with a copy of their licences and a copy of their annual returns to the Licensing Authority. These must be kept up to date for the duration of the above work. In this connection, you are requested to provide the Sub-committee with the updated license for the project when available.

Dr Maureen Boost
Chairman
Animal Subjects Ethics Sub-committee

c.c. Chairman, DRC (RS)

THE HONG KONG
POLYTECHNIC UNIVERSITY
香港理工大學

MEMO

To : Dr Guo Xia, Department of Rehabilitation Sciences

From : Dr Maureen Boost, Chairman, Animal Subjects Ethics Sub-committee

Ref. : _____ Your Ref. : _____

Tel. No. : Ext. 6391 Date : 28 MAR 2006

Ethical approval granted for teaching / research projects using animals
[Effect of low intensity pulsed ultrasound on PhBMP-4 induced osteogenesis in an spinal fusion model]
(ASESC No. 03/9)

I am pleased to inform you that approval has been given to extend the approval validity period for the above project up to 6 April 2007. You will be invited to advise on the status of your project by the end of the approval validity period.

You are required to inform the Animal Subjects Ethics Sub-committee if at any time the conditions under which the animals are kept and cared for no longer fully meet the requirements of the Procedures for the Care of Laboratory Animals. If you are keeping animals in the University's animal holding room, you should state the full title of the approved project and the ASESC no. on the cage cards of the cages holding the animals. The members of the Sub-committee may visit the animal holding room unannounced at any reasonable time.

I would like to draw your attention to the University requirement that holders of licences under Cap. 340 must provide the Animal Subjects Ethics Sub-committee with a copy of their licences and a copy of their annual returns to the Licensing Authority. These must be kept up to date for the duration of the above work. In this connection, you are requested to provide to Sub-committee with the updated license for the project when available.

Dr Maureen Boost
Chairman
Animal Subjects Ethics Sub-committee

c.c. Chairman, DRC (RS)

Table1. Raw data of BMC at day 3 postoperation

	Low dose rhBMP-4 group		High dose rhBMP-4 group	
	Sham LIPU side	LIPU treated side	Sham LIPU side	LIPU treated side
BMC	207.7967	204.3874	210.4296	242.6096
BMC	223.0448	230.0825	265.4349	254.5730
BMC	217.6694	219.3339	218.6142	220.2243
BMC	223.4057	206.1942	222.1486	241.1124
BMC	211.9577	221.0200	258.9967	252.2564
BMC	213.1048	226.5660	213.2846	224.0068

Table2. Raw data of BMC at week 1 postoperation

	Low dose rhBMP-4 group		High dose rhBMP-4 group	
	Sham LIPU side	LIPU treated side	Sham LIPU side	LIPU treated side
BMC	186.4503	157.6636	201.5707	217.7388
BMC	298.9205	324.536	291.6364	275.9261
BMC	253.8073	220.4745	243.5623	255.6438
BMC	185.8489	151.0589	286.5617	277.0964
BMC	270.2272	298.5414	206.8339	207.7022
BMC	275.0593	233.0999	227.3525	221.0417

Table3. Raw data of BMC at week 3 postoperation

	Low dose rhBMP-4 group		High dose rhBMP-4 group	
	Sham LIPU side	LIPU treated side	Sham LIPU side	LIPU treated side
BMC	228.6850	251.4626	242.2076	250.6832
BMC	223.8580	247.6220	297.6010	297.9028
BMC	247.1213	235.0525	252.5711	262.6993
BMC	223.5576	254.9308	276.8066	262.6496
BMC	223.2400	259.0808	211.5064	213.3530
BMC	232.8633	236.7322	297.6786	295.7400

Table4. Raw data of BMC at week 7 postoperation

	Low dose rhBMP-4 group		High dose rhBMP-4 group	
	Sham LIPU side	LIPU treated side	Sham LIPU side	LIPU treated side
BMC	211.3642	300.0045	345.5200	360.6440
BMC	239.8734	268.2450	140.5200	150.5640
BMC	216.1829	238.0165	279.8402	296.3928
BMC	197.4790	213.5775	255.6351	308.7980
BMC	281.1489	368.8290	147.3985	157.3290
BMC	244.5876	322.4094	359.8459	397.6150

Table5. Raw data of BMC at week 12 postoperation

	Low dose rhBMP-4 group		High dose rhBMP-4 group	
	Sham LIPU side	LIPU treated side	Sham LIPU side	LIPU treated side
BMC	247.3240	251.8340	247.3240	251.8340
BMC	300.6352	371.0950	300.6352	371.0950
BMC	307.4980	386.1614	307.4980	386.1614
BMC	318.1103	440.5095	318.1103	440.5095
BMC	274.7975	290.6702	274.7975	290.6702
BMC	268.5399	295.8677	268.5399	295.8677

Table6. Raw data of bone volume and BMD at day 3 postoperation

	Low dose rhBMP-4 group		High dose rhBMP-4 group	
	Sham LIPU side	LIPU treated side	Sham LIPU side	LIPU treated side
Bone volume	0.045876	0.051204	0.049873	0.055223
Bone volume	0.058260	0.051500	0.058678	0.060621
Bone volume	0.057344	0.056744	0.052264	0.055944
Bone volume	0.057272	0.050520	0.051016	0.060208
Bone volume	0.045728	0.050704	0.060328	0.057540
Bone volume	0.054720	0.054064	0.050112	0.053576
BMD	382.58	411.00	415.08	430.53
BMD	462.54	432.62	432.39	432.11
BMD	399.53	415.23	419.63	392.39
BMD	363.37	410.74	425.97	400.00
BMD	455.71	429.68	427.19	436.74
BMD	387.11	417.81	413.93	418.28

Table7. Raw data of bone volume and BMD at week 1 postoperation

	Low dose rhBMP-4 group		High dose rhBMP-4 group	
	Sham LIPU side	LIPU treated side	Sham LIPU side	LIPU treated side
Bone volume	0.061920	0.060842	0.059345	0.057320
Bone volume	0.041727	0.032847	0.05928	0.056642
Bone volume	0.050544	0.050144	0.04376	0.048282
Bone volume	0.051360	0.054120	0.06522	0.061040
Bone volume	0.042360	0.033380	0.05032	0.052080
Bone volume	0.060540	0.052720	0.05076	0.052360
BMD	433.95	462.12	429.61	428.96
BMD	523.22	534.58	431.61	424.68
BMD	470.80	452.17	456.70	459.55
BMD	448.33	456.39	438.35	454.73
BMD	517.69	522.60	427.47	424.55
BMD	441.97	478.27	452.07	434.18

Table8. Raw data of bone volume and BMD at week 3 postoperation

	Low dose rhBMP-4 group		High dose rhBMP-4 group	
	Sham LIPU side	LIPU treated side	Sham LIPU side	LIPU treated side
Bone volume	0.055368	0.063220	0.068430	0.063380
Bone volume	0.050864	0.061324	0.069650	0.059240
Bone volume	0.057200	0.061540	0.059240	0.057048
Bone volume	0.049040	0.064220	0.061160	0.064827
Bone volume	0.058120	0.058400	0.066560	0.065800
Bone volume	0.060880	0.060033	0.068784	0.065280
BMD	459.95	407.97	350.05	402.65
BMD	454.15	400.68	349.03	380.65
BMD	400.08	403.64	479.66	483.60
BMD	400.53	385.44	476.06	443.27
BMD	400.39	404.52	433.31	450.83
BMD	400.21	408.85	319.37	332.79

Table9. Raw data of bone volume and BMD at week 7 postoperation

	Low dose rhBMP-4 group		High dose rhBMP-4 group	
	Sham LIPU side	LIPU treated side	Sham LIPU side	LIPU treated side
Bone volume	0.070945	0.084253	0.079245	0.085440
Bone volume	0.044035	0.060400	0.051464	0.074550
Bone volume	0.067602	0.080808	0.042200	0.055660
Bone volume	0.045080	0.058024	0.079600	0.081500
Bone volume	0.072220	0.085460	0.038640	0.043680
Bone volume	0.061380	0.084400	0.079780	0.085654
BMD	455.12	431.85	347.22	313.79
BMD	351.22	330.48	457.00	420.17
BMD	385.68	381.71	419.93	415.40
BMD	438.40	375.84	376.18	325.20
BMD	352.26	342.81	389.30	389.06
BMD	401.40	381.91	478.68	453.11

Table10. Raw data of bone volume and BMD at week 12 postoperation

	Low dose rhBMP-4 group		High dose rhBMP-4 group	
	Sham LIPU side	LIPU treated side	Sham LIPU side	LIPU treated side
Bone volume	0.091640	0.093134	0.082756	0.105578
Bone volume	0.060120	0.071723	0.068033	0.070900
Bone volume	0.094720	0.095920	0.087384	0.102160
Bone volume	0.086586	0.094200	0.069952	0.072440
Bone volume	0.060000	0.074960	0.083896	0.102928
Bone volume	0.094880	0.097060	0.069272	0.072744
BMD	462.31	487.87	339.21	316.00
BMD	369.65	358.88	392.53	423.95
BMD	428.44	410.70	363.03	411.77
BMD	399.44	437.96	365.50	364.79
BMD	464.31	486.12	334.91	295.53
BMD	396.65	424.55	400.02	407.73

Table11. Raw data of percentage of new bone at week 3 postoperation

Tissue	Low dose rhBMP-4 group		High dose rhBMP-4 group	
	Sham LIPU side	LIPU treated side	Sham LIPU side	LIPU treated side
New bone %	2.51	2.19	3.89	5.42
New bone %	2.81	2.99	3.89	5.51
New bone %	1.90	2.99	3.85	5.42
New bone %	2.16	2.91	4.05	4.80
New bone %	1.92	2.99	3.38	7.99
New bone %	2.22	3.85	4.02	3.68

Table12. Raw data of percentage of new bone at week 7 postoperation

Tissue	Low dose rhBMP-4 group		High dose rhBMP-4 group	
	Sham LIPU side	LIPU treated side	Sham LIPU side	LIPU treated side
New bone %	4.97	5.48	16.57	24.88
New bone %	4.96	5.44	15.86	22.80
New bone %	4.97	5.48	16.69	23.83
New bone %	4.73	5.80	16.13	26.05
New bone %	5.72	5.49	17.82	21.81
New bone %	4.50	4.89	15.95	23.74

Table13. Raw data of percentage of new bone at week 12 postoperation

Tissue	Low dose rhBMP-4 group		High dose rhBMP-4 group	
	Sham LIPU side	LIPU treated side	Sham LIPU side	LIPU treated side
New bone %	14.39	15.21	23.07	27.25
New bone %	13.79	15.14	23.07	27.56
New bone %	13.93	15.13	23.18	27.15
New bone %	13.44	14.99	23.40	28.10
New bone %	14.38	15.46	23.70	27.15
New bone %	13.69	15.39	22.03	26.68

Table14. Raw data of percentage of cartilage and fibrous tissue at week 3 postoperation

	Low dose rhBMP-4 group		High dose rhBMP-4 group	
	Sham LIPU side	LIPU treated side	Sham LIPU side	LIPU treated side
Cartilage %	0.39	1.0379	0.4791	2.5546
Cartilage %	0.39	0.7063	0.4724	3.1454
Cartilage %	0.39	0.7065	0.4823	2.8234
Cartilage %	0.40	0.2021	0.3634	3.5479
Cartilage %	0.31	0.7093	0.2976	2.2685
Cartilage %	0.47	0.9230	0.7721	4.0236
Fibrous tissue %	97.72	97.6200	96.3819	94.5620
Fibrous tissue %	97.77	96.8573	95.9956	94.6923
Fibrous tissue %	97.78	96.8563	95.9989	92.5022
Fibrous tissue %	97.55	97.6050	95.9901	95.2962
Fibrous tissue %	97.99	96.8544	96.5267	93.3877
Fibrous tissue %	97.66	96.2643	95.9945	96.5060

Table15. Raw data of percentage of cartilage and fibrous tissue at week 7 postoperation

	Low dose rhBMP-4 group		High dose rhBMP-4 group	
	Sham LIPU side	LIPU treated side	Sham LIPU side	LIPU treated side
Cartilage %	0	0.09	0	0.71
Cartilage %	0	0.09	0	0.69
Cartilage %	0	0.09	0	0.70
Cartilage %	0	0.11	0	0.59
Cartilage %	0	0.05	0	0.79
Cartilage %	0	0.10	0	0.71
Fibrous tissue %	95.03	94.43	83.42	74.41
Fibrous tissue %	95.04	94.47	84.13	76.51
Fibrous tissue %	95.03	94.43	83.31	75.47
Fibrous tissue %	95.50	94.06	83.87	73.40
Fibrous tissue %	94.28	94.56	82.19	77.42
Fibrous tissue %	95.26	94.93	84.10	75.55

Table16. Raw data of percentage of cartilage and fibrous tissue at week 12 postoperation

	Low dose rhBMP-4 group		High dose rhBMP-4 group	
	Sham LIPU side	LIPU treated side	Sham LIPU side	LIPU treated side
Cartilage %	0	0	0	0
Cartilage %	0	0	0	0
Cartilage %	0	0	0	0
Cartilage %	0	0	0	0
Cartilage %	0	0	0	0
Cartilage %	0	0	0	0
Fibrous tissue %	85.51	84.79	78.00	72.90
Fibrous tissue %	86.21	84.86	75.65	72.34
Fibrous tissue %	86.67	84.87	76.62	72.95
Fibrous tissue %	86.36	85.21	76.06	71.44
Fibrous tissue %	85.02	84.34	77.26	72.55
Fibrous tissue %	86.61	84.61	77.99	73.92

Table17. Raw data of density of CGRP-positive nerve fibers in fibrous tissue at day 3

	Sham LIPU side	LIPU side
Fibrous tissue	0.001310	0.002614
Fibrous tissue	0.001206	0.002352
Fibrous tissue	0.001261	0.002997
Fibrous tissue	0.001249	0.002527
Fibrous tissue	0.001231	0.002476
Fibrous tissue	0.001309	0.002972

Table18. Raw data of density of CGRP-positive nerve fibers in fibrous tissue at week 1

	Sham LIPU side	LIPU side
Fibrous tissue	0.001048	0.002402
Fibrous tissue	0.001039	0.002357
Fibrous tissue	0.001090	0.002505
Fibrous tissue	0.001048	0.002352
Fibrous tissue	0.001050	0.002433
Fibrous tissue	0.001094	0.002485

Table19. Raw data of density of CGRP-positive nerve fibers in fibrous and bone marrow tissues at week 3

	Sham LIPU side	LIPU side
Fibrous tissue	0.002235	0.002796
Fibrous tissue	0.002004	0.002686
Fibrous tissue	0.002452	0.002408
Fibrous tissue	0.002028	0.002435
Fibrous tissue	0.002338	0.002668
Fibrous tissue	0.002320	0.002769
Bone marrow	0.000859	0.001479
Bone marrow	0.000867	0.001445
Bone marrow	0.000818	0.001472
Bone marrow	0.000825	0.001497
Bone marrow	0.000870	0.001479
Bone marrow	0.000851	0.001462

Table20. Raw data of density of CGRP-positive nerve fibers in fibrous and bone marrow tissues at week 7

	Sham LIPU side	LIPU side
Fibrous tissue	0.001454	0.001652
Fibrous tissue	0.001474	0.001648
Fibrous tissue	0.001413	0.001658
Fibrous tissue	0.001486	0.001680
Fibrous tissue	0.001434	0.001681
Fibrous tissue	0.001442	0.001665
Bone marrow	0.003075	0.004016
Bone marrow	0.003108	0.004072
Bone marrow	0.003060	0.004068
Bone marrow	0.003077	0.004110
Bone marrow	0.003072	0.004045
Bone marrow	0.003039	0.004083

Table21. Raw data of density of CGRP-positive nerve fibers in fibrous and bone marrow tissues at week 12

	Sham LIPU side	LIPU side
Fibrous tissue	0.001112	0.001242
Fibrous tissue	0.001080	0.001330
Fibrous tissue	0.001112	0.001235
Fibrous tissue	0.001100	0.001224
Fibrous tissue	0.001089	0.001290
Fibrous tissue	0.001085	0.001312
Bone marrow	0.001552	0.001835
Bone marrow	0.001532	0.001871
Bone marrow	0.001530	0.001841
Bone marrow	0.001587	0.001838
Bone marrow	0.001612	0.001848
Bone marrow	0.001549	0.001870